Next-Generation Technologies for the Development of Novel C–C and C–X Bond Formation Pathways from Functionalized Nitroolefins

Muhammad Ehtisham Ibraheem Khan

International School of Advance Studies
University of Camerino
2025

Università degli Studi di Camerino

School of Advanced Studies

Doctoral Course in

Chemical and Pharmaceutical Sciences and Biotechnology

Curriculum in *Chemical Sciences*

CYCLE XXXVII

Next-Generation Technologies for the Development of Novel C–C and C–X Bond Formation Pathways from Functionalized Nitroolefins

PhD Candidate

Muhammad Ehtisham Ibraheem Khan

Supervisor

Prof. Alessandro Palmieri

2022-2025

“ We created man from an extract of clay. Then We made him a seed, in a secure repository. Then We developed the seed into a clot. Then We developed the clot into a lump. Then We developed the lump into bones. Then We clothed the bones with flesh. Then We produced it into another creature. Most Blessed is Allah, the Best of Creators.**”**

(Al Quran 23: 12–14)

Acknowledgements

First and foremost, I am profoundly grateful to Almighty **Allah**, the Most Beneficent and Most Merciful, for granting me the strength, wisdom, and perseverance to complete this dissertation.

I would like to express my heartiest gratitude to my supervisor, **Professor Alessandro Palmieri,** for his invaluable guidance, encouragement, and expertise throughout this journey. His dedication to academic excellence and his constructive and continuous feedback have been a constant source of inspiration.

I am deeply indebted to my **Parents** for their endless love, support, and prayers, which have always been a source of strength in my life. To my **Brothers,** thank you for your encouragement and constant belief in my abilities, even from afar. Your unwavering support means more than words can express.

To my **Better Half,** I owe my heartfelt thanks for her endless patience, understanding, and love. Your encouragement during the most challenging times has been invaluable. To my boys **Muhammad Azhan** and **Muhammad Rayan**, being away from you while you were in Pakistan was one of the hardest parts of this journey. I missed you dearly, and your love and smiles from afar were a constant source of motivation.

I am sincerely grateful to **Indena S.p.A.,** Milan, for their generous support and collaboration, which played a vital role in shaping the outcomes of this research.

My deepest thanks go to the **Green Chemistry Group** for providing such a friendly, collaborative, and stimulating research environment. The camaraderie and mutual support within the group have made this journey not only productive but also enjoyable.

Finally, my heartfelt thanks go to the **University of Camerino** for providing a nurturing academic environment, as well as the resources and opportunities necessary to pursue this work.

To everyone who has supported me, whether through guidance, encouragement, or prayers, I am deeply grateful. This journey has been one of immense growth and learning, and it is a testament to the collective support of so many individuals.

Abbreviations

AI	Artificial Intelligence
BINAP	2,2'-bis(diphenylphosphino)-1,1'-binaphthyl
CPBA	Chloroperoxybenzoic acid
CPME	Cyclopentyl methyl ether
CTAB	Cetyltrimethylammonium bromide
DCM	Dichloromethane
DFT	Density Functional Theory
DMF	Dimethylformamide
DMSO	Dimethyl sulfoxide
DMTMM	4-(4,6-dimethoxy-1,3,5-triazin-2-yl)-4-methyl-morpholinium chloride
EnT	Triplet energy transfer
ET	Energy transfer
FDA	Food and Drug Administration
GSK	Glaxo Smith Kline
GVL	γ-valerolactone
HAT	Hydrogen atom transfer
HFIP	Hexafluoroisopropanol
HOMO	Highest Occupied Molecular Orbital
HTS	High-throughput synthesis
IC	Internal Conversion
ICA	Independent Component Analysis
IR	Infra-red
ISC	Intersystem Crossing
LED	Light emitting diode

LUMO	Lowest unoccupied molecular orbital
MH	Microwave heating
NHPI	*N*-Hydrophthalimide
NMR	Nuclear magnetic Resonance
NOSEY	Nuclear Overhauser Effect Spectroscopy
OLED	Organic light-emitting diodes
OPV	Organic photovoltaics
PEG	Polyethylene glycol
PPA	Polyphthalamide
S_0	Ground state
S_1	Lowest/First excited singlet state
SDG	Sustainable Development Goals
T_1	Lowest exited triplet state
TEMPO	2,2,6,6-tetramethylpiperidine-1-oxyl
XAT	Halogen atom transfer

Contents

Preface

This thesis explores the "*Next-Generation Technologies for the Development of Novel C–C and C–X Bond Formation Pathways from Functionalized Nitroolefins"* with the aim of developing green and sustainable synthetic methodologies for biologically important molecules.

The First chapter enlights the emerging trends and technologies being used in the modern organic synthesis with a focus on photochemistry, flow-chemistry, microwave irradiation and one-pot reactions.

The second chapter encounters my research work conducted at University of Camerino (Chemistry Interdisciplinary Project, ChIP, Camerino, Italy) in the Green Chemistry Group, under the supervision of Prof. Alessandro Palmieri, where I specifically studied the reactivity of β-nitroenones and explored the possibility to utilize them as a precursor for various bioactive heterocyclic systems including pyridazines, Isoxazoles, and conjugated nitrotriene systems. These works promoted sustainability in terms of green energy conditions including microwave, photochemistry and flow chemistry.

The third chapter describes my research work performed during visiting research stay at the State key laboratory of Green Chemistry and Chemical process at East China Normal University, Shanghai, China. Where I worked with Prof. Xuefeng Jiang on the selective C-H activation of alkyl benzenes under photochemical conditions. In parallel to the core project, I was also involved in co-authorship of a review article published in Artificial Intelligence Chemistry.

Chapter 1

1. Emerging Trends in Green and Sustainable Organic Synthesis

As we face environmental imbalances and climate change, sustainability has become paramount. Consequently, synthetic organic chemistry has been undergoing a subtle transformation. Green chemistry, better known as sustainable or eco-friendly chemistry, has become a driving force for this change. By allowing safety, efficiency, and reducing environmental impacts, it provides a promising pathway to align industrial practices with ecological balance for a sustainable future.

In 1998 Paul Anastas and John Warner took the lead by devising some core principles of green chemistry and presented the first comprehensive introduction to design, development and evolution process central to green chemistry [1]. Guided by these core set of principles (**Figure 1.1**), researchers are pioneering innovative solutions to overcome the challenges of conventional chemical processes in academia as well as in industry [2].

Figure 1.1 Core principles of green chemistry

Moving a step further, the implementation of the United Nations sustainable development goals (SDGs) in 2016 endorsed the use of green chemical practices. These SDGs serve as a roadmap for fostering a more sustainable way of life on Earth, with public health being a critical focus. Whereas green chemistry acts as an efficient tool in achieving these SDGs, addressing public health challenges from a technical side [3, 4].

The influence of organic chemistry on contemporary society is profound as it caters to the fields of essential requirements like drug discovery, pharmaceuticals, agrochemical, and many others [5-7]. Particularly in the realm of synthetic chemistry, strides in green chemistry have resulted in cleaner processes that has transposed the traditional synthetic methodologies, these improvements are based on newer concepts like *step-* and *atom- economy* [8] and *E- factor* [9], the adoption of greener solvents such as water, polyethylene glycol (PEG), hexafluoroisopropanol (HFIP), supercritical CO_2 etc. is gaining attention as a replacement to the traditional solvents [10-12]. On other hand modern molecular design particularly emphasizes green features including alternative activation and energy sources like light-controlled reactions, electrocatalysis, ultrasound & microwave irradiations in combination with flow chemistry [13-21].

In this dissertation we will briefly discuss some of the emerging fields like Photochemistry (**1.1**), Flow chemistry (**1.2**), Microwave reactions (**1.3**) and One-pot reactions (**1.4**).

1.1 Harnessing light: The Photochemistry

Since the creation of the world various light driven reactions are happening autonomously. Countless photochemical processes often go unnoticed including photosynthesis, the way our eyes perceive colors, the color change in light exposed materials and many more. Even though, thousand years back ancient civilizations explored how to harness the power of sunlight [22].

Modern history

The history of laboratory-based light-driven chemical reactions goes back to the 19th century and with the golden age in the beginning of 20th century [23], when Ciamician and Silber at Bologna pioneered the study of chemical effects of light exposure on various transformations, like photoreduction of carbonyl groups, photopinacolization, α- β cleavage and intramolecular cycloadditions. They specifically studied the photo-reduction of benzoquinone to hydroquinone and acetaldehyde, in alcoholic solutions under sunlight. Further expanding the understanding of light-induced chemical changes, Silber identified the

transformation of nitrobenzene in aniline, acetaldehyde and methylquinoline in alcoholic solution [24].

The evolution of the concept of "*quanta*" by Plank and explanation of "*photoelectric effect*" by Einstein led the foundations of first law of photochemistry [25]. While the concept of the existence of a "*metastable*" activated triplet state (T_1) by Perrin in combination to Jablonsky's findings on "*phosphorescence*", encouraged further studies on triplet energy transfer events, advancing how energy transfer occurs between molecules in their triplet states by paving a new direction towards photochemical research [26].

Photochemistry or chemistry of excited state is a captivating field of study which has significantly reshaped organic chemistry by providing advances in understanding and application of photoredox catalysis, energy transfer, organometallic excitation and light induced atom-transfer to tackle with the longstanding problems in the field [27].

Renaissance of photochemistry

The 21st century came with the renaissance of photochemistry, specifically the last two decades espied the spike incorporation of various technologies in organic synthesis to achieve reproducibility and sustainability. In this new wave, chemists discovered ways to harness the light absorbing properties of certain species to drive chemical reactions by fusion of photochemistry and catalysis. **Figure 1.2** depicts a Web of Science based yearly contribution of research published in the fields of photochemistry and catalysis, with a primary focus on investigating the Electron transfer (ET), Energy transfer (EnT), C-H activations or Hydrogen atom transfer (HAT), Halogen atom transfer (XAT) and the incorporation of flow chemistry to achieve automation.

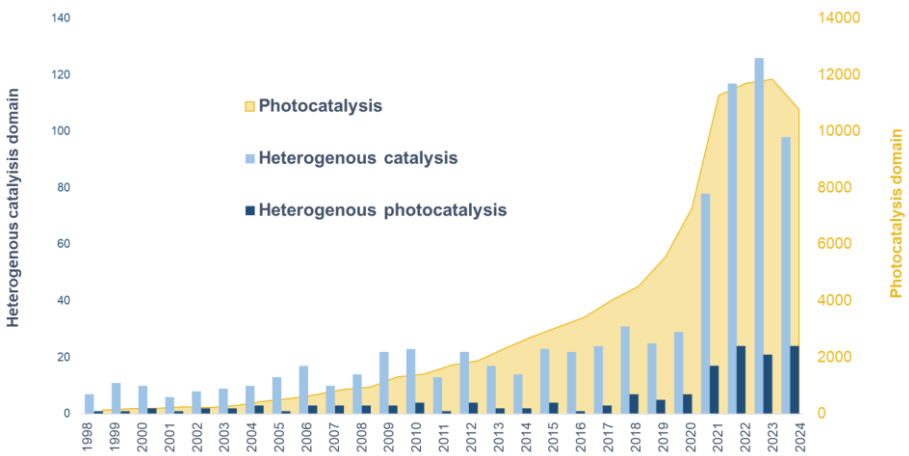

Figure 1.2 Plot of yearly publications count in photocatalysis

Photoexcitation is the very first stage of photochemical reactions, where reactants move to higher energy levels after absorbing light, in other words "*light absorption is essential for a photochemical reaction to take place*" precisely known as Grotthuss–Draper law or the first law of photochemistry. This law highlights the importance of light source selection to conduct any successful photochemical transformation. An effective photochemical transformation is obliged to the light source selection, proper matching of the emitted wavelengths to the absorption spectrum of reaction mixture is essential for the rich light absorption and attaining successful transformations [28-30]. Actinometry helps in precise evaluation of light source by measuring the actual amount of light penetrated through the sample or photon flux [31].

Light is generally categorized into three main types, ultraviolet (100-380nm), visible region (380-700), and infrared (>700 nm), sunlight being blend of all these. Most of the chemical transformations occur in near UV and visible regions, as there photons are with suitable energy to make transition possible. While in lower wavelengths high energy radiation can cause distortion of molecules.

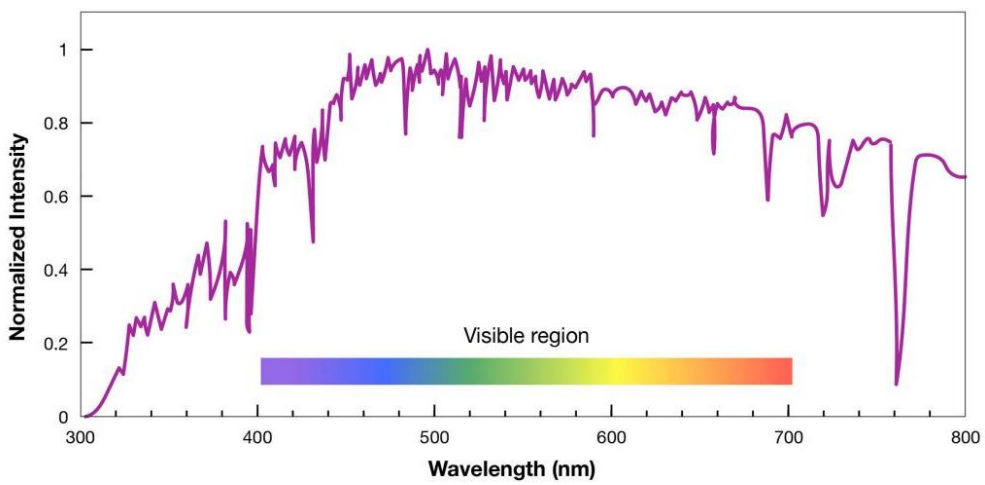

Figure 1.3 ASTM standard "AM1.5" based solar spectrum [32]

The second law in photochemistry was proposed by *Stark-Einstein* also known as "*quantum equivalence law*" which states that "*Each photon of light absorbed causes one equivalent of a subsequent chemical reaction*".

$$E = h\nu = h\, c/\lambda \text{ [j. photon } ^{-1}\text{]}$$

Where:

h: Planck's constant (6.6256 x 10 $^{-34}$ J·S·photon^{-1})

ν: radiation frequency [s^{-1}]
c: speed of light (2.9979 x 10^{-8} m·s^{-1})
λ: wavelength of light [m]

Beer-Lambert Law explains when a molecule and photon interact, the molecule absorbs that photon which subsequently leads to the excitation of one electron. The absorption probability (A) typically lies on molar extinction coefficient (ελ) fixed at a specific irradiation wavelength, sample concentration (C) and the path length (I). This law is only applicable in homogeneous, non-emissive diluted solutions, where there is no interaction between the absorbing species [33].

$$log\frac{I_0}{I} = A = \varepsilon_\lambda lC$$

Where:

ε_λ: molar absorption coefficient $[L \cdot mol^{-1} \cdot cm^{-1}]$
C: molar concentration of absorbing species [M]
l: "path length" travelled by light [cm]
I_0/I: initial intensity/ experimental intensity

Interaction of photons with molecules typically leads to the electronic transition from the highest occupied molecular orbital (HOMO) to the lowest unoccupied molecular orbital (LUMO), generating electronically excited-state molecules, which are fundamentally distinct reactive entities as compared to their ground-state counterparts [34, 35]. These excited intermediates exhibit different electronic distributions, energy levels, and lifespans, which enable their involvement in the formation of complex molecular structures. Precisely, a photochemical reaction is a deactivation process of an excited state.

The general concept of photo driven transformations can be better understood by Jablonski's diagram [36] (**Figure 1.4**). Where in the primary step absorption of light leads to molecular excitation from ground state S_0 to higher excited singlet states (S_2, S_3, . . .) followed by the transition to first or lowest excited singlet state S_1 via internal conversion (IC). In further transitions from S_1 to S_0 molecule can follow any of the following possible path

- It may lose the rest of energy and follow transition.
- Molecule may exhibit fluorescence (UV radiations)
- Undergo loss of some energy during inter system crossing (ISC) by generating T_1 state (the lowest excited triplet state or reactive state)
- Or by exhibiting phosphorescence after ISC

As a quick return happens from singlet excited state to ground state S_0, there are very few chances of chemical transformation, whereas transition from triplet excited state T_1 to ground state S_0 takes time by providing an opportunity for a chemical conversion.

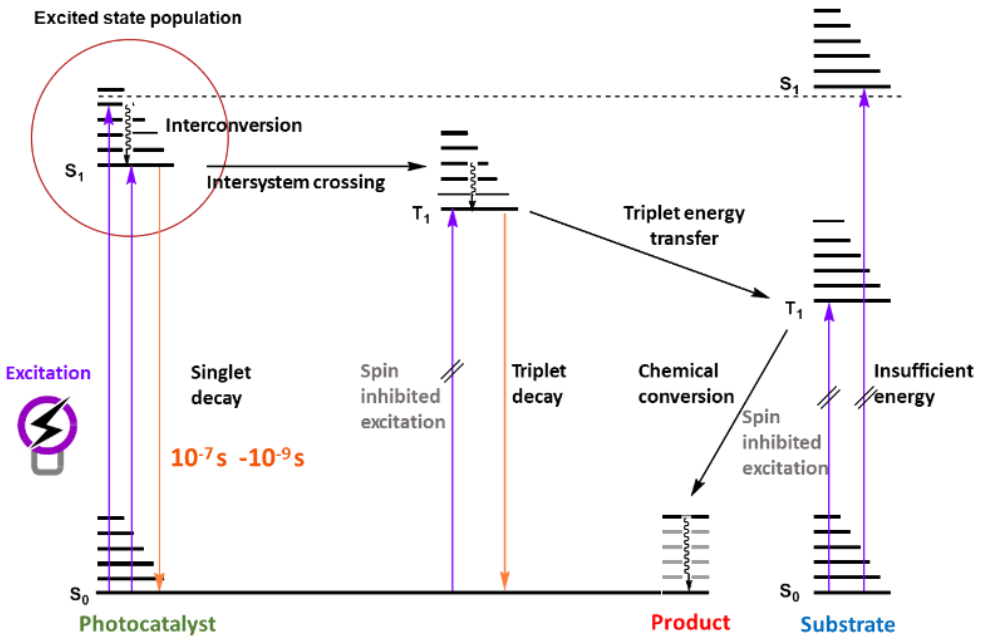

Figure 1.4 Jablonski Diagram: A general mechanism of photo driven reactions

1.1.1 Photochemical Transformations

Various photochemical reactions conducted under specific sustainable conditions often require no chemical activation, as photons are considered as traceless reagents. These chemical reactions enable the formation of unique molecular structures, important from synthetic chemistry point of view, specifically in the field of heterocyclic chemistry.

Photo induced isomerization

Photoisomerization is a widely used process in molecular switches[37] and biological systems, based on a concept in which light energy induces the transformation of one isomer into another. In organic molecules photoisomerization occurs via $\pi \rightarrow \pi^*$ transition, as their singlet (S_1) and triplet (T_1) excited states adopt a perpendicular geometry instead of planer geometry and during excitation the difference between *E* & *Z* isomer is lost, resultantly

generating either of isomer upon return to the ground state (S_0) [38]. Simulation studies suggest that mechanical isomerization initially proceeds through a mechanical induced inversion, which leads to an energetically favorable ultrafast rotation to bring effective isomerization [39]. This photoisomerization is not just limited to geometry but can also lead to stereodivergence under certain conditions [40, 41].

Styrylbenzazoles represent a promising but underexplored class of photo-switches that can undergo a light driven *E*/*Z* isomerization of central alkene bond, recently Dr. Ben's group at Groningen explored this possibility and synthesized a library of styrylbenzazole based E to *Z* isomers under visible light irradiation around 460nm, with a successful conversion of E to Z isomer in very high quantum yields.

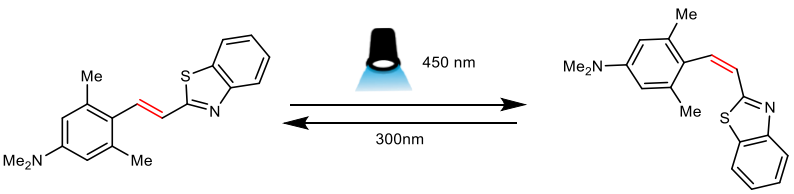

Scheme 1.1 Synthesis of Styrylbenzazole based Photoswitches.[42]

During the course of my PhD, I employed the photoisomerization technique to explore the preparation of *Z* Isomer of *β*-nitroacrylate derivatives under visible light irradiations (**Chapter 2**).

Photochemical C-H activations

One of the significant chemical problem in modern organic chemistry is the activation and functionalization of C-H bonds [43]. The C-H activation strategies are highly desirable as they help the sleek synthesis of organic molecules by skipping the traditional pre-functionalization steps [44-47]. Use of light to activate C-H bonds requires a photocatalyst to promote the cleavage of C-H bond in organic molecules, these photochemical reactions provide selectivity and tuneability under mild reaction conditions, which are difficult to achieve in contrast [48, 49].

Commonly photochemical C-H activations can be achieved by photoredox catalysis [50], energy transfer via photosensitizer [51], metal catalyzed activation or via ligand-metal or metal-ligand charge transfers [52-54]. Ackermann's group reported a photo-induced remote meta C-H activation using the cyclometalated ruthenium complex, which was difficult to achieve priorly (Scheme 1.2), without any use of an external photosensitizer [55].

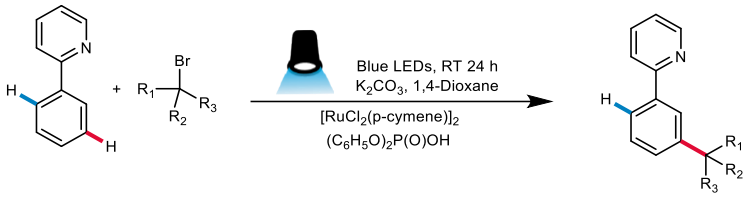

Scheme 1.2 C-H activation by photocatalysis.

During my visiting research stay at State key laboratory of green chemistry and chemical process in Shanghai China, I worked on C-H activations of electronically poor substrates like alkylbenzenes promoted by tungsten(V) oxide as a photocatalyst. Which I will discuss briefly in **Chapter 3.**

Photochemical cyclization

In heterocyclic chemistry, photochemical cyclization with at least two unsaturated moieties is crucial, these cyclization reactions involve a pericyclic ring closure induced by light. Producing an intermediate which evolves in a way to afford stable cyclized product. These reactions are widely applicable in the synthesis of photochromic compounds [56].

Photochemical cyclization reaction used to synthesize the compounds like carbazoles, dibenzofurans and dibenzothiophenes [57, 58]. In these reactions a 6π electronic system is involved to generate an intermediate, these intermediates undergo tautomerism to form the final product under mild oxidation conditions by 1,3 dipolar cycloaddition reactions [59].

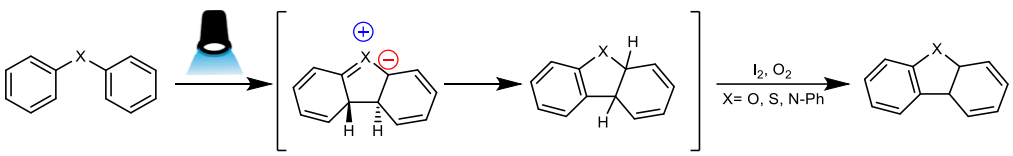

Scheme 1.3 Photochemical cyclization to synthesize carbazole, dibenzofurans and dibenzothiophens.

Widespread ability of photochemical reactions to generate highly reactive intermediates in mild conditions, often leading to increased selectivity, efficiency, and sustainability, make it an invaluable tool in modern organic synthesis. As a result, photochemistry not only provides the accessible toolset to the organic chemists, but also broadens to support the rising initiatives in green and sustainable chemistry.

1.2 Flow Chemistry

Traditionally organic synthesis has been conducted in batches, which implies in test tubes, closed containers, or round bottom flasks. However, recently organic chemistry witnessed a spike of interest in continuous flow conditions among the chemical fraternity [60-63]. Flow chemistry or continuous flow chemistry is a process in which chemical reactions take place in a stream that flows continuously in contrast to batch reactors. The reactants are introduced to a tube or microchannel, where mixing and transformation occurs. It is a revolutionary tool in organic synthesis, combined with enhanced safety, heat transfer, scalability, and precision. With a wide range of applications ranging from multistep synthesis to handling hazardous reactions, and ecofriendly sustainable chemistry both in academia and pharmaceutical industry [64, 65]. It is an interdisciplinary field that integrates concepts from both chemistry and chemical engineering. While having a basic understanding of general concepts of flow chemistry is often sufficient for setting up experiments in flow conditions. The growing interest in photo and electrochemistry has made flow technology an increasingly essential tool, thanks to their combined ability to address the scalability challenges inherent in these synthetic methods.

The flow setup

A typical flow reactor can be divided into three zones, the first where reactants are inserted and moved towards mixing unit, then pushed further to the substantial portion; the reaction zone or coil where under controlled conditions a transformation occurs, leading to exit point of product collection. On further stages, this system can include the purifications unit or analysis unit right after product collection. The following **Figure 1.5** can help to better understand a general representation of the flow-chemical reactor.

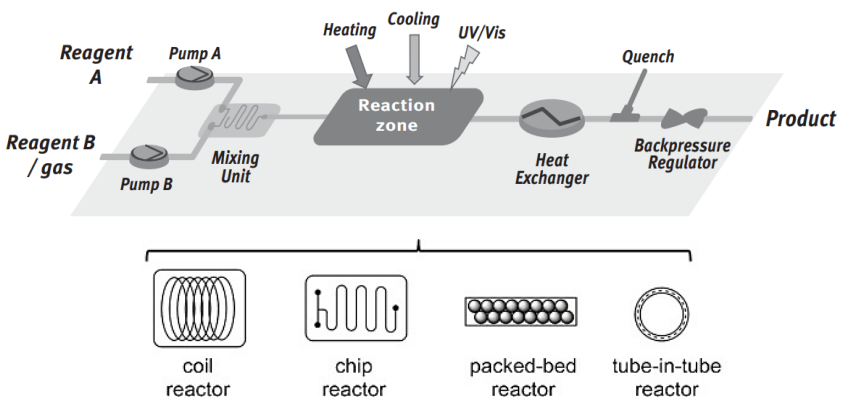

Figure 1.5 General representation of flow reactor [66]

According to Kobayashi and colleagues, so far documented literature suggests the broadly categorized four types of flow systems being commonly used [67]. In type **I** systems, all reagents flow through the reactor, and the product is collected at the end. In type **II** systems, one of reactant is immobilized on a solid support within the reactor, while substrate flows through it. If the reactions go to completion, the exit product will be solely the desired one. But in both cases no catalyst is used during the reactions. In type **III** systems, a homogenous catalyst is used, flowing through the reactor along with the reactants, at the product collection point a separation step can be required to segregate the catalyst of the potential byproducts. In type **IV** systems, the catalyst is immobilized in the reactor while allowing the reactants to flow through. This type of system eliminates the product-catalyst separation phase and enables straightforward catalyst recycling.

Reaction characteristics: Flow vs Batch

Figure 1.6 Advantages of flow chemistry [68, 69]

The batch reaction conditions are widely used on lab scale to industrial scales, but with the emergence of new techniques like flow, their use is getting limited. Although batch methods may remain more flexible for exploration or low-throughput studies but here we can understand how flow chemistry offers significant advantages in area like control safety and scalability. [70]

- **Reaction control :** In batch it is limited by mixing and heat transfer, while flow chemistry provides precise control over reaction conditions.
- **Scalability :** Scale-UP of batch performed reaction often requires redesign, while in flow it is intrinsically scalable by extending reactors.
- **Reaction time :** Reactions under batch conditions usually require longer times to complete due to inefficiencies, where enhanced kinetics in flow conditions leads to shorter reaction times.
- **Safety :** Hazardous reactions are highly risky in batch, but flow reactors support improved safety for handling hazardous materials.
- **Heat transfer :** Usually heat transfer in batch reactors leads to hot spots and can be inefficient, where large surface area in flow reactors provide superior heat transfers.
- **Reproducibility :** In batch conditions reproducibility is highly variable depending on batch-to-batch differences, on other hand continuous operations in flow conditions lead to high reproducibility.
- **Reagent usage :** larger volumes of reagents are often required in batch reactions, while efficient reagent usage in flow promotes waste minimization.
- **Flexibility :** Batch conditions are suitable for small and diverse reactions where flow conditions are ideal for continuous and high-throughput synthesis.

1.2.1 Synthesis with Flow

Flow chemistry has brought transformative changes to various areas in chemistry, with one of its most significant impacts observed in medicinal chemistry. This field thrives on multidisciplinary collaborations to create new, safe, and effective drugs. Unquestionably, the disruptive expansion of flow technology favored the synthesis of complex chemicals from smaller building blocks. As a result, it is being widely used in drug discovery, synthesis of natural products, heterocyclic systems, and active pharmaceutical ingredients (API's) [69, 71, 72]. Numerous C-C and C-X bond formation reactions have benefited from the effective use of flow chemistry, leading to notable developments in scalability, process optimization and catalyst development [73-79].

Ackermann and coworkers reported Mn-catalyzed C–H arylations in continuous flow mode. In a batch comparison, the authors obtained comparable and occasionally better yields. However, because of inherent benefits of flow chemistry to operate at feverish temperature and quick screening of reaction conditions, the initial optimizations were carried out in flow conditions [80].

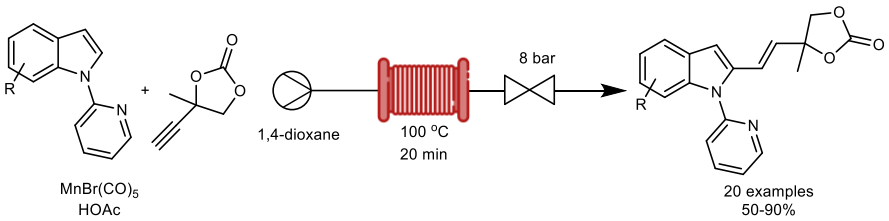

Scheme 1.4 Flow-based C–H alkynylation reaction.

The Lay group recently developed a new strategy for synthesizing homoallylic alcohols using flow chemical conditions (**Scheme 1.5**). A set of fifteen derivatives were successfully produced, using TMS-diazomethane, E-vinyl boronic acids, and aldehydes in good yields. Following its initial success in flow conditions the method was adopted for batch processing, in order to promote its broader adoption [81].

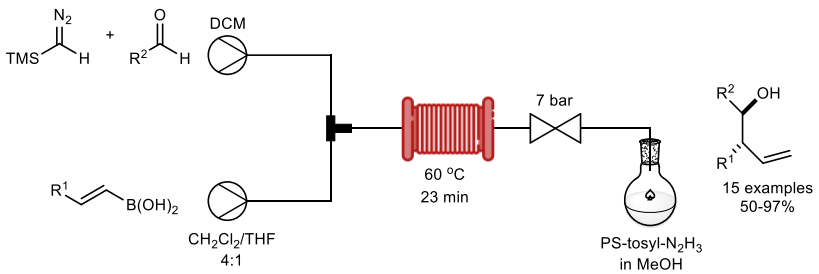

Scheme 1.5 Synthesis of homoallyl alcohols in flow chemical conditions.

Diazonium salts can be quite difficult to scale up in batch systems and present number of safety concerns because they are unstable and produce an unusual amount of nitrogen gas, during synthetic procedures. Novartis has developed a scalable, multistep continuous-flow process for the synthesis of 2H-indoles. This method enables the safe handling of precarious diazonium salts and azides in large scales as 200g (**Scheme 1.6**). [82]

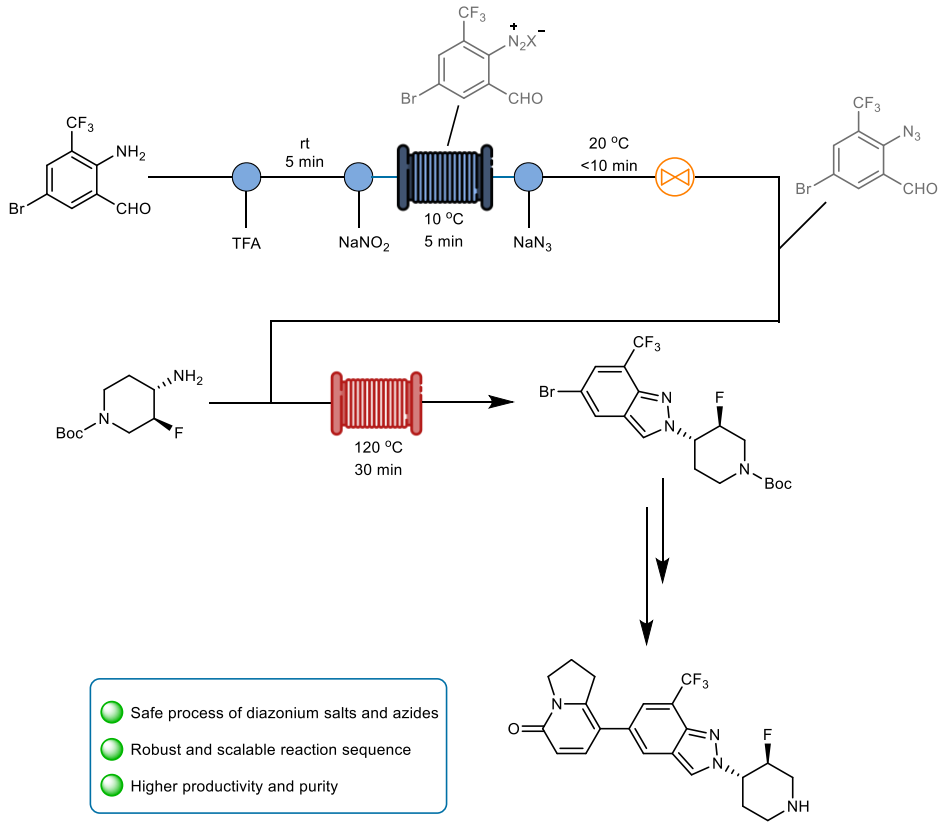

Scheme 1.6 Multistep Continuous flow synthesis of indazoles.

Around 80-90% hydrazine is used in the production of organic derivatives, including pharmaceuticals and pesticides, while the rest of the portion is employed as a reducing agent in various applications [83, 84]. Cantillo and colleagues demonstrated the use of hydrazine to reduce aromatic nitro compounds. They used in situ generated iron oxide nanocrystals as catalyst. Initially they optimized the conversion of nitrobenzene to aniline in batch microwave conditions in 2 minutes at 150 ℃. While under flow conditions, reaction was completed at the same temperature cutting the reaction time by 20% (**Scheme 1.7**). Following the flow-chemical conditions, they developed a library of 20 aniline derivatives [85]. As an extension, this process was used to reduce a range of aliphatic nitro compounds and azides [86].

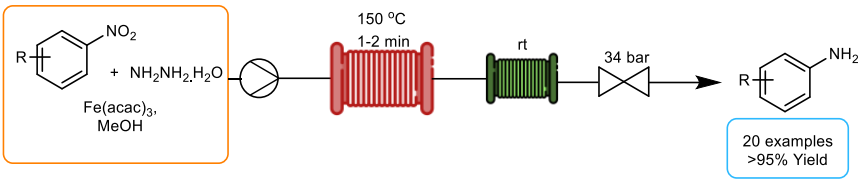

Scheme 1.7 Flow supported reduction of Nitro compounds.

1.2.2 Synergizing Technologies: Integrating Photo and flow chemistry

Photochemical reactions pose special challenges, particularly due to intrinsic complexity and scalability issues often associated with the attenuation of photon transfer. Scaling up in batch reactors make these issues even more complex. Nonhomogeneous irradiation can lead to the production of byproducts and can complicate the purification process. This challenge is specially faced in photochemical rearrangements like Wolff, Favorskii, Beckmann, Fries, and Claisen reactions, where conditions are uncontrollable due to extended photolysis reaction times and decreased light penetrations.

The compatibility of flow technology with photochemical transformations was quickly demonstrated when continuous processing was introduced in organic chemistry. The small-scale dimensions of flow chemical reactors were very advantageous for the reactions, which typically rely on the traceless reagents like photons. Moreover, precise control over key reaction parameters like reaction time and temperature, amplifies the efficiency and reach of these reactions. Therefore, the integration of flow techniques with photochemistry has played a significant role in recent resurgence of sustainable modern technologies, and to overcome the long-standing issues in photochemical rearrangements by providing uniform irradiation to the reaction mixtures [87-90]. Furthermore, reduced reaction times and lower photocatalyst loadings compared to batch operations can significantly boost the productivity of photochemical rearrangements in flow and of photochemical reactions in general [91].

Baumann and colleagues recently reported a novel photo-flow cascade reaction, utilizing alkyne bearing chalcones to produce a transitory carbene (**Scheme 1.8**). This reactive intermediate was captured by a neighboring aryl ring system, resulting in isolable cycloheptatrienes and ultimately complex cyclobutene through a series of pericyclic reactions [92].

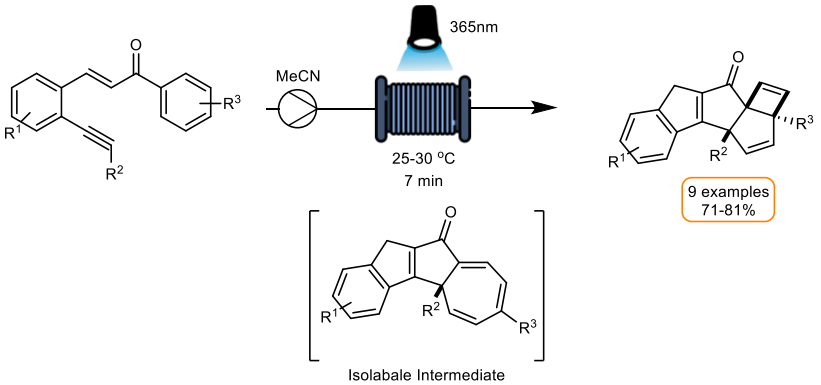

Scheme 1.8 Photo-flow Cascade reaction for complex cyclobutene synthesis.

Short residence times and uniformed irradiations with a 365nm LED enabled the isolation of late-stage intermediates, supporting the possible mechanistic approach. Additionally, continuous flow process explored the expansion of substrate scope, by uncovering the highly regioselective route to synthesize multi substituted polycyclic products. Thus, this approach demonstrates the usefulness of combination photo-flow technologies for reaction discovery [35].

Karl Fries demonstrated the Fries rearrangement in 1908, a rearrangement of an aryl ester to a hydroxy aryl ketone, promoted by a Lewis acid catalyst [93, 94]. Recently, Wu and Co-workers reported another method for this rearrangement in photo-flow conditions [95]. They used a practical and green approach under aqueous micellar conditions by employing a number of aryl-benzoates (**Scheme 1.9**). A LED of 245nm was used in an FEP made photo-flow reactor, while CTAB (cetyltrimethylammonium bromide) was used as a surfactant. They successfully devised a library of 11 compounds in satisfactory yields.

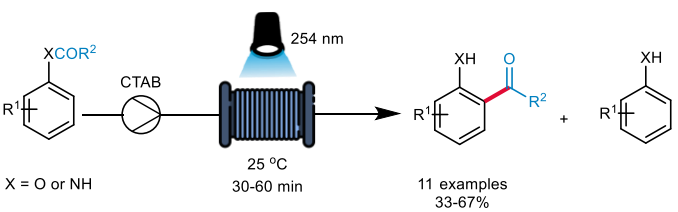

Scheme 1.9 Photo-Fries Rearrangement under Flow conditions.

This widespread use of photo and flow chemistry in organic synthesis led us to use these techniques for our researches. I used flow chemistry and a combination of both photo and flow chemistry in my PhD research, which will be discussed further in **Chapter 2.**

1.3 Microwaves: A Green Energy Source

The serendipitous discovery that microwaves can be used for cooking happened in 1949 when a Raytheon engineer *Percy Spencer* observed a melted candy in his pocket while working on radar equipment in the lab, opened new doors of advancements in domestic cooking styles. In mid-1980's chemists began using these domestic microwaves for synthesis purposes. In late 20th century microwave irradiations become a widely recognized chemical techniques in synthesis, better recognized for its capability to enhance reaction efficiency, accelerations and reducing its environmental impacts [96]. Microwave reactions are predominantly more favored in organic chemistry, as they have ability to directly couple with the molecules, while bypassing the legacy thermal conductivity mechanisms and promoting rapid temperature elevations [97].

Microwaves are such types of electromagnetic radiations, which lies between radio waves and infrared radiation on electromagnetic spectrum, with wavelengths ranging from *1m* to *1mm* and frequencies between *300 MHz* to *300 GHz*, making them ideal for energy transfers over short distances. They are a combination of electric (E) and magnetic (B) fields, with a travel speed of light (c).

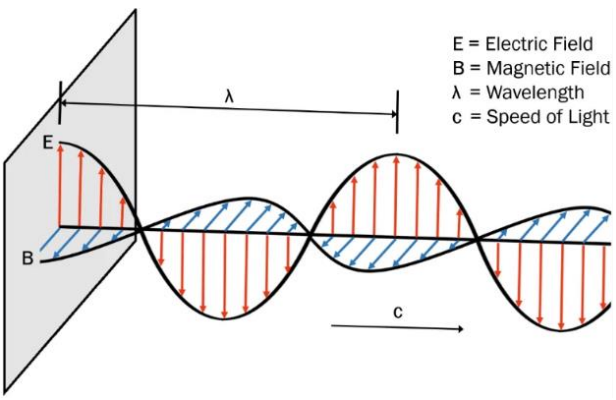

Figure 1.7 Microwave's component representation. [98]

1.3.1 The Principle of Microwave Heating

Since electromagnetic waves are comprised of both electric and magnetic fields, the primary responsibility of heat generation lies on electric (E) field. The electric field applies a force on the charged particles causing them to rotate or migrate. Rotation of the charged bodies is regarded as "*dipolar rotation*" in which a molecule persistently rotates back and forth in an effort to align its dipole with ever fluctuating electric field. This rapid rotation causes continuous friction, resulting in heat generation. While migration is associated as "*ionic conduction*", where a

charged species moves translationally along the space, causing friction same as in dipolar rotation and generating heat. This coordination of both electric and magnetic components of microwaves results in rapid warming [99].

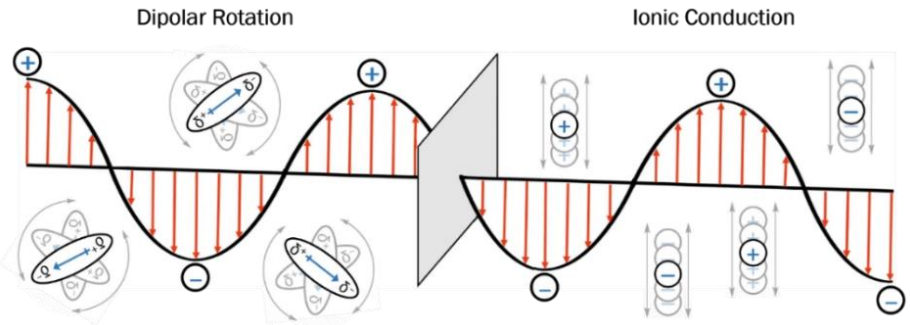

Figure 1.8 Microwave heating mechanism. [98]

A material's dielectric properties determine how it will behave when exposed to microwave irradiations. Thus, the ability of any substance to convert electromagnetic energy into heat at a particular frequency and temperature, is determined by *loss angle* or *loss factor* (*tan δ*).

$$tan\,\delta = \frac{e''}{e'}$$

Where:

e'': dielectric loss (indicative of the conversion efficiency of electromagnetic radiation into heat)
e' : dielectric constant

On the basis of loss tangent or loss factor (*tan δ*) we can idealize the absorption efficiency of the reaction. Generally, if the value of loss factor is higher than the dielectric heating of the material will also be higher. Absorbance of solvents in microwave reactors can be adjusted according to the value of *tan δ*.
If

tan $\delta > 0.5$: high absorbance
tan $\delta = 0.1$- 0.5 : medium absorbance
tan $\delta < 0.1$: low absorbance

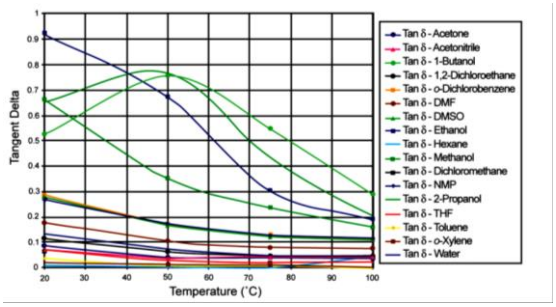

Figure 1.9 Different solvent's loss tangent vs temperature. [98]

Thus, temperature will increase in proportion to how high the absorbance is in **Figure 1.9.** We can observe that higher values of loss tangents lead to rapid achievement of temperatures. But it is also important to mention that heating hot solvents is much more difficult than heating cold solvents, because most of the solvents experience a decrease in loss tangent with the rise in temperature.

1.3.2 Conduction vs Microwave heating (MH)

Conventional synthesis typically relies on conduction, an oil bath or a heating mantle is used for heating the reaction mixture. But the pitfall is homogenous heating, where the outer side of vessel gets heated earlier, and the inner temperature remains significantly low. This drawback results in causing wall effect, temperature gradient inside the vessel and poor control over reaction conditions. However, this issue can be resolved by stirring, but it can take a long time to reach thermal equilibrium.

In microwave reaction conditions the wall effect is almost negligible, as the vessels are generally transparent to microwaves and they couple directly with the reaction molecules. This direct interaction leads to a rapid increase in temperature and localized superheating in the system, promoting dipolar rotation or ionic conduction [100, 101]. A general representation of heat transfer via conventional method vs microwave irradiation can be understood by **Figure 1.10**.

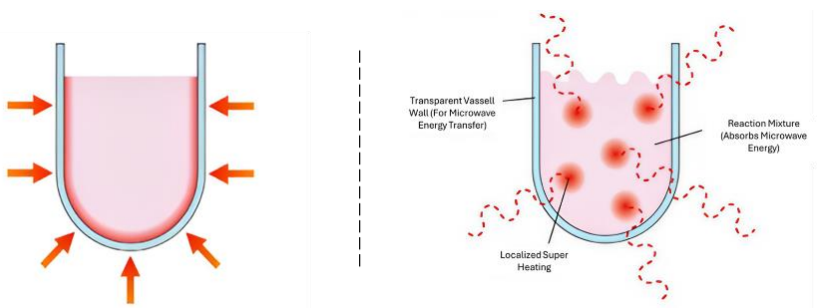

Figure 1.10 Conventional heating vs microwave irradiation [98]

In comparison to conventional heating, MH offers numerous benefits [102-105] like:

- Reduced reaction times and rapid heat transfer
- Dielectric heating, volumetric and selective (for molecules with dipole)
- Energy efficient and cost effective
- Prevention of overheating
- Good yields and clean products
- Reduced side products & degradation due to fast reaction times

1.3.3 Microwave Irradiation in Organic Synthesis

Number of researches encounter the use of MW-assisted organic synthesis, including multicomponent reactions, cross-coupling reactions, C-H activations, insertion reactions, peptide synthesis and many more. Applications in metal-organic-frameworks (MOFs), nanomaterials and MW-assisted continuous flow chemistry are among some of the most recent advancements, drawing interest.

The very first organic reaction under microwave irradiation was reported back in 1986, by *Richerd Gedye* and colleagues [97], where they studied the hydrolysis of benzamide to benzoic acid and obtaining an enhancement of reactivity since the reaction time decreased from one hour to 10 minutes and the yield improved from 90% to 99% (**Scheme 1.10**).

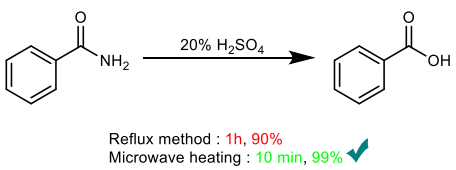

Scheme 1.10 The very first microwave-based organic reaction.

Following this great modern shift in organic synthesis, multiple studies involving Claisen rearrangement, Diels-Alder reaction and ene reaction were published in the same year [106].

Microwave-Assisted Synthesis of *N*-Heterocycles

Efficient synthesis of *N*-heterocycles is a key area in organic synthesis. Since the majority of nitrogen containing heterocyclic compounds show biological functions and are therefore highly desirable in drug development, therapeutics and diagnostics [107-110]. It is increasingly clear from an economic and environmental standpoint that classical synthetic techniques are unsustainable and

require an upgrade. In this regard use of MW conditions in multicomponent reactions is particularly attractive [111].

Imidazole and pyrazoles serve as essential building blocks of various pharmaceutical and agrochemical products. **Scheme *1.11*** represents the synthesis of 2,4,5-trisubstituesd imidazoles under MW conditions.

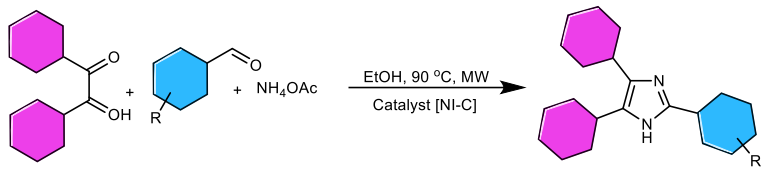

Scheme 1.11 MW-assisted 2,4,5-trisubstituted imidazoles synthesis.

Another nitrogen containing biologically important heterocycle pyrrole, was synthesized under microwave heating by Tu and colleagues (**Scheme 1.12**), which enables the C-4 substituted pyrroles formation [112]. The reaction generally proceeds by the interaction of β-enaminones and arylglyoxal monohydrates with indoles or benzenethiols, leading cyclodehydration to final product, in the presence of acetic acid.

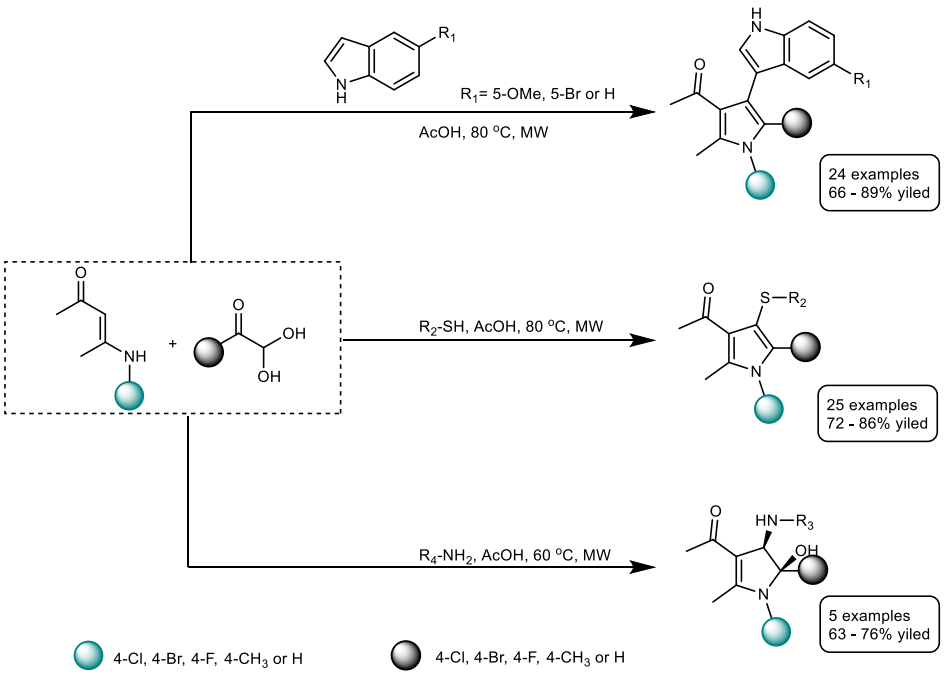

Scheme 1.12 MW assisted three component Domino reaction for pyrrole synthesis.

Cross coupling reactions

In organic synthesis, the quick formation of carbon-carbon (C-C) and carbon-heteroatom (C-X) bonds is quite crucial [113]. The quest to hunt for alternatives to conventional, frequently inefficient, and energy-intensive protocols has been fueled by the desire for more sustainable and efficient coupling techniques. Many of the coupling reactions often require prolonged heating, while MW controlled synthesis provides key benefits like fast and safe heating beyond boiling temperatures in sealed vessels, shortening the reaction times and rising the yields. Efficiency of microwaves in accelerating these coupling reactions has been well documented [114-116].

Pioneering coupling reactions like *Suzuki* coupling reactions, *Heck* reaction and *Sonogashira* coupling reaction are broadly studied under microwave conditions with and without metal catalysts [117-120].

In a recent study, Abrarbi and colleagues demonstrated the use of Suzuki–Miyaura coupling reaction under microwave conditions for arylation and heteroarylation of 4-(trifluoromethyl)pyrimido[1,2-b]indazol-2(1H)-one using aryl or heteroaryl boronic acids. The reaction was carried out in EtOH/H_2O (4:1) solvent system at 135 °C. The intended coupling products were obtained in 45 minutes of reaction time, with yields as high as 89% [121] (**Scheme 1.13**).

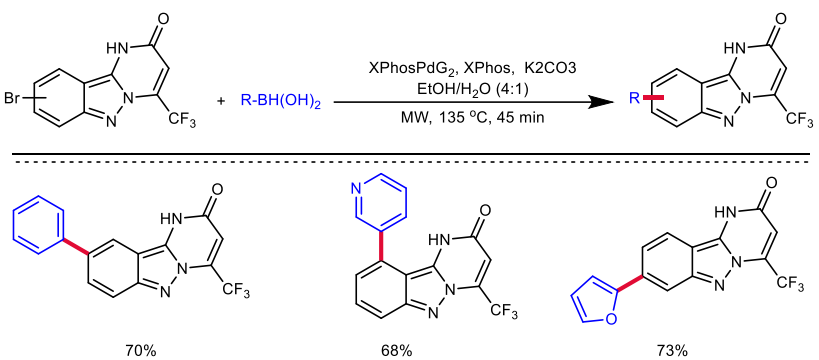

Scheme 1.13 Microwave-assisted Suzuki–Miyaura coupling reaction.

Erik's group has documented a successful domino Heck/borylation of acrylamides to yield indolinone-3-methyl boronic esters under microwave conditions. Where C-C and C-B bonds were produced in a single step using a $Pd(PPh_3)_4$ /Na_2CO_3 catalytic system in ACN/water at 120 °C for 40 min (**Scheme 1.14**) [122].

This method demonstrates exceptional selectivity for domino reaction against well-known hurdles like alkene's hydroarylation and direct Miyaura borylation.

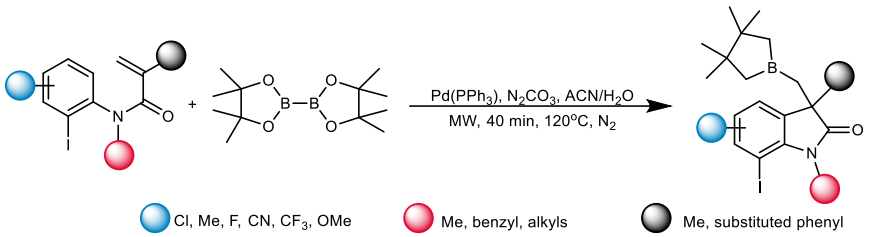

Scheme 1.14 MW-assisted domino Heck/borylation to yield C-C and C-B bonds.

In summary it is evident that by offering a technique for rapid and efficient reaction heating, microwave conditions have drastically changed the classical practices of synthetic chemistry. I used this opportunity and utilized MW conditions broadly during my PhD research for the synthesis of Pyridazines and Isoxazoles.

1.4 One-pot Reactions

Multistep reactions which requires the isolation of each intermediate, and a consequence higher production of waste and energy consumption, can be altered with very efficient one-pot synthesis which is a method of increasing reaction's efficiency, reducing waste and extra purifications.

One-pot synthesis is an active field from the past few decades, it is such a type of synthetic strategy where multiple transformations take place sequentially in a single reaction vessel, without isolating and purifying the intermediates. [123]

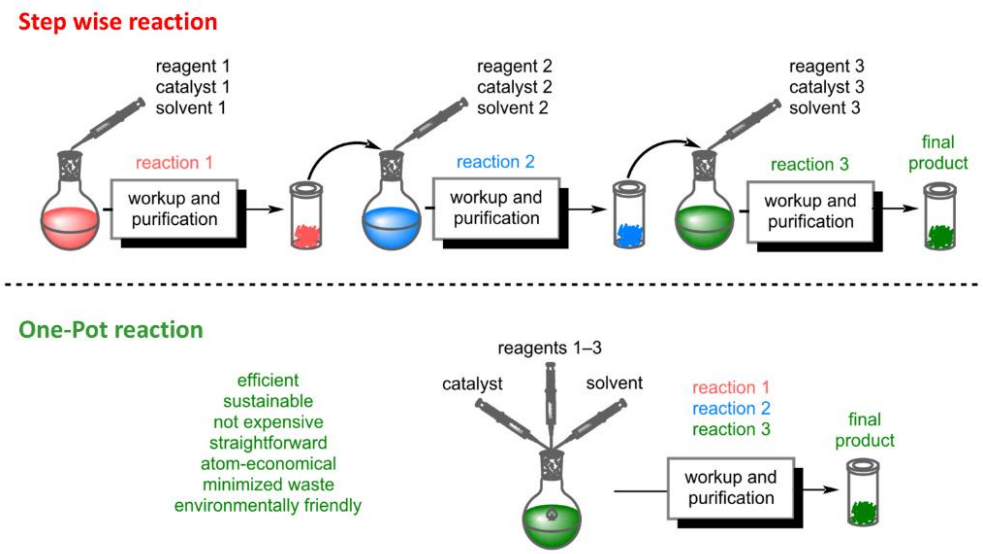

Figure 1.11 Representation of classical synthesis vs One-pot reaction. [124]

These reactions are very advantageous across various aspects of synthetic chemistry. Some of the key advantages are explored here:

Enhanced efficiency

- Reduces the number of reactions steps, eliminates the need of purification and handling intermediates.
- Streamlines the processes, leading to rapid reaction completion.

Cost and waste efficiency

- Reduces the amount of energy, solvents and reagents required to form intermediate processing.
- Less chemical waste is produced which aligns with the principles of green chemistry.

Better atom economy

- Enhances overall yield and efficiency by promoting the consumption of all starting materials in product formation phase.
- Minimizes material loss associated with intermediate isolation.

Improved selectivity

- Provides precise control over reaction conditions, improving stereoselectivity and regioselectivity.
- Undesired products and side reaction are decreased due to sequential transformations in same vessel.

Compatibility with flow-chemistry

- Ideally matched for integration with flow chemistry, which provides safe, scalable and controlled reaction conditions.
- Enables real-time optimizations of multistep reactions.

Access to chemically complex molecules

- Enables the construction of complex molecular architectures via cascade and tandem reactions.
- Provides novel approaches to explore new chemical spaces in drug discovery.

Reproducibility and scalability

- Improves uniformity by lowering batch variability.
- Simplifies the processes, easier to be scaled up at industrial level.

Overall, one-pot processes act as a cornerstone for modern synthetic chemistry by enabling more innovative, sustainable, and cost-effective, approaches to molecule construction.

The cycloaddition reactions are more powerful than cyclization reactions, when there is a need of increasing molecular diversity and complexity [125]. Integration of cycloaddition reaction in one-pot reactions can be more difficult than cyclization due to stereochemical restrictions, particularly while performing consecutive cycloadditions [126].

Recently, Zhang and group reported a two-step process via [3+2] cycloaddition and nucleophilic annulation, for the modular synthesis of dihydrobenzoxazines (A), tetrahydrobenzoxazepines (B), and tetrahydrobenzoxazocines (C) (**Scheme 1.15)** [127]. In situ produced, azomethine ylides from amino esters and benzaldehydes undergoes 1,3-dipolar cycloaddition with maleimides to yield [3 + 2] adducts, which serves as a common intermediate three different nucleophilic annulation reaction to form 6-, 7-, and 8-membered ring-fused tetracyclic compounds, respectively

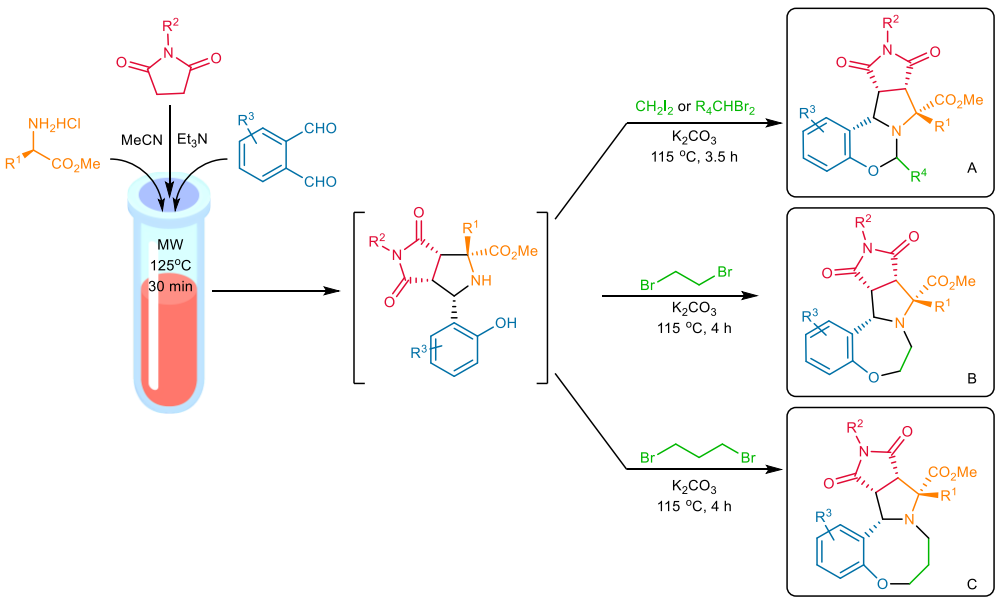

Scheme 1.15 A modular synthesis of three distinct ring scaffolds in two steps.

K_2CO_3 was used to support the nucleophilic [4 + n] annulation under conventional heating at 125°C for 3.5–4 hours. On the other hand, triethylamine (Et_3N) was used as a base for the first step cycloaddition under microwave heating at 125°C for 30 minutes.

In summary, One-pot ractions are an effective and flexible tool in contemporary syntheic chemistry that allow the efficient construction of complex molcules by a series of transformations in one go. These approaches meet with the tenets of green chemistry and have the potential to significantly advance the synthesis in pharmaceutical and material research fields.

All the aforementioned technologies including photochemistry, flow chemistry, microwave reactions and one-pot processess are revolutioning the green and sustainable organic synthesis by deeply intergrating with the core principles of green chemistry. These technologies help to mitigate the environmental challenges as well as enhancing the reaction effeciencies, paving the way for sustainable and innovative solutitions in modern synthetic chemistry. Their continued advancements offer an intriguing avenue for further research developments.

1.4.1 References

[1] P. T. Anastas and J. C. Warner, *Green Chemistry: Theory and Practice* (Theory and Practice). Oxford, 2000; online edn, Oxford Academic, 2000/5/25.

[2] J. Song and B. Han, "Green chemistry: a tool for the sustainable development of the chemical industry," *National Science Review,* vol. 2, no. 3, 2015/09/01, doi: 10.1093/nsr/nwu076.

[3] P. T. Anastas and J. B. Zimmerman, "The United Nations sustainability goals: How can sustainable chemistry contribute?," *Current Opinion in Green and Sustainable Chemistry,* vol. 13, 2018/10/01, doi: 10.1016/j.cogsc.2018.04.017.

[4] T.-L. Chen, H. Kim, S.-Y. Pan, P.-C. Tseng, Y.-P. Lin, and P.-C. Chiang, "Implementation of green chemistry principles in circular economy system towards sustainable development goals: Challenges and perspectives," *Science of The Total Environment,* vol. 716, 2020/05/10, doi: 10.1016/j.scitotenv.2020.136998.

[5] Q. Liu, B.-B. Zhang, H. Sheng, S. Qiao, Z.-X. Wang, and X.-Y. Chen, "Visible-Light-Induced Photoreduction of Carborane Phosphonium Salts: Efficient Synthesis of Carborane-Oxindole-Pharmaceutical Hybrids," *Angewandte Chemie International Edition,* vol. 62, no. 31, 2023/08/01, doi: 10.1002/anie.202305088.

[6] J. Yu and X. Jiang, "Synthesis and perspective of organosulfur chemicals in agrochemicals," *Advanced Agrochem,* vol. 2, no. 1, 2023/03/01, doi: 10.1016/j.aac.2022.12.003.

[7] M. G. Martina, L. Giannessi, and M. Radi, "Multicomponent Synthesis of Purines and Pyrimidines: From the Origin of Life to New Sustainable Approaches for Drug-Discovery Applications," *European Journal of Organic Chemistry,* vol. 26, no. 2, 2023/01/10, doi: 10.1002/ejoc.202201288.

[8] B. Trost, "The Atom Economy—A Search for Synthetic Efficiency," *Science,* vol. 254, no. 5037, 1991-12-6, doi: 10.1126/science.1962206.

[9] R. A. Sheldon and R. A. Sheldon, "Green chemistry and resource efficiency: towards a green economy," *Green Chemistry,* vol. 18, no. 11, 2016/05/31, doi: 10.1039/C6GC90040B.

[10] Fatemeh Asilpour, Dariush Saberi, Alireza Hasaninejad, Fatemeh Asilpour, Dariush Saberi, and Alireza Hasaninejad, "Synthesis of novel chromeno[1,6]naphthyridine derivatives in PEG-400 via catalyst-free, one-pot, and multicomponent reactions," *New Journal of Chemistry,* vol. 48, no. 1, 2023/12/18, doi: 10.1039/D3NJ03273F.

[11] H. F. Motiwala *et al.*, "HFIP in Organic Synthesis," *Chemical Reviews,* vol. 122, no. 15, July 17, 2022, doi: 10.1021/acs.chemrev.1c00749.

[12] S. H. Vahidi, H. Monhemi, M. Hojjatipour, M. Hojjatipour, M. Eftekhari, and M. Vafaeei, "Supercritical CO2/Deep Eutectic Solvent Biphasic System as a New Green and Sustainable Solvent System for Different Applications: Insights from Molecular Dynamics Simulations," *The Journal of Physical Chemistry B,* vol. 127, no. 37, September 8, 2023, doi: 10.1021/acs.jpcb.3c04292.

[13] R. S. Varma, "Clay and clay-supported reagents in organic synthesis," *Tetrahedron,* vol. 58, no. 7, 2002/02/11, doi: 10.1016/S0040-4020(01)01216-9.

[14] R. S. Varma and R. S. Varma, "Chemical activation by mechanochemical mixing, microwave and ultrasonic irradiation," *Green Chemistry,* vol. 10, no. 11, 2008/11/01, doi: 10.1039/B817559B.

[15] M. B. Gawande, S. N. Shelke, R. Zboril, and R. S. Varma, "Microwave-Assisted Chemistry: Synthetic Applications for Rapid Assembly of Nanomaterials and Organics," March 25, 2014, doi: 10.1021/ar400309.

[16] R. B. N. Baig, R. B. N. Baig, R. S. Varma, and R. S. Varma, "Alternative energy input: mechanochemical, microwave and ultrasound-assisted organic synthesis," *Chemical Society Reviews,* vol. 41, no. 4, 2012/01/30, doi: 10.1039/C1CS15204A.

[17] K. Yue *et al.*, "Trends and Opportunities in Organic Synthesis: Global State of Research Metrics and Advances in Precision, Efficiency, and Green Chemistry," *The Journal of Organic Chemistry,* vol. 88, no. 7, 2023/04/07, doi: 10.1021/acs.joc.2c03057.

[18] Luca Capaldo, Zhenghui Wen, Timothy Noël, Luca Capaldo, Zhenghui Wen, and Timothy Noël, "A field guide to flow chemistry for synthetic organic chemists," *Chemical Science,* vol. 14, no. 16, 2023/04/26, doi: 10.1039/D3SC00992K.

[19] Y. H. Budnikova *et al.*, "Electrochemistry in organics: a powerful tool for "green" synthesis," *Journal of Solid State Electrochemistry 2023 28:3,* vol. 28, no. 3, 2023/04/18, doi: 10.1007/s10008-023-05507-9.

[20] V. Polshettiwar and R. S. Varma, "Microwave-Assisted Organic Synthesis and Transformations using Benign Reaction Media," *Accounts of Chemical Research,* vol. 41, no. 5, 2008/04/18, doi: 10.1021/ar700238.

[21] R. S. Varma, "Greener and Sustainable Trends in Synthesis of Organics and Nanomaterials," *ACS Sustainable Chemistry & Engineering,* vol. 4, no. 11, 2016/08/18, doi: 10.1021/acssuschemeng.6b01623.

[22] H. D. Roth, "The Beginnings of Organic Photochemistry," *Angewandte Chemie International Edition in English,* vol. 28, no. 9, 1989/09/01, doi: 10.1002/anie.198911931.

[23] H. D. Roth, "Twentieth century developments in photochemistry. Brief historical sketches," *Pure and Applied Chemistry,* vol. 73, no. 3, 2001-01-01, doi: 10.1351/pac200173030395.

[24] G. Ciamician, "The Photochemistry of the Future," *Science,* vol. 36, no. 926, 1912-09-27, doi: 10.1126/science.36.926.385.

[25] A. Einstein, "Concerning a Heuristic Point of View Toward the Emission and Transformation of light," *Annalen der Physik,* vol. 17, pp. 132-148, 1905/01/01.

[26] G. S. Hammond and N. J. Turro, "Organic Photochemistry," *Science,* vol. 142, no. 3599, 1963-12-20, doi: 10.1126/science.142.3599.1541.

[27] M. H. Shaw, J. Twilton, and D. W. C. MacMillan, "Photoredox Catalysis in Organic Chemistry," *The Journal of Organic Chemistry,* vol. 81, no. 16, August 1, 2016, doi: 10.1021/acs.joc.6b01449.

[28] H. E. Bonfield *et al.*, "Photons as a 21st century reagent," *Nature Communications 2020 11:1,* vol. 11, no. 1, 2020/02/06, doi: 10.1038/s41467-019-13988-4.

[29] S. Protti, D. Ravelli, and M. Fagnoni, S. G. Newman, Ed. *Introduction to Photochemistry for the Synthetic Chemist*. 2023/08/31.

[30] F. Guba, Ü. Tastan, K. Gugeler, M. Buntrock, T. Rommel, and D. Ziegenbalg, "Rapid Prototyping for Photochemical Reaction Engineering," *Chemie Ingenieur Technik,* vol. 91, no. 1-2, 2019/01/01, doi: 10.1002/cite.201800035.

[31] J. Rabani, H. Mamane, D. Pousty, and J. R. Bolton, "Practical Chemical Actinometry—A Review," *Photochemistry and Photobiology,* vol. 97, no. 5, 2021/09/01, doi: 10.1111/php.13429.
[32] J. C. T. Scaiano, *Photochemistry Essentials*. American Chemical Society, 2022.
[33] "The Beer-Lambert Law," *Journal of Chemical Education,* vol. 39, no. 7, 1962, doi: 10.1021/ed039p333.
[34] A. Albini, A. Albini, M. Fagnoni, and M. Fagnoni, "Green chemistry and photochemistry were born at the same time," *Green Chemistry,* vol. 6, no. 1, 2004/01/14, doi: 10.1039/B309592D.
[35] M. D. Filippo, M. D. Filippo, M. Baumann, and M. Baumann, "Carbene-controlled regioselectivity in photochemical cascades," *Organic & Biomolecular Chemistry,* vol. 21, no. 14, 2023/04/05, doi: 10.1039/D3OB00122A.
[36] T. Schweizer, H. Kubach, T. Koch, T. Schweizer, H. Kubach, and T. Koch, "Investigations to characterize the interactions of light radiation, engine operating media and fluorescence tracers for the use of qualitative light-induced fluorescence in engine systems," *Automotive and Engine Technology 2021 6:3,* vol. 6, no. 3, 2021-10-23, doi: 10.1007/s41104-021-00092-3.
[37] D. Bléger and S. Hecht, "Visible-Light-Activated Molecular Switches," *Angewandte Chemie International Edition,* vol. 54, no. 39, 2015/09/21, doi: 10.1002/anie.201500628.
[38] C. D. and and L. Demange‡, "Cis−Trans Isomerization of Organic Molecules and Biomolecules: Implications and Applications†," *Chemical Reviews,* vol. 103, no. 7, May 30, 2003, doi: 10.1021/cr0104375.
[39] J. Li *et al.*, "Automatic discovery of photoisomerization mechanisms with nanosecond machine learning photodynamics simulations," *Chemical Science,* vol. 12, no. 14, 2021/04/15, doi: 10.1039/D0SC05610C.
[40] J. Wang *et al.*, "Photocatalytic Z/E isomerization unlocking the stereodivergent construction of axially chiral alkene frameworks," *Nature Communications 2024 15:1,* vol. 15, no. 1, 2024-04-16, doi: 10.1038/s41467-024-47404-3.
[41] C. Z. Rubel *et al.*, "Stereodivergent, Kinetically Controlled Isomerization of Terminal Alkenes via Nickel Catalysis," *Angewandte Chemie International Edition,* vol. 63, no. 21, 2024/05/21, doi: 10.1002/anie.202320081.
[42] C. N. Stindt, S. Crespi, and B. L. Feringa, "Synthesis of Styrylbenzazole Photoswitches and Evaluation of their Photochemical Properties," *Chemistry – A European Journal,* vol. 30, no. 39, 2024/07/11, doi: 10.1002/chem.202401409.
[43] J. A. Labinger, J. E. Bercaw, J. A. Labinger, and J. E. Bercaw, "Understanding and exploiting C–H bond activation," *Nature 2002 417:6888,* vol. 417, no. 6888, 2002/05, doi: 10.1038/417507a.
[44] T. Dohi, N. Takenaga, A. Goto, H. Fujioka, and Y. Kita, "Clean and Efficient Benzylic C−H Oxidation in Water Using a Hypervalent Iodine Reagent: Activation of Polymeric Iodosobenzene with KBr in the Presence of Montmorillonite-K10," *The Journal of Organic Chemistry,* vol. 73, no. 18, August 26, 2008, doi: 10.1021/jo8012435.
[45] K.-J. Liu *et al.*, "Clean Oxidation of (Hetero)benzylic Csp3–H Bonds with Molecular Oxygen," *ACS Sustainable Chemistry & Engineering,* vol. 7, no. 12, May 28, 2019, doi: 10.1021/acssuschemeng.9b00002.

[46] J. Ma *et al.*, "DDQ/tert-Butyl nitrite-catalyzed aerobic oxidation of diarylmethane sp3 C–H bonds," *Tetrahedron,* vol. 71, no. 38, 2015/09/23, doi: 10.1016/j.tet.2015.07.042.

[47] Y. Qin, L. Zhu, and S. Luo, "Organocatalysis in Inert C–H Bond Functionalization," *Chemical Reviews,* vol. 117, no. 13, February 13, 2017, doi: 10.1021/acs.chemrev.6b00657.

[48] J.-H. Mao *et al.*, "Organocatalyst-controlled site-selective arene C–H functionalization," *Nature Chemistry 2021 13:10,* vol. 13, no. 10, 2021-08-09, doi: 10.1038/s41557-021-00750-x.

[49] A. Mardani, F. Kazemi, and B. Kaboudin, "Photo-tunable oxidation of toluene and its derivatives catalyzed by TBATB," *Journal of Photochemistry and Photobiology A: Chemistry,* vol. 414, 2021/06/01, doi: 10.1016/j.jphotochem.2021.113301.

[50] N. A. Romero and D. A. Nicewicz, "Organic Photoredox Catalysis," *Chemical Reviews,* vol. 116, no. 17, June 10, 2016, doi: 10.1021/acs.chemrev.6b00057.

[51] S. Protti *et al.*, "Activation of aliphatic C–H bonds by tetracyanobenzene photosensitization. A time-resolved and steady-state investigation," *RSC Advances,* vol. 2, no. 5, 2012/02/13, doi: 10.1039/C2RA01054B.

[52] F. Juliá, "Ligand-to-Metal Charge Transfer (LMCT) Photochemistry at 3d-Metal Complexes: An Emerging Tool for Sustainable Organic Synthesis," *ChemCatChem,* vol. 14, no. 19, 2022/10/10, doi: 10.1002/cctc.202200916.

[53] N. Sinha and O. S. Wenger, "Photoactive Metal-to-Ligand Charge Transfer Excited States in 3d6 Complexes with Cr0, MnI, FeII, and CoIII," *Journal of the American Chemical Society,* vol. 145, no. 9, February 21, 2023, doi: 10.1021/jacs.2c13432.

[54] A. Marie May, J. L. Dempsey, A. Marie May, and J. L. Dempsey, "A new era of LMCT: leveraging ligand-to-metal charge transfer excited states for photochemical reactions," *Chemical Science,* vol. 15, no. 18, 2024/05/08, doi: 10.1039/D3SC05268K.

[55] I. Choi, J. Struwe, L. Ackermann, I. Choi, J. Struwe, and L. Ackermann, "C–H activation by immobilized heterogeneous photocatalysts," *Photochemical & Photobiological Sciences 2021 20:12,* vol. 20, no. 12, 2021-11-16, doi: 10.1007/s43630-021-00132-9.

[56] M. Irie and M. Irie, "Discovery and development of photochromic diarylethenes," *Pure and Applied Chemistry,* vol. 87, no. 7, 2015-07-01, doi: 10.1515/pac-2015-0208.

[57] K.-H. Grellmann, G. M. Sherman, and H. Linschitz, "Photo-Conversion of Diphenylamines to Carbazoles, and Accompanying Transient Species," May 1, 2002, doi: 10.1021/ja00895.

[58] K.-P. Zeller, K.-P. Zeller, S. Berger, and S. Berger, "Steric hindrance in substituted dibenzofurans," *Journal of the Chemical Society, Perkin Transactions 2,* no. 1, 1977/01/01, doi: 10.1039/P29770000054.

[59] A. G. Schultz and M. B. DeTar, "Thiocarbonyl ylides. Photogeneration, rearrangement, and cycloaddition reactions," *Journal of the American Chemical Society,* vol. 96, no. 1, doi: 10.1021/ja00808.

[60] J. Wegner, S. Ceylan, and A. Kirschning, "Flow Chemistry – A Key Enabling Technology for (Multistep) Organic Synthesis," *Advanced Synthesis & Catalysis,* vol. 354, no. 1, 2012/01/01, doi: 10.1002/adsc.201100584.

[61] K. F. Jensen, B. J. Reizman, S. G. Newman, K. F. Jensen, B. J. Reizman, and S. G. Newman, "Tools for chemical synthesis in microsystems," *Lab on a Chip,* vol. 14, no. 17, 2014/07/29, doi: 10.1039/C4LC00330F.

[62] M. Movsisyan *et al.*, "Taming hazardous chemistry by continuous flow technology," *Chemical Society Reviews,* vol. 45, no. 18, 2016/09/12, doi: 10.1039/C5CS00902B.

[63] D. Cantillo, D. Cantillo, C. O. Kappe, and C. O. Kappe, "Halogenation of organic compounds using continuous flow and microreactor technology," *Reaction Chemistry & Engineering,* vol. 2, no. 1, 2017/02/07, doi: 10.1039/C6RE00186F.

[64] M. B. Plutschack, B. Pieber, K. Gilmore, and P. H. Seeberger, "The Hitchhiker's Guide to Flow Chemistry‖," *Chemical Reviews,* vol. 117, no. 18, June 1, 2017, doi: 10.1021/acs.chemrev.7b00183.

[65] M. Guidi, M. Guidi, P. H. Seeberger, P. H. Seeberger, K. Gilmore, and K. Gilmore, "How to approach flow chemistry," *Chemical Society Reviews,* vol. 49, no. 24, 2020/12/14, doi: 10.1039/C9CS00832B.

[66] B. Gutmann, D. Cantillo, and C. O. Kappe, "Continuous-Flow Technology—A Tool for the Safe Manufacturing of Active Pharmaceutical Ingredients," *Angewandte Chemie International Edition,* vol. 54, no. 23, 2015/06/01, doi: 10.1002/anie.201409318.

[67] T. Tsubogo, H. Oyamada, S. Kobayashi, T. Tsubogo, H. Oyamada, and S. Kobayashi, "Multistep continuous-flow synthesis of (R)- and (S)-rolipram using heterogeneous catalysts," *Nature 2015 520:7547,* vol. 520, no. 7547, 2015-04-15, doi: 10.1038/nature14343.

[68] M. Comito *et al.*, "Towards Antibiotic Synthesis in Continuous-Flow Processes," *Molecules 2023, Vol. 28, Page 1421,* vol. 28, no. 3, 2023-02-02, doi: 10.3390/molecules28031421.

[69] A. S. Burange, S. M. Osman, and R. Luque, "Understanding flow chemistry for the production of active pharmaceutical ingredients," *iScience,* vol. 25, no. 3, 2022/03/18, doi: 10.1016/j.isci.2022.103892.

[70] M. Baumann, T. S. Moody, M. Smyth, and S. Wharry, "A Perspective on Continuous Flow Chemistry in the Pharmaceutical Industry," *Organic Process Research & Development,* vol. 24, no. 10, January 10, 2020, doi: 10.1021/acs.oprd.9b00524.

[71] A. R. Bogdan and A. W. Dombrowski, "Emerging Trends in Flow Chemistry and Applications to the Pharmaceutical Industry," *Journal of Medicinal Chemistry,* vol. 62, no. 14, February 22, 2019, doi: 10.1021/acs.jmedchem.8b01760.

[72] Y. Chen and J.-C. M. Monbaliu, "Continuous-Flow Multistep Synthesis of Active Pharmaceutical Ingredients," doi: 10.1002/9783527824595.ch7.

[73] Z. Zhang, A. Ohno, H. Takaya, and Y. M. A. Yamada, "Continuous-Flow Suzuki-Miyaura Coupling in Water and Organic Solvents Promoted by Blends of Stabilized Convoluted Polymeric Palladium Catalysts and Polymeric Auxiliary Materials," *Chemistry – A European Journal,* vol. 29, no. 34, 2023/06/19, doi: 10.1002/chem.202300494.

[74] C. Len *et al.*, "Palladium-Catalyzed Suzuki–Miyaura Cross-Coupling in Continuous Flow," *Catalysts 2017, Vol. 7, Page 146,* vol. 7, no. 5, 2017-05-09, doi: 10.3390/catal7050146.

[75] T. Hattori *et al.*, "Palladium on Carbon-Catalyzed Suzuki-Miyaura Coupling Reaction Using an Efficient and Continuous Flow System," *Catalysts 2015, Vol. 5, Pages 18-25,* vol. 5, no. 1, 2015-01-12, doi: 10.3390/catal5010018.

[76] N. Alonso, L. Z. Miller, J. d. M. Muñoz, J. Alcázar, and D. T. McQuade, "Continuous Synthesis of Organozinc Halides Coupled to Negishi Reactions," *Advanced Synthesis & Catalysis,* vol. 356, no. 18, 2014/12/15, doi: 10.1002/adsc.201400243.

[77] A. Herath, V. Molteni, S. Pan, and J. Loren, "Generation and Cross-Coupling of Organozinc Reagents in Flow," *Organic Letters,* vol. 20, no. 23, November 14, 2018, doi: 10.1021/acs.orglett.8b03156.

[78] N. Nikbin, M. Ladlow, and S. V. Ley, "Continuous Flow Ligand-Free Heck Reactions Using Monolithic Pd(0) Nanoparticles.," *ChemInform,* vol. 38, no. 40, 2007/10/02, doi: 10.1002/chin.200740062.

[79] P. Yaseneva *et al.*, "Continuous flow Buchwald–Hartwig amination of a pharmaceutical intermediate," *Reaction Chemistry & Engineering,* vol. 1, no. 2, 2016/03/30, doi: 10.1039/C5RE00048C.

[80] H. Wang, F. Pesciaioli, J. C. A. Oliveira, S. Warratz, and L. Ackermann, "Synergistic Manganese(I) C−H Activation Catalysis in Continuous Flow: Chemoselective Hydroarylation," *Angewandte Chemie International Edition,* vol. 56, no. 47, 2017/11/20, doi: 10.1002/anie.201708271.

[81] J.-S. Poh *et al.*, "A multicomponent approach for the preparation of homoallylic alcohols," *Chemical Science,* vol. 7, no. 11, 2016/10/18, doi: 10.1039/C6SC02581A.

[82] H. Lehmann, T. Ruppen, and T. Knoepfel, "Scale-Up of Diazonium Salts and Azides in a Three-Step Continuous Flow Sequence," *Organic Process Research & Development,* vol. 26, no. 4, March 22, 2022, doi: 10.1021/acs.oprd.2c00016.

[83] J.-P. Schirmann and P. Bourdauducq, "Hydrazine," *Ullmann's Encyclopedia of Industrial Chemistry,* 2001, doi: 10.1002/14356007.a13_177.

[84] "Hydrazine as a Reducing Agent for Organic Compounds (Catalytic Hydrazine Reductions)," *Chemical Reviews,* vol. 65, no. 1, 1965, doi: 10.1021/cr60233a002.

[85] D. Cantillo, M. Baghbanzadeh, and C. O. Kappe, "In Situ Generated Iron Oxide Nanocrystals as Efficient and Selective Catalysts for the Reduction of Nitroarenes using a Continuous Flow Method," *Angewandte Chemie International Edition,* vol. 51, no. 40, 2012/10/01, doi: 10.1002/anie.201205792.

[86] D. Cantillo, M. M. Moghaddam, and C. O. Kappe, "Hydrazine-mediated Reduction of Nitro and Azide Functionalities Catalyzed by Highly Active and Reusable Magnetic Iron Oxide Nanocrystals," April 15, 2013, doi: 10.1021/jo400556.

[87] F. Raymenants, T. M. Masson, J. Sanjosé-Orduna, and T. Noël, "Efficient C(sp3)−H Carbonylation of Light and Heavy Hydrocarbons with Carbon Monoxide via Hydrogen Atom Transfer Photocatalysis in Flow**," *Angewandte Chemie International Edition,* vol. 62, no. 36, 2023/09/04, doi: 10.1002/anie.202308563.

[88] F. Bonassi, D. Ravelli, S. Protti, and M. Fagnoni, "Decatungstate Photocatalyzed Acylations and Alkylations in Flow via Hydrogen Atom Transfer," *Advanced Synthesis & Catalysis,* vol. 357, no. 16-17, 2015/11/16, doi: 10.1002/adsc.201500483.

[89] C. Yang *et al.*, "Heterogeneous photoredox flow chemistry for the scalable organosynthesis of fine chemicals," *Nature Communications 2020 11:1,* vol. 11, no. 1, 2020-03-06, doi: 10.1038/s41467-020-14983-w.

[90] K. Donnelly, M. Baumann, K. Donnelly, and M. Baumann, "Scalability of photochemical reactions in continuous flow mode," *Journal of Flow Chemistry 2021 11:3,* vol. 11, no. 3, 2021-05-17, doi: 10.1007/s41981-021-00168-z.

[91] L. Buglioni, F. Raymenants, A. Slattery, S. D. A. Zondag, and T. Noël, "Technological Innovations in Photochemistry for Organic Synthesis: Flow Chemistry, High-Throughput Experimentation, Scale-up, and Photoelectrochemistry," *Chemical Reviews,* vol. 122, no. 2, August 10, 2021, doi: 10.1021/acs.chemrev.1c00332.

[92] M. D. Filippo *et al.*, "Discovery of a photochemical cascade process by flow-based interception of isomerising alkenes," *Chemical Science,* vol. 12, no. 29, 2021/07/28, doi: 10.1039/D1SC02879K.

[93] K. Fries and G. Finck, "Über Homologe des Cumaranons und ihre Abkömmlinge," *Berichte der deutschen chemischen Gesellschaft,* vol. 41, no. 3, 1908/10/01, doi: 10.1002/cber.190804103146.

[94] H. Bestian, "Karl Fries. 1875–1962," *Chemische Berichte,* vol. 117, no. 11, 1984/11/01, doi: 10.1002/cber.19841171102.

[95] C.-C. Chien *et al.*, "Photo-Fries rearrangement in flow under aqueous micellar conditions," *Chemical Communications,* vol. 56, no. 98, 2020/12/17, doi: 10.1039/D0CC07331H.

[96] H. M. T. Albuquerque, D. C. G. A. Pinto, A. M. S. Silva, H. M. T. Albuquerque, D. C. G. A. Pinto, and A. M. S. Silva, "Microwave Irradiation: Alternative Heating Process for the Synthesis of Biologically Applicable Chromones, Quinolones, and Their Precursors," *Molecules 2021, Vol. 26, Page 6293,* vol. 26, no. 20, 2021-10-18, doi: 10.3390/molecules26206293.

[97] R. Gedye *et al.*, "The use of microwave ovens for rapid organic synthesis," *Tetrahedron Letters,* vol. 27, no. 3, 1986/01/01, doi: 10.1016/S0040-4039(00)83996-9.

[98] https://cem.com/de/microwave-heating-mechanism-and-theory (accessed.

[99] S. A. Galema and S. A. Galema, "Microwave chemistry," *Chemical Society Reviews,* vol. 26, no. 3, 1997/01/01, doi: 10.1039/CS9972600233.

[100] O. Algul *et al.*, "Comparative Studies on Conventional and Microwave Synthesis of Some Benzimidazole, Benzothiazole and Indole Derivatives and Testing on Inhibition of Hyaluronidase," *Molecules 2008, Vol. 13, Pages 736-748,* vol. 13, no. 4, 2008-03-27, doi: 10.3390/molecules13040736.

[101] P. Lidstrom, J. Westman, and A. Lewis, "Enhancement of Combinatorial Chemistry by Microwave-Assisted Organic Synthesis," *Combinatorial Chemistry & High Throughput Screening,* vol. 5, no. 6, 2002, doi: 10.2174/1386207023330147.

[102] N. Kuhnert, "Microwave-Assisted Reactions in Organic Synthesis—Are There Any Nonthermal Microwave Effects?," *Angewandte Chemie International Edition,* vol. 41, no. 11, 2002/06/03, doi: 10.1002/1521-3773(20020603)41:11<1863::AID-ANIE1863>3.0.CO;2-L.

[103] F. Langa *et al.*, "Microwave irradiation: more than just a method for accelerating reactions," *Contemporary Organic Synthesis,* vol. 4, no. 5, 1997/01/01, doi: 10.1039/CO9970400373.

[104] M. Nüchter, U. Müller, B. Ondruschka, A. Tied, and W. Lautenschläger, "Microwave-Assisted Chemical Reactions," *Chemical Engineering & Technology,* vol. 26, no. 12, 2003/12/10, doi: 10.1002/ceat.200301836.

[105] N. E. Leadbeater and N. E. Leadbeater, "In situ reaction monitoring of microwave-mediated reactions using IR spectroscopy," *Chemical Communications,* vol. 46, no. 36, 2010/08/31, doi: 10.1039/C0CC01921F.

[106] R. J. Giguere, T. L. Bray, S. M. Duncan, and G. Majetich, "Application of commercial microwave ovens to organic synthesis.," *Tetrahedron Letters,* vol. 27, no. 41, 1986/01/01, doi: 10.1016/S0040-4039(00)85103-5.

[107] A. P. Taylor *et al.*, "Modern advances in heterocyclic chemistry in drug discovery," *Organic & Biomolecular Chemistry,* vol. 14, no. 28, 2016/07/12, doi: 10.1039/C6OB00936K.

[108] C. Cabrele and O. Reiser, "The Modern Face of Synthetic Heterocyclic Chemistry," *The Journal of Organic Chemistry,* vol. 81, no. 21, October 10, 2016, doi: 10.1021/acs.joc.6b02034.

[109] S. Ghosh and K. Biswas, "Microwave-assisted synthesis of indolizine derivatives: Recent developments: A review (2003-present)," *Synthetic Communications,* vol. 54, no. 7, 2024-4-2, doi: 10.1080/00397911.2023.2297064.

[110] A. Majumder, R. Gupta, and A. Jain, "Microwave-assisted synthesis of nitrogen-containing heterocycles," *Green Chemistry Letters and Reviews,* vol. 6, no. 2, 2013-6-1, doi: 10.1080/17518253.2012.733032.

[111] A. Kruithof, E. Ruijter, and R. V. A. Orru, "Microwave-Assisted Multicomponent Synthesis of Heterocycles," *Current Organic Chemistry,* vol. 15, no. 2, 2011, doi: 10.2174/138527211793979817.

[112] J.-Y. Liu *et al.*, "Three-component domino reactions providing rapid and efficient routes to fully substituted pyrroles," *RSC Advances,* vol. 3, no. 15, 2013/03/18, doi: 10.1039/C3RA40252E.

[113] K. S. M. Salih, "Modern Development in Copper- and Nickel-Catalyzed Cross-Coupling Reactions: Formation of Carbon-Carbon and Carbon-Heteroatom bonds under Microwave Irradiation Conditions," *Asian Journal of Organic Chemistry,* vol. 11, no. 4, 2022/04/01, doi: 10.1002/ajoc.202200023.

[114] V. P. Mehta, E. V. V. d. Eycken, V. P. Mehta, and E. V. V. d. Eycken, "Microwave-assisted C–C bond forming cross-coupling reactions: an overview," *Chemical Society Reviews,* vol. 40, no. 10, 2011/09/20, doi: 10.1039/C1CS15094D.

[115] V. P. Mehta, V. P. Mehta, B. Punji, and B. Punji, "Recent advances in transition-metal-free direct C–C and C–heteroatom bond forming reactions," *RSC Advances,* vol. 3, no. 30, 2013/07/10, doi: 10.1039/C3RA40813B.

[116] M. Rahman, S. Ghosh, D. Bhattacherjee, G. V. Zyryanov, A. K. Bagdi, and A. Hajra, "Recent Advances in Microwave-assisted Cross-Coupling Reactions," *Asian Journal of Organic Chemistry,* vol. 11, no. 8, 2022/08/01, doi: 10.1002/ajoc.202200179.

[117] L. Y. and and J. Liebscher*, "Carbon−Carbon Coupling Reactions Catalyzed by Heterogeneous Palladium Catalysts," *Chemical Reviews,* vol. 107, no. 1, December 21, 2006, doi: 10.1021/cr0505674.

[118] K. Ramesh and G. Satyanarayana, "Microwave-assisted intramolecular reductive Heck in aqueous medium: Synthesis of 3,3'-Disubstituted heterocyclic

compounds," *Journal of Organometallic Chemistry,* vol. 902, 2019/12/01, doi: 10.1016/j.jorganchem.2019.120963.

[119] F. Arcudi *et al.*, "Efficient Synthesis and Microwave-Assisted Sonogashira Reactions of Triflate-Substituted Porphyrin," *European Journal of Organic Chemistry,* vol. 26, no. 43, 2023/11/14, doi: 10.1002/ejoc.202300772.

[120] W. Chang, J. Shin, G. Chae, S. R. Jang, and B. J. Ahn, "Microwave-assisted Sonogashira cross-coupling reaction catalyzed by Pd-MCM-41 under solvent-free conditions," *Journal of Industrial and Engineering Chemistry,* vol. 19, no. 3, 2013/05/25, doi: 10.1016/j.jiec.2012.11.002.

[121] B. Jismy, G. Guillaumet, M. Akssira, A. Tikad, and M. Abarbri, "Efficient microwave-assisted Suzuki–Miyaura cross-coupling reaction of 3-bromo pyrazolo[1,5-a]pyrimidin-5(4H)-one: towards a new access to 3,5-diarylated 7-(trifluoromethyl)pyrazolo[1,5-a]pyrimidine derivatives," *RSC Advances,* vol. 11, no. 3, 2021/01/04, doi: 10.1039/D0RA07959F.

[122] D. D. Vachhani *et al.*, "Domino Heck/borylation sequence towards indolinone-3-methyl boronic esters: trapping of the σ-alkylpalladium intermediate with boron," *Chemical Communications,* vol. 51, no. 80, 2015/09/24, doi: 10.1039/C5CC05193B.

[123] Yujiro Hayashi and Yujiro Hayashi, "Pot economy and one-pot synthesis," *Chemical Science,* vol. 7, no. 2, 2016/01/26, doi: 10.1039/C5SC02913A.

[124] S. B. Tsogoeva and S. B. Tsogoeva, "Catalytic multi-step domino and one-pot reactions," *Beilstein Journal of Organic Chemistry,* vol. 20, no. 1, 2024-02-08, doi: 10.3762/bjoc.20.25.

[125] B. Gabriele, R. Mancuso, L. Veltri, I. Ziccarelli, and N. D. Ca', "Palladium-Catalyzed Double Cyclization Processes Leading to Polycyclic Heterocycles: Recent Advances," *European Journal of Organic Chemistry,* vol. 2019, no. 31-32, 2019/09/01, doi: 10.1002/ejoc.201900481.

[126] J. E. Sears and D. L. Boger, "Tandem Intramolecular Diels–Alder/1,3-Dipolar Cycloaddition Cascade of 1,3,4-Oxadiazoles: Initial Scope and Applications," *Accounts of Chemical Research,* vol. 49, no. 2, January 27, 2016, doi: 10.1021/acs.accounts.5b00510.

[127] A. Muthengi *et al.*, "Sequential (3 + 2) cycloaddition and (5 + n) annulation for modular synthesis of dihydrobenzoxazines, tetrahydrobenzoxazepines and tetrahydrobenzoxazocines," *Green Chemistry,* vol. 20, no. 13, 2018/07/02, doi: 10.1039/C8GC01099D.

Chapter 2

2. Functionalized Nitroolefins: As precursors of novel C–C and C–X bond formations.

2.1 Nitro Compounds

Nitro compound's exceptional synthetic significance has guaranteed a long-term research application in organic synthesis. Nitro compounds, particularly aromatic ones have historically been crucial for azo dye and explosive precursors. Naturally, the significance of nitro compounds as azo dye and explosive materials remains unchanged, but additionally they have demonstrated an immense value as a synthetic reagent for various complex molecular targets. Potent electron withdrawing ability and presence of an acidic α-H make these nitro compounds highly desirable in variety of reactions like *Henry reaction* and *Michael additions* [1], moreover their versatility makes them a good choice for nucleophilic and electrophilic reactions [2].

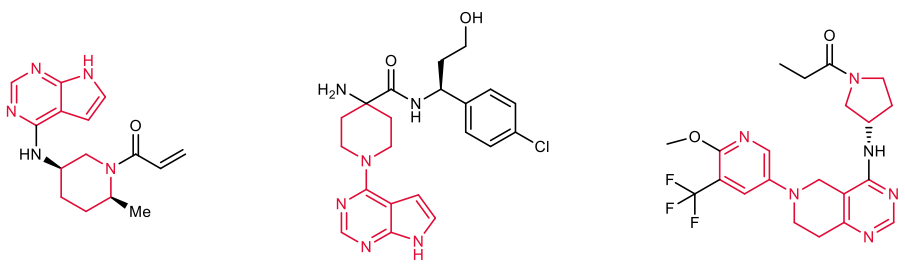

Figure 2.1 Nitrogen-containing drugs approved by the US FDA in 2023. [3]

These compounds have shown extensive applications as chemical feedstocks for the production of dyes, drugs, fertilizers, plastics, energy materials, explosives and anticancer medicines [4-8]. Their versatility in synthetic chemistry is primarily attributed due to their ready availability and ability to convert into a diverse range of functional groups. In a recent list of FDA approved drugs 75% of them contain

nitrogen moieties, which highlights their importance as a key component in medicinal chemistry [9].

Conventional synthetic methods to obtain N-heterocycles rely on anilines, as anilines serve as a vital building block for C-N bond formation [10, 11]. While anilines are commonly obtained from hydrogenation, electron transfer, hydride transfer and electrochemical reduction of nitroarenes [12-14]. Recent advancements in synthesis of nitro compounds have critically focused on enhancing efficiency, selectivity and environmental sustainability. Radical nitration with tert-butyl nitrite has emerged as a green and efficient approach for a wide range of substrates like alkenes, alkynes and aromatics [15]. In this context, present day research is focused on developing controllable and stereo-chemically selective methods for nitro compounds, aligned with the green chemistry basics.

2.1.1 Aliphatic Nitro compounds

The remarkable synthetic efficiency of aliphatic nitro compounds represent a significant class of molecules in modern organic chemistry, due to their extensive and enduring synthetic utility in various synthetic processes. Their ability to act as nucleophile as well as electrophile makes them a crucial part of C-C single and C=C double bonds formations [16].

2.1.1.1. Nitroalkanes

Nitroalkanes typically yield 'Nitronate anions' upon various basic actions, which leads to C-C bond formation by functioning as carbon nucleophile and react with common electrophiles like aldehydes in nitroaldol or Henry reaction and electronically poor alkenes in Micheal addition reactions [17-19]. Although there are numerous ways to obtain nitroalkanes, the most prominent and widely used one is to employ metal nitrite (silver, potassium or silver nitrate) to convert alkyl halides (R-X) into nitroalkanes (R-NO_2) [20, 21]. Many advancements have been reported regarding the use of efficient green solvents instead of the conventional one, like Ballini and colleagues reported the use of aqueous media and PEG 400 as solvent for nitration of alkyl halides [21-24].

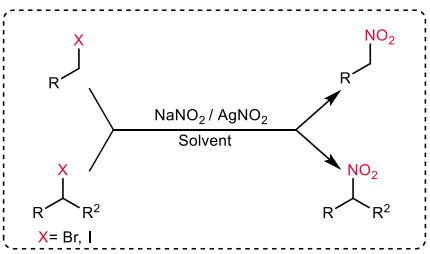

Scheme 2.1 Nitroalkanes from alkyl halides.

Since classically nitroalkane's preparation is bound to alkyl halides, the same group explored an interesting and direct synthesis of nitroalkanes from readily available compounds like alcohols. The nitration process completes in almost 3 hours at room temperature, starting form mesylates or tosylates in the presence of tetrabutylammonium nitrite (Bu_4NNO_2), using toluene as a solvent [25].

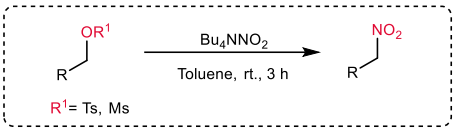

Scheme 2.2 Nitroalkanes from tosylates or mesylates.

2.1.1.2. Nitroalkenes

Conversely, Nitroolefins are extremely useful electron poor alkenes that are most likely to function as nucleophilic acceptors, primarily in Diels-Alder cycloaddition reactions and Micheal addition reactions [26, 27]. There are many direct nitration reactions of alkenes to afford nitroalkenes including Nitro-decarboxylation of aromatic *a,β*-unsaturated carboxylic acids, ipso-nitration of vinylboronic acids, direct nitration of olefinic C-H bonds, and many more. But the most common and classical method for the synthesis of nitroolefins is a two-step Henry reaction–condensation sequence [28-32]. The first step is C-C bond formation which is normally supported by mild basic conditions, whereas dehydration demands harsh reaction conditions, which significantly impact the overall yield of reaction. In recent past, many advancements have been made to improve the synthetic conditions of this widely used method [33].

In 2011, Pujol and colleagues came up with a novel approach to synthesize nitroolefins in microwave conditions using ammonium acetate as a catalyst (**Scheme 2.3**)[34]. This synthetic approach offers significant benefits like, reduced reactions times and eliminated the formation of side products such as dimers of nitro-compounds or nitrostyrenes.

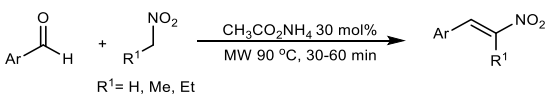

Scheme 2.3 Microwave assisted condensation of aldehydes with nitroalkanes.

In another development, Maiti and colleagues revealed the use of silver nitrite ($AgNO_2$) in combination with 2,2,6,6-tetramethylpiperidine-1-oxyl (TEMPO), to obtain a highly regio- and stereoselective and efficient nitration of olefins (**Scheme 2.4**) [35]. This innovative approach offers a very safe and practical

method to obtain nitroolefins. It not only demonstrates a wide functional group tolerance but also promotes the direct nitration of a diverse range of aliphatic, aromatic, and heteroaromatic olefins. Importantly, this method is quite efficient for gram-scale production of *β*-nitrostyrene.

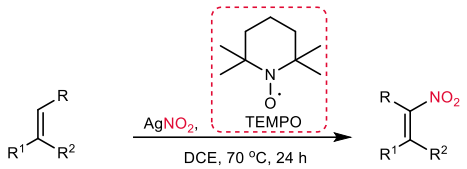

Scheme 2.4 Nitration of olefins with $AgNO_2$ & TEMPO.

Later year the same team reported another study of olefinic nitration, using a cheap alternative (ferric nitrate) to silver nitrite ($AgNO_2$). This protocol predominantly supports *E*-selectivity in contrast to the silver nitrite, and also accommodates the chloromethyl groups which were a limitation of priorly used nitrating reagent ($AgNO_2$) [36].

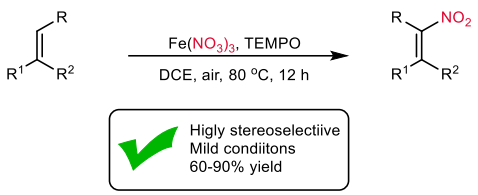

Scheme 2.5 Nitration of olefins with $Fe(NO_3)_3$ & TEMPO

Very recently Katayev and colleagues utilized the blue LED's to bring a stable transfer of nitronium radical to alkenes, from a succinimide derived NO_2-transfer reagent [37]. This procedure enables unique and selective access to functionalized isoxazole motifs and valuable nitrohydrin building blocks, by employing a single reagent in a single step initiated by the reactivity of *N*-nitrosuccinimide and commercially available $[Ru(bpy)_3](PF_6)_2$ under 350W blue light irradiations for six hours to afford this nitration technique (**Scheme 2.6**).

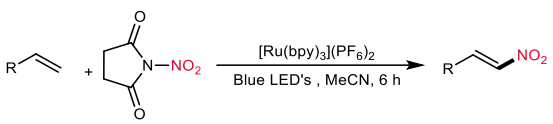

Scheme 2.6 Visible-light-mediated nitration of alkenes.

Among various synthetic methods, the use of solid supported reagents have been widely explored [38]. The solid reagents like Amberlyst A21 and *N*,*N*-

diethylpropylamine supported on amorphous silica were widely studied by the Ballini group in Henry or Nitroaldol reactions [39-41].

Scheme 2.7 Examples of nitroaldol reaction promoted by supported bases.

Although this nitroaldol reaction is not a direct path to nitroolefins, the subsequent dehydration of the *β*-nitroalcohols can be employed further to afford nitroalkenes by using different reagents like basic alumina [42], trifluoracetic anhydride with triethylamine[43] etc. (**Scheme 2.8**)

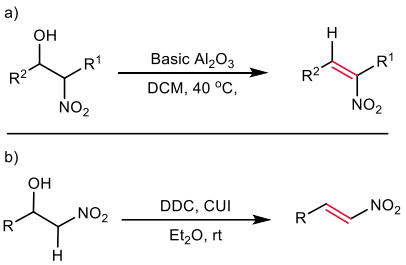

Scheme 2.8 Dehydration of *β*-nitroalcohols.

Wide range of applications of nitroolefins often bound to their reactivity which have been extensively demonstrated in the literature, where nitroalkenes are regarded as an acyl methyl cation equivalent and the nitro group is equivalent to an acyl anion [44, 45]. The unbeatable ability of nitro group to activate electrophiles and stabilize nucleophiles by coordination with Lewis and Bronsted acids, combined with the capability of nitroalkenes to undergo activation by Lewis bases, have established nitroalkenes as preferred substrates in asymmetric reactions.

Versatile ability of nitro group in various functional group transformations has broadened its utility in synthetic organic chemistry, particularly that of nitroalkenes based transformations [46-49]. Some of the notable transformations include conversion to carbonyl compounds via the Nef reaction, reduction to oximes, hydroxylamines, and amines, dehydration to form nitriles, and generation of reactive 1,3-dipoles such as nitrile oxides, nitrones, and silyl nitronates, supported by a variety of reagents.

2.1.1.3. *β*–Nitroenones & *β*–Nitroacrylates

The *β*-nitroenones and *β*-nitroacrylates (**Figure 2.2**) belong to a distinct subclass of nitroolefins. As such they have the ability to participate in the characteristic

reactions typical of nitroolefins. The presence of the carbonyl group provides an additional opportunity for further functionalization.

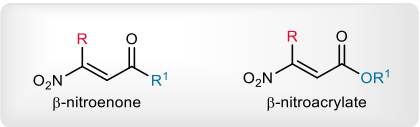

Figure 2.2 General structure of *β*-nitroenones and acrylates

In the past few years our research group utilized the conjugated nitro-olefinic systems like unsaturated *β*-nitroketones and esters to synthesize numerous functionalized heterocycles in efficient ways including indoles, pyrroles, quinolones, etc. (**Scheme 2.9**). Specifically, the *β*-nitro esters/acrylates are a highly reactive class of doubly activated olefins having two electron-withdrawing groups in both *α*- and *β*-positions.

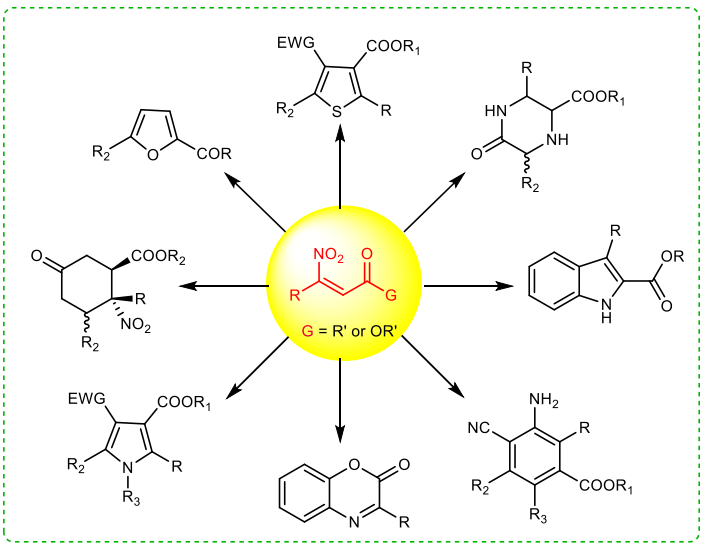

Scheme 2.9 Application of *β*-nitroenones and *β*-nitroacrylates to synthesize heterocyclic systems.. [50-59]

Among many synthetic methods, the most practical one to afford these conjugated nitroolefinic derivatives proceed in three simple steps, starting from the commercially available nitroalkanes and alkyl or aryl glyoxal or glyoxylate (**Scheme 2.10**). In the very 1st step (**step-I**), the starting materials (nitroalkanes & glyoxal) undergo a Henry reaction to yield nitro-alcohol in the presence of a basic polymeric resin Amberlyst® A21, at room temperature.

In secondary step (**step-II**) nitro-alcohol is treated with acetic anhydride (Ac_2O) in solvent free conditions, supported by an acidic resin (Amberlyst®15) to promote protonation. Which resultantly provides an acetylated product. In the last step (**step-III**), this acetylated product undergoes elimination in presence of a base like potassium carbonate (K_2CO_3) to yield the respective *β*-nitroenones or *β*-nitroacrylate.

However, we can bypass the second step by directly converting the nitro-alcohol into the eliminated product using triethylamine (Et_3N) and methanesulfonyl chloride (CH_3SO_2Cl) in dichloromethane at -10 ºC.

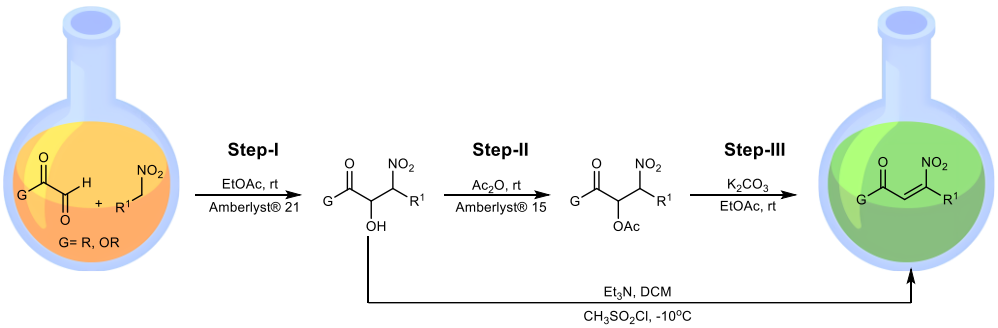

Scheme 2.10 Preparation of conjugated nitroolefins.

Deconjugation of *β*-nitroenones

Reactivity of *β*-nitroenones is widely explored in literature, but isomerization of these compound to convert into *β*-nitro-*β*,γ-unsaturated ketones (**Figure 2.3 b**) is not much focused. The shifting of double bond from *α*-*β* to *β*-*γ* can provide us with an additional reactivity of these nitroenones and can pave a way further for diverse utilities in heterocycles synthesis.

Figure 2.3 Deconjugation of *β*-nitroenones.

Recently our research group developed an efficient isomerization technique to afford these compounds. The starting molecules (*β*-nitroenones) were prepared by the method discussed in **Scheme 2.10**. These *β*-nitro-*α*, *β*-unsaturated ketones were irradiated under microwave conditions at 120 ºC, using ethanol as solvent to yield *β*-nitro-*β*,*γ*-unsaturated ketones [60] (**Scheme 2.11a)**.

In another isomerization method, we can use butanol and heat at reflux for 5-8 hours to obtain the desired *β*-nitro-*β*,*γ*-unsaturated ketones (**Scheme 2.11b)**.

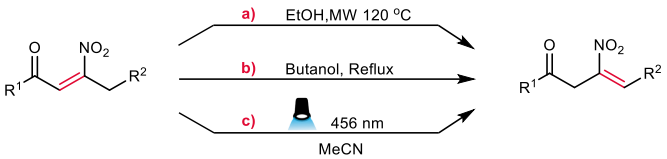

Scheme 2.11 Isomerization of *β*-Nitroenones into *β*-Nitro-*β*,*γ*-Unsaturated Ketones.

Very recently, our group in collaboration with Prof. Protti at University of Pavia developed another sustainable isomerization technique. They utilized the unprecedented photo- reactivity of *(E)*-*β*-nitroenones to afford *β*-nitro-*β*,*γ*-unsaturated ketones under mild conditions [61] (**Scheme 2.11c)**.

In summary, the versatile reactivity, intriguing chemistry, and wide range-utility of these β-nitroolefins serves as a cornerstone for understanding the challenges and opportunities in their further reactivity. The subsequent chapters will delve into the specific research endeavors undertaken to explore the fascinating chemistry of these compounds in novel C-C and C-X bond formations, during my doctoral research. Where I aimed to contribute to the growing body knowledge of these nitroolefinic compounds, by addressing gaps and advancing their applications in green and sustainable organic chemistry.

2.2 Visible-Light-Driven Photocatalyst-Free Preparation of (*Z*) β-Nitroacrylate Isomers

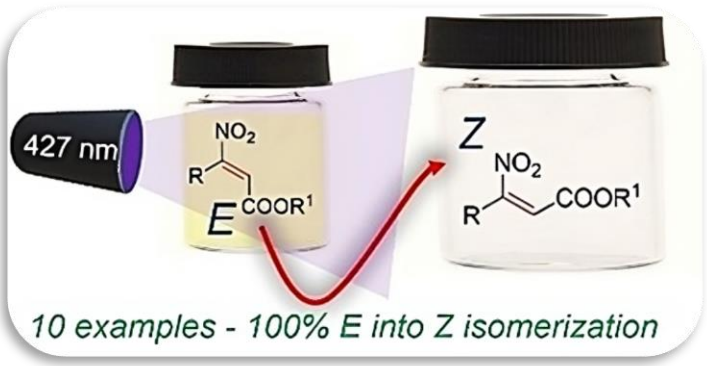

This chapter is based on the results obtained from:

Khan, M. E. I., Di Terlizzi, L., Protti, S., & Palmieri, A. (2022). Visible-Light-Driven Photocatalyst-Free Preparation of (*Z*) β-Nitroacrylate Isomers. *European Journal of Organic Chemistry*, *2022*(26), e202200635.

2.2.1 Introduction

Over the past decade, *β*-nitroacrylates **1** have gained attention as excellent building blocks for synthesizing highly functionalized materials and heterocycles [45, 62, 63]. Furthermore, owing to their enhanced reactivity compared to general nitroolefins, reactions involving this class of compounds are frequently performed under solvent-free and/or promoter free conditions [64], aligning with the core principles of green chemistry [65-67].

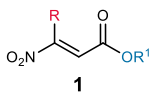

1

Figure 2.4 General structure of *β*-nitroacrylates **1**.

Regardless of their demonstrated versatility, the major synthetic routes for preparing *β*-nitroacrylates are primarily restricted to the *E*-stereoisomer [68]. While this limitation is inconsequential for many other reactions where these compounds are used, such as Michael additions. Conversely, it poses a significant challenge in processes where the stereochemistry of the starting materials directly influences the products configuration, including cycloaddition reactions [69]. Consequently, the development of innovative methodologies to enable access to (*Z*) geometry is highly desirable and would greatly expand the scope of applications for β-nitroacrylates for further reactivity.

The *E*/*Z* isomerizations under photochemical conditions are regarded as ideal approaches, as they leverage reactive excited states to facilitate stereochemical changes under mild conditions [70, 71]. These strategies have been effectively employed in diverse fields like molecular switches and rotors, energy storage systems, and in photomedicines [72-76]. Beside the classical example of provitamin D, applications of photoisomerization can be found in various recent synthetic contexts, including the preparation of coumarins, [77] (*Z*)-β-ionyl derivatives,[78] and as a method to control racemization [79].

In the past, studies regarding the photochemical behavior of *β*-nitrocarbonyl compounds received very little attention. A noteworthy contribution regarding the large-scale *E*/*Z* isomerization of *a*-(hetero)aryl-nitro-*a*,*β*-enals in polar solvents was reported by Alonso and colleagues. Nonetheless, an equilibrium combination of the two isomers was regularly produced by this method [80]. To study the further photochemical behavior of these *β*-nitroolefinic compounds, Prof. Palmieri's research group recently conducted a thorough analysis of the photo reactivity of (*E*)-*β*-nitroacrylates under both UV and visible light

irradiation, revealing two competing pathways: *E*/*Z* isomerization and deconjugation to *β*-nitro-*β*,*γ*-enones [61].

Building on all these findings and inspired by cited previous research works, I directed my efforts toward developing a photochemical approach for synthesizing (*Z*)-*β*-nitroacrylates under mild conditions.

2.2.2 Results and discussion

Initially we conducted the experiments on ethyl (*E*) 3-nitropent-2-enoate **1a**, using it as a standard compound. The studied substrate exhibits a main absorption band located in the UV, with a maximum located at 234 nm and an absorption tail which exceeds the UV region (>400 nm).

We thus studied the photochemical behavior of **1a** in acetonitrile (0.1 M solution) under five different wavelengths. The substrate containing solution was placed in a sealed vial at a distance of 6 cm from the light source (**Table 2.1**). Pleasantly in just two hours, the irradiation at 427 nm generated a quantitative isomerization of **1a** into **2a** (**Table 2.1, entry c**). Remarkably, the isomerization efficiency dropped as one moved into the UV region 370 and 390 nm, (**Table 2.1, entries a, b**), while the process proceeded inefficiently at higher wavelengths like 456 and 525 nm, (**Table 2.1entries d, e**).

Table 2.1 Photochemical behavior of **1** under different wavelengths.

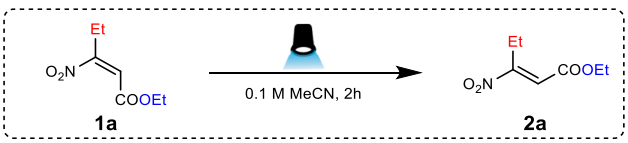

Entry	Wavelength (nm)	*E* : *Z*
a	370	15:85
b	390	07:93
c	427	0:100
d	456	72:28
e	525	96:04

This behavior has been attributed to the distinct UV absorption spectra of compounds **1a** and **2a**, particularly the blue-shifted spectrum of stereoisomer **2a**, which minimizes competitive absorption between the substrate and the desired product (**Figure 2.5**). Notably, we also observed the isomerization also under natural sunlight exposure, yielding a 12:88 ratio of the two isomers after 9 hours. Prolonged exposure did not result in further improvement.

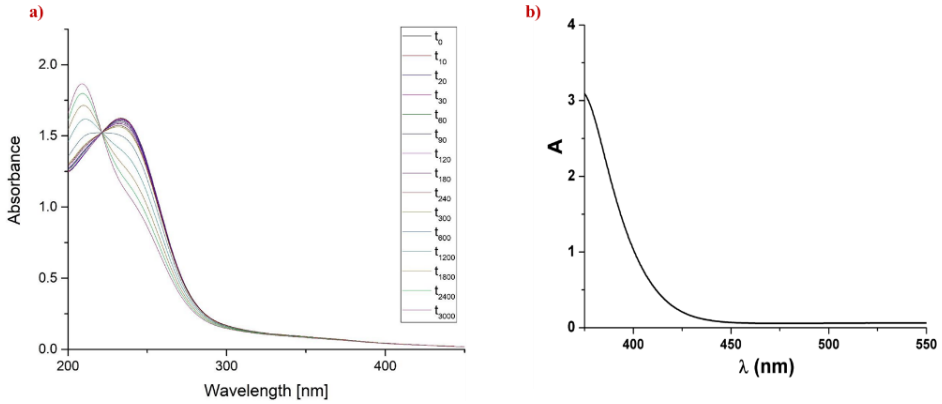

Figure 2.5 a) UV-absorption spectra of compounds **1a** and **2a** **b)** UV-Vis spectra of compound **1a** in MeCN solution 0.1 M

According to NMR investigations, under our particular experimental conditions, the isomerization of **1a** at 427 nm occurs at a constant rate of 8.1 x 10^{-4} ^{S} (**Figure 2.6**). Interestingly, after 15 hours of heating the compound at 40°C, no retro-isomerization of **2a** was seen.

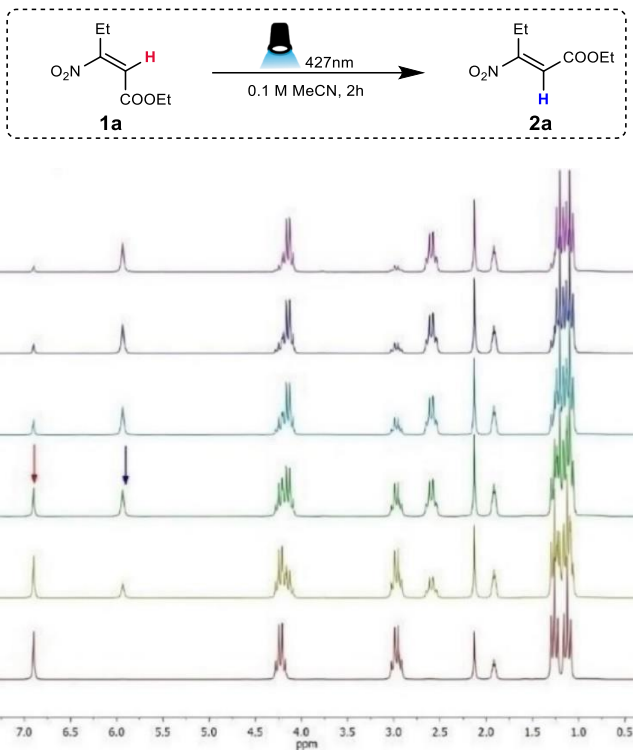

Figure 2.6 Isomerization of **1a** to **2a** followed by 1H NMR analyses (t_{irr} 0 to50 min).

With these encouraging results in hand, we expanded this technique to a range of functionalized (*E*) *β*-nitroacrylates **1** in order to show the adaptability of our methodology. Compounds **1** undergo quantitative (*Z*) isomerization to **2** under all circumstances, regardless of the existence of functionalities such halides, double bonds, aromatic systems, and ether groups. Overall, the reaction time depends on the type of substituent R. Longer isomerization durations are required for (*E*) *β*-nitroacrylates with bulky substituents.

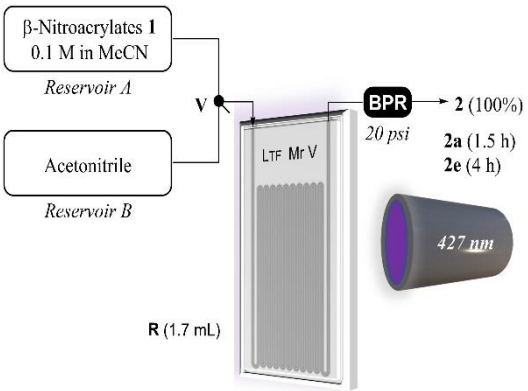

Figure 2.7 Photo-flow setup for *E*/*Z* Isomerization.

2.2.2.1. Substrate Scope

The viability of carrying out the demonstrated reaction procedure under flow chemical conditions was then investigated. In this sense, the flow apparatus consisted of (i) two syringe pumps, each of which contained the solution of (*E*) β-nitroacrylates **1** (reservoir A) and acetonitrile (reservoir B), which served as carriers to move the solution into the line; (ii) a three-way valve (V) for connecting and selecting the reservoirs to a (iii) borosilicate glass reactor type LTF-V.

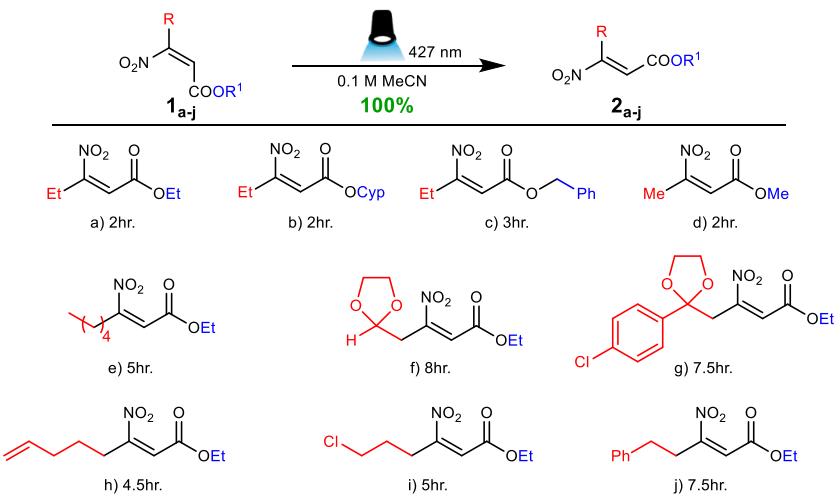

Figure 2.8 Substrate scope of β-nitroacrylate E/Z isomerization.

Thus, the flow apparatus was used to process the compounds **1a** and **1e**. The conversion to the equivalent (*Z*) isomer happened quantitatively in both situations. Notably, the reaction times dropped from two and five hours to one

and a half and four hours, respectively. Using flow microreactors instead of batch allows for more uniform and thorough irradiation, which explains the improved efficiency (reaction time < 20%) [81-83].

2.2.3 Conclusions

In a nutshell, the reported strategy offers an efficient way to convert (*E*) isomers of *β*-nitroacrylates to the hardly obtainable (*Z*)-*β*-nitroacrylates using visible light. Since, it can be carried out in both batch and flow conditions, this reaction is versatile and has quick reaction times (2–8 hours). Furthermore, there are obvious benefits from a sustainability standpoint because the reaction mixture can be evaporated to produce the desired products in high purity without the need for laborious and wasteful work-up methods.

2.2.4 Experimental section

^{1}H NMR analyses were recorded at 400 MHz on a Varian Mercury Plus 400. ^{13}C NMR analyses were recorded at 100 MHz. IR spectra were recorded with a Perkin Elmer FTIR spectrometer Spectrum Two UATR. Microanalyses were performed with a CHNS-O analyzer Model EA 1108 from Fisons Instruments. GS-MS analyses were obtained on a Hewlett-Packard GC/MS 6890 N that works with the EI technique (70 eV). Solutions in the flow apparatus were injected using syringe pumps model NE-300 (New Era Pump Systems Inc.) LTF-V microreactor (I.D. channel 1 mm; volume reactor 1.7 mL) was purchased by Little Things Factory GmbH. Photochemical irradiation was performed by using 40 W Kessil lamp (emission centred at 370 nm, 390 nm, 427, 456 nm and 525 nm).

2.2.4.1. General procedure for the preparation of compounds 2 under batch conditions.

The suitable (*E*) *β*-nitroacrylate **1 a–j** (0.25 mmol)was solubilized in acetonitrile (2.5 mL) and placed in a 2 mL vial. The solution was purged with argon and placed at a distance of 6 cm from the lamp (427 nm) and irradiated for the appropriate time (see **Figure 2.8**). After that, the pure (*Z*) *β*-nitroacrylate **2 a–j** were obtained by concentrating the solution under reduced pressure.

2.2.4.2. General procedure for the preparation of compounds 2 underflow conditions.

A 0.1 M solution of the (*E*) *β*-nitroacrylate **1a** or **1e** in acetonitrile was injected through a pump at a flow rate of 1.13 mL/h for **1a** and 0.42 mL/h for **1e**, into the three-way valve V. Then the LTF-V microreactor R irradiated with a lamp of 427 nm, placed at distance of 6 cm, while the pressure was adjusted by a BPR set at 20 psi. When the allotted volume from reservoir A was delivered, valve V was

switched from reservoir A to B, and a stream of acetonitrile was flowed through the system to push out the residual solution. The resulting outflow from reactor R was collected in a 25 mL round bottom flask and then concentrated on the solution at reduced pressure to afford the pure product **2a** or **2e**.

2.2.4.3. Characterization data

Ethyl (*Z*)-3-nitropent-2-enoate (2a) (100%, 0.25 mmol, 43 mg).

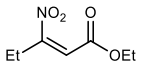

Clear oil. IR (cm-^{1} , neat): 1333, 1435, 1546, 1671, 1730. ^{1}H-NMR ($CDCl_3$, 400 MHz) δ: 5.79 (s, 1H), 4.22 (q, J = 7.2 Hz, 2H), 2.62 (dq, J = 7.4, 1.5 Hz, 2H), 1.27 (t, J = 7.1 Hz, 3H), 1.18 (t, J = 7.4 Hz, 3H). ^{13}C-NMR: ($CDCl_3$, 100 MHz) δ: 162.3, 120.6, 113.6, 61.7, 13.8, 26.3, 10.7. MS (EI, 70 eV) m/z (%): 173 (M+ , 2), 128 (100), 99 (90), 81 (30), 72 (21), 55 (39), 53 (50), 43 (49), 29 (92). Anal. Calcd. For $C_7H_{11}NO_4$ (173.17): C, 48.55; H, 6.40; N, 8.09. Found: C, 48.59; H, 6.43; N, 8.11.

Cyclopentyl (*Z*)-3-nitropent-2-enoate (2b) (100%, 0.25 mmol, 53 mg).

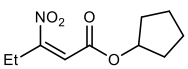

Clear oil. IR (cm^{-1} , neat): 1352, 1449, 1544, 1672, 1731. ^{1}H-NMR ($CDCl_3$, 400 MHz) δ: 5.75 (s, 1H), 5.26-5.20 (m, 1H), 2.61 (dq, J = 7.4, 1.5 Hz, 2H), 1.90-1.50 (m, 8H), 1.16 (t, J = 7.4 Hz, 3H). ^{13}C-NMR: ($CDCl_3$, 100 MHz) δ: 162.1, 160.7, 114.1, 78.9, 32.4, 26.2, 23.6, 10.6. MS (EI, 70 eV) m/z (%): 129 (30), 128 (56), 99 (76), 85 (55), 69 (82), 68 (50), 67 (96), 57 (40), 53 (39), 43 (57), 41 (100), 30 (60). Anal. Calcd. For $C_{10}H_{15}NO_4$ (213.23): C, 56.33; H, 7.09; N, 6.57. Found: C, 56.36; H, 7.13; N, 7.00.

Benzyl (*Z*)-3-nitropent-2-enoate (2c) (100%, 0.25 mmol, 58 mg).

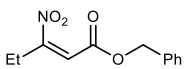

Clear oil. IR (cm^{-1} , neat): 649, 697, 724, 904, 1379, 1456, 1543, 1675, 1730. ^{1}H-NMR ($CDCl_3$, 400 MHz) δ: 7.40-7.32 (m, 5H), 5.83 (s, 1H), 5.19 (s, 2H), 2.62 (dq, J = 7.4, 1.5 Hz, 2H), 1.18 (t, J = 7.4 Hz, 3H). ^{13}C-NMR: ($CDCl_3$, 100 MHz) δ: 162.1, 161.7, 134.8, 128.7, 128.6, 128.5, 113.1, 67.5, 26.4, 10.6. MS (EI, 70 eV) m/z (%): 129 (11), 107 (32), 99 (21), 91 (100), 79 (22), 65 (19), 43 (25). Anal. Calcd. For $C_{12}H_{13}NO_4$ (235.24): C, 61.27; H, 5.57; N, 5.95. Found: C, 61.31; H, 5.60; N, 5.92.

Methyl (*Z*)-3-nitrobut-2-enoate (2d) (100%, 0.25 mmol, 36 mg).

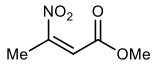

Clear oil. IR (cm^{-1} , neat): 1324, 1437, 1541, 1677, 1731. ^{1}H-NMR ($CDCl_3$, 400 MHz) δ: 5.90 (s, 1H), 3.77 (s, 3H), 2.30 (d, J = 1.4 Hz, 3H). ^{13}C-NMR: ($CDCl_3$, 100 MHz) δ: 162.8, 155.0, 115.8, 52.6, 19.1. MS (EI, 70 eV) m/z (%): 114 (45), 99 (100), 59 (57), 39 (54), 30 (44). Anal. Calcd. For $C_5H_7NO_4$ (145.11): C, 41.38; H, 4.86; N, 9.65. Found: C, 41.42; H, 4.89; N, 9.69.

Ethyl (*Z*)-3-nitrooct-2-enoate (2e) (100%, 0.25 mmol, 53 mg).

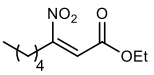

Clear oil. IR (cm^{-1} , neat): 1343, 1439, 1545, 1671, 1732. ^{1}H-NMR ($CDCl_3$, 400 MHz) δ: 5.77 (s, 1H), 4.21 (q, J = 7.1 Hz, 2H), 2.58-2.52 (m, 2H), 1.59-1.46 (m, 2H), 1.38-1.30 (m, 4H), 1.27 (t, J = 7.1 Hz, 3H), 0.89 (t, J = 7.1 Hz, 3H). ^{13}C-NMR: (CDCl3, 100 MHz) δ: 162.2, 160.2, 114.0, 61.7, 32.9, 30.6, 25.8, 22.2, 13.8. MS (EI, 70 eV) m/z (%): 170 (36), 141 (21), 95 (100), 81 (35), 37 (35), 55 (55), 41 (47), 29 (75). Anal. Calcd. For $C_{10}H_{17}NO_4$ (215.25): C, 55.80; H, 7.96; N, 6.51. Found: C, 55.77; H, 7.93; N, 6.49.

Ethyl (*Z*)-4-(1,3-dioxolan-2-yl)-3-nitrobut-2-enoate (2f) (100%, 0.25 mmol, 57 mg).

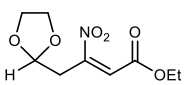

Clear oil. IR (cm^{-1} , neat): 1344, 1441, 1548, 1672, 1733. ^{1}H-NMR ($CDCl_3$, 400 MHz) δ: 6.09 (s, 1H), 5.11 (t, J = 4.1 Hz, 1H), 4.23 (q, J = 7.1 Hz, 2H), 4.00-3.86 (m, 4H), 2.94 (dd, J = 4.1, 0.9 Hz, 2H), 1.28 (t, J = 7.1 Hz, 3H). ^{13}C-NMR: ($CDCl_3$, 100 MHz) δ: 162.4, 152.6, 119.8, 100.8, 65.4, 61.9, 36.8, 13.8. MS (EI, 70 eV) m/z (%): 73 (100), 45 (21), 29 (8). Anal. Calcd. For $C_9H_{13}NO_6$ (231.20): C, 46.75; H, 5.67; N, 6.06. Found: C, 46.79; H, 5.70; N, 6.03.

Ethyl(*Z*)-4-(2-(4-chlorophenyl)-1,3-dioxolan-2-yl)-3-nitrobut-2-enoate (2g) (100%, 0.25 mmol, 85 mg).

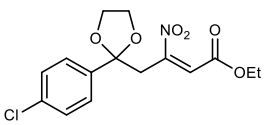

Clear oil. IR (cm^{-1} , neat): 730, 1014, 1033, 1370, 1489, 1541, 1598, 1673, 1730. ^{1}H-NMR ($CDCl_3$, 400 MHz) δ: 7.42- 7.38 (m, 2H), 7.34-7.30 (m, 2H), 5.98 (s, 1H), 4.23 (q, J = 7.2 Hz, 2H), 4.05-3.98 (m, 2H), 3.79-3.72 (m, 2H), 3.14 (s, 2H), 1.28 (t, J = 7.2 Hz, 3H). ^{13}C-NMR: ($CDCl_3$, 100 MHz) δ: 162.5, 152.4, 139.5, 134.7, 128.6, 127.0, 121.0, 107.8, 65.3, 61.9, 42.6, 13.7. MS (EI, 70 eV) m/z (%): 185 (53), 183 (100), 141 (23), 139 (74), 11 (22). Anal. Calcd. For $C_{15}H_{16}ClNO_6$ (341.74): C, 52.72; H, 4.72; N, 4.10. Found: C, 52.76; H, 4.69; N, 4.13.

Ethyl (Z)-3-nitroocta-2,7-dienoate (2h) (100%, 0.25 mmol, 53 mg).

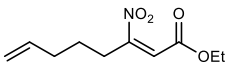

Clear oil. IR (cm^{-1} , neat): 1371, 1442, 1542, 1641, 1675, 1732, 3078. ^{1}H-NMR ($CDCl_3$, 400 MHz) δ: 5.81-5.66 (m, 1H), 5.79 (s, 1H), 5.10-4.98 (m, 2H), 4.21 (q, J = 7.1 Hz, 2H), 2.60-2.53 (m, 2H), 2.14 (q, J = 7.1 Hz, 2H), 1.70-1.59 (m, 2H), 1.27 (t, J = 7.1 Hz, 3H). ^{13}CNMR: ($CDCl_3$, 100 MHz) δ: 162.2, 159.7, 136.7, 116.2, 114.4, 61.7, 32.3, 32.1, 25.2, 13.8. MS (EI, 70 eV) m/z (%): 196 (7), 168 (7), 137 (16), 125 (36), 91 (82), 77 (53), 55 (62), 39 (68). 29 (100). Anal. Calcd. For $C_{10}H_{15}NO_4$ (213.23): C, 56.33; H, 7.09; N, 6.57. Found: C, 56.37; H, 7.12; N, 6.54.

Ethyl (*Z*)-6-chloro-3-nitrohex-2-enoate (2i) (100%, 0.25 mmol, 55 mg).

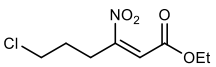

Clear oil. IR (cm^{-1} , neat): 1538, 1675, 1726. ^{1}H-NMR ($CDCl_3$, 400 MHz) δ: 5.90 (s, 1H), 4.23 (q, J = 7.1 Hz, 2H), 3.64-3.59 (m, 2H), 2.77 (td, J = 7.4, 1.1 Hz, 2H), 2.07-1.98 (m, 2H), 1.28 (t, J = 7.2 Hz, 3H). ^{13}C-NMR: ($CDCl_3$, 100 MHz) δ: 162.0, 157.7, 116.0, 61.9, 42.8, 29.9, 28.8, 13.8. MS (EI, 70 eV) m/z (%): 176 (80), 175 (78), 147 (81), 129 (22), 111 (23), 67 (75), 39 (64), 29 (100). Anal. Calcd. For $C_8H_{12}ClNO_4$ (221.64): C, 43.35; H, 5.46; N, 6.32. Found: C, 43.39; H, 5.49; N, 6.29.

Ethyl (*Z*)-3-nitro-5-phenylpent-2-enoate (2j) (100%, 0.25 mmol, 62 mg)

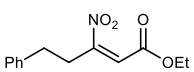

Clear oil. IR (cm^{-1} , neat): 700, 1031, 1370, 1454, 1540, 1604, 1676, 1728. ^{1}H-NMR ($CDCl_3$, 400 MHz) δ: 7.36-7.17 (m, 5H), 5.73 (s, 1H), 4.22 (q, J = 7.1 Hz, 2H), 2.87 (s, 4H), 1.27 (t, J = 7.2 Hz, 3H). ^{13}C-NMR: ($CDCl_3$, 100 MHz) δ: 162.2, 158.4, 138.5, 128.8, 128.4, 126.9, 115.4, 61.8, 34.6, 32.6, 13.8. MS (EI, 70 eV) m/z (%): 173 (7), 155 (30), 129 (16), 91 (100), 65 (11), 29 (7). Anal. Calcd. For $C_{13}H_{15}NO_4$ (249.27): C, 62.64; H, 6.07; N, 5.62. Found: C, 62.60; H, 6.04; N, 5.64.

2.3 Overcoming the Usual Reactivity of β-Nitroenones: Synthesis of Polyfunctionalized Homoallylic Alcohols and Conjugated Nitrotriene Systems

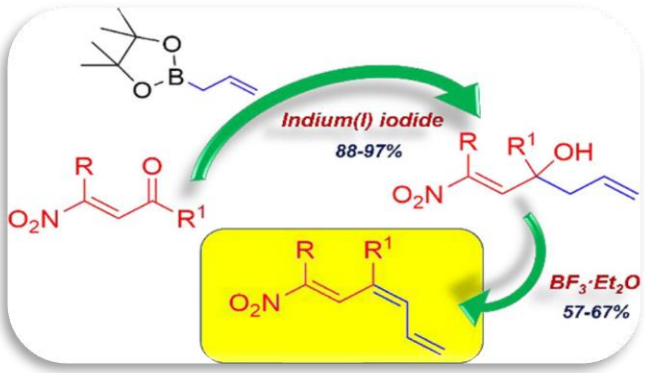

This chapter is based on the results derived from:

Yuan, L., Kachalova, L., **Khan, M. E. I.**, Ballini, R., Petrini, M., & Palmieri, A. (2023). Overcoming the Usual Reactivity of β-Nitroenones: Synthesis of Polyfunctionalized Homoallylic Alcohols and Conjugated Nitrotriene Systems. *The Journal of Organic Chemistry*, *88*(7), 4770-4777.

2.3.1 Introduction

The presence of nitro and ketone functionalities in the *a* and *β* positions to a double bond distinguishes the valuable family of nitroolefins known as *β*-nitroenones **1**. The proximity of these functionalities make them a highly reactive class of compounds, active to a wide range of nucleophiles due to juxtaposition. Specifically, reaction occur chemoselectively in β position due to the higher electron-withdrawing power of the nitro group (**Figure 2.9**). Use of these compounds in the synthesis of heterocyclic systems over time has shown their synthetic significance [51, 60, 62, 84, 85].

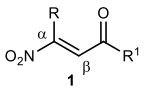

Figure 2.9 General structure of *β*-Nitroenones **1**.

As we continue to study the chemistry of *β*-nitroenones **1**, we have recently found that when exposed to metal allylating agents **2**, they exhibit an odd reactivity of **1**. Actually, metal allylating agents only react with the carbonyl group and not the nitroalkene moiety, producing the corresponding homoallylic alcohols **3** in contrast to the reactivity frequently seen with other nucleophilic species (**Scheme 2.12**).

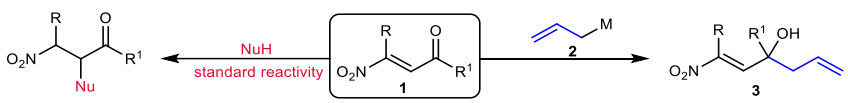

Scheme 2.12 Reactivity of *β*-Nitroenones **1**.

As essential building blocks for the synthesis of highly functionalized materials [86-90], homoallylic alcohols are also essential precursors for the common structures of numerous natural products and bioactive substances [91-93].

Keeping in view to their importance and the unique structure of compound **3**, where the homoallylic alcohol segment is linked to the nitroalkene system, prompted us to investigate and successfully accomplish its dehydration, which resultantly yields the conjugated nitrotriene systems **4** (**Scheme 2.13**).

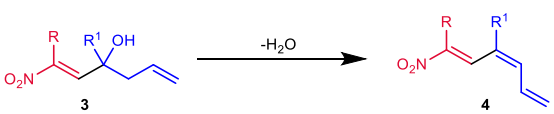

Scheme 2.13 Synthesis of Nitro-Functionalized Triene Systems.

Literature studies shows that the chemistry of conjugated nitrodienes **5** has been extensively explored [94-97], while very limited information is available regarding their homologues **4**. This is due to the challenges in synthesizing these compounds, which often demands complex starting materials and/or harsh reaction conditions [98-102]. In this context, our method stands out as the very first general and straightforward approach to access the conjugated nitrotriene systems **4**.

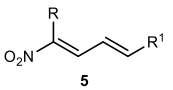

Figure 2.10 General structure of conjugated nitrodienes **5**.

2.3.2 Results and discussion

Homoallylic alcohols

We began with a focus on the optimizing studies of allylation reaction. To this end, the conversion of **1a** (*β*-nitroenone) to **3a** (homoallylic alcohol) was chosen as a representative reaction, and various allylation systems and reaction conditions were systematically evaluated.

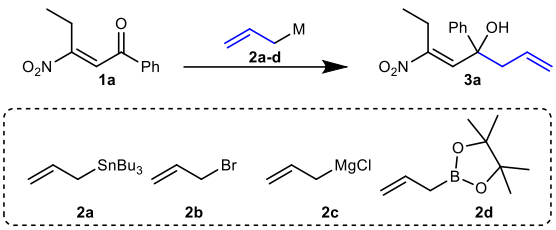

Scheme 2.14 Test Reaction: Conversion of **1a** into **3a**.

Drawing the inspiration from the work of Kalita and Phukan on allylation of chalcones [103], we initially investigated the conversion of **1a** to **3a** using allyltributylstannane (**2a**) in the presence of CuI (0.25 equiv) and DMF as the reaction medium. The reaction ended in a modest outcome, with 3a being isolated in a 56% yield. While, changing the solvent with MeCN and *γ*-valerolactone was not efficient to bring satisfactory yield improvements (**Table 2.2, entries a-c**).

Subsequently, the literature studies reveal the increasing use of indium as an efficient metal for promoting the Barbier reaction [104-106], motivated us to explore the synthesis of **3a** starting from allyl bromide (**2b**) and **1a.** Unfortunately, the results were not much different from the previous trial, as the product **3a** was obtained in a yield of 58%, requiring a significant excess of both **2b** and indium to achieve this result (**Table 2.2, entries d–g**).

In a further trial we took inspiration from the work of Schneider and Kobayashi [107], and investigated the allylation of **1a** using pinacolyl allylboronate (**2d**) in the presence of a catalytic amount of indium(I) iodide. To our delight, this reaction yielded **3a** in 94% (**Table 2.2, entry h**).

In addition to this, we also did an optimization study on other catalytic systems based on indium species, such as In/$InBr_3$ and In/$InCl_3$, which are thought to produce the corresponding in-situ In(I) halides. However, none of these systems proved to be more effective than InI, by delivering lower yields and requiring longer reaction times, which is likely due to the reduced thermodynamic stability of the In-situ generated halides, as previously reported [107]. In additional trial we also assessed the use of allylmagnesium chloride (**2c**), but the reaction ended up without any appreciable results (**Table 2.2, entry k**).

Table 2.2 Optimization Studies of the Allylation Reaction.

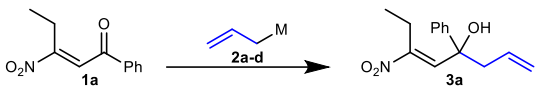

Entry	Compound 2	Catalyst	Solvent	Temperature	Time	Yield of 3a
a	**2a** (1.2 equiv)	K_2CO_3 + CuI	DMF	70 °C	20 h	56%
b	**2a** (1.2 equiv)	K_2CO_3 + CuI	MeCN	70 °C	20 h	31%
c	**2a** (1.2 equiv)	K_2CO_3 + CuI	γ-Valerolactone	70 °C	20 h	50%
d	**2b** (1.3 equiv)	In (1.5 equiv)	EtOH	0 °C	7 h	21%
e	**2b** (2 equiv)	In (2 equiv)	EtOH	0 °C	6 h	43%
f	**2b** (2 equiv)	In (2 equiv)	EtOH	r.t	3 h	49%
g	**2b** (3 equiv)	In (2 equiv)	EtOH	r.t	3 h	58%
h	**2c** (1.5 equiv)	InI(0.05 equiv)	THF	40 °C	7 h	94%
i	**2c** (1.5 equiv)	In (0.20 equiv) + $InBr_3$	THF	40 °C	30 h	85%
j	**2c** (1.5 equiv)	In (0.20 equiv) + $InCl_3$	THF	40 °C	34 h	71%
k	**2d** (1.2 equiv)	-	THF	0 °C	20 h	-

After a thorough screening of appropriate reaction conditions, we further investigated the substrate scope for the allylation of *β*-nitroenones **1a–o** with **2d**, catalyzed by 5 mol% indium(I) iodide, as well as the scalability of the protocol by converting **1a** to **3a** on a 5 mmol scale. Encouragingly, both studies resulted in excellent outcomes. The reaction displayed broad generality, producing the desired homoallylic alcohols **3a–o** in very high yields (**Figure 2.11**), while the reaction at large-scale afforded **3a** with a 95% yield.

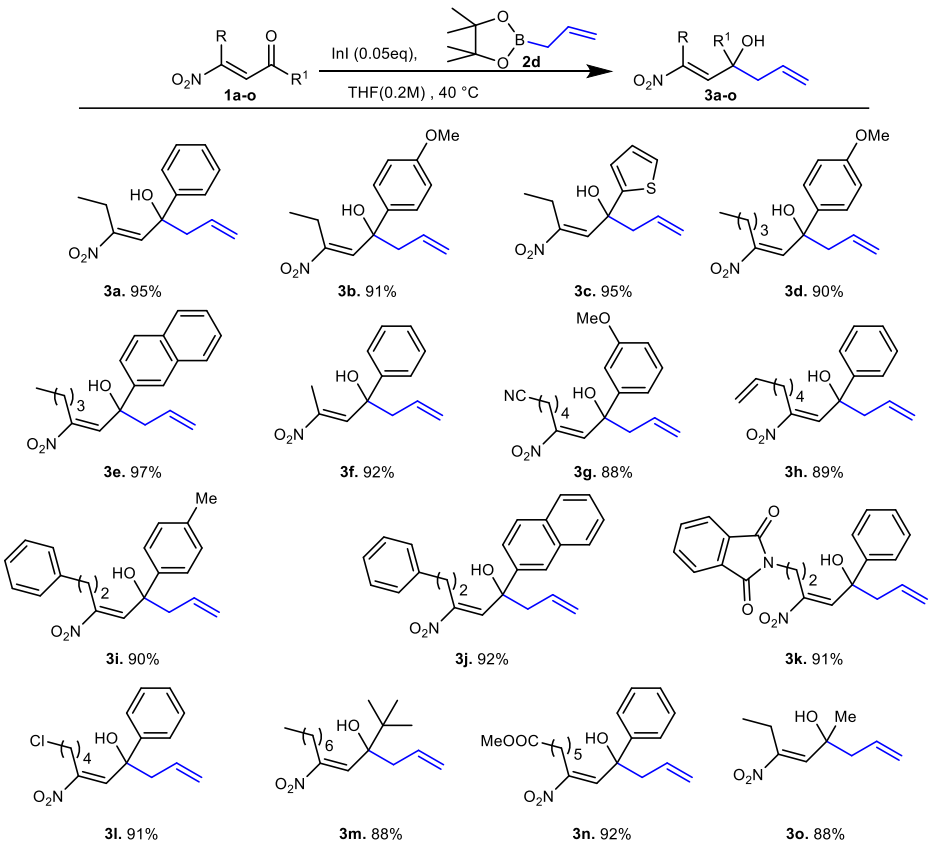

Figure 2.11 Substrate scope demonstration: synthesis of homoallylic alcohols **3**.

Subsequently, we studied the potential of nitroalkenyl alcohols **3** as versatile building blocks for synthesizing conjugated nitrotriene systems **4**. This previously less explored class of nitro derivatives holds promise for advancing the synthesis of functionalized molecules by leveraging the unique reactivity of trienes systems [108]. To optimize the suitable reaction conditions and guided by the literature studies [109, 110], firstly we attempted the conversion of **3a** into **4a** using p-toluenesulfonic acid under reflux, in toluene as solvent system. However, this approach resulted in a complex mixture of inseparable compounds. While the

same reaction was performed at room temperature, resulting in complete ineffectiveness.

Nitrotrienes systems

Next, we tested the dehydration reaction using boron trifluoride diethyl etherate in dichloromethane [111] at room temperature, we successfully isolated regioisomeric nitrotrienes **4a** and **5a** in a 75:25 ratio, achieving a combined yield of 43%. After a meticulous optimization of reaction conditions, we were able to achieve the highest yield (67%) at -10 ºC using 1.5 equivalents of $BF_3.Et_2O$. Notably, the isomeric ratio was changed with the minimized production of **5a**, which was around 10%. The enhanced regioselectivity observed at lower temperatures (-10 ºC) is likely attributed to improved kinetic control during the formation of compound **4**.

In search of complete selectivity of product, we attempted the conversion of **4a** into **5a**, the reaction was stirred at room temperature for 24 h; however, we observed extensive degradation of the product without any change in their regioisomeric ratios (**Table 2.3, entry f**).

Table 2.3 Optimization Studies of the Dehydration Reaction Using BF_3. Et_2O.

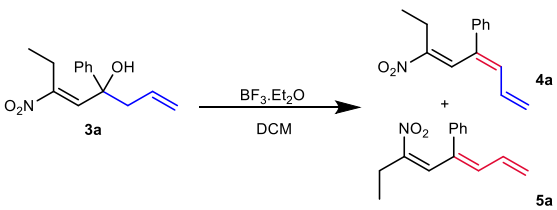

Entry	$BF_3.Et_2O$ eq	Temperature	Time	Overall Yield (4a : 5a)
a	1.2	rt	2.5 h	43% (75:25)
b	1.2	0 °C	2.5 h	49% (80:20)
c	1.5	0 °C	2.5 h	54% (80:20)
d	1.5	-10 °C	5 h	67% (90:10)
e	1.5	-20 °C	24 h	traces
f	1.5	rt	24 h	17% (75:25)
g	1.5	-10 °C	5 h	69% (90:10)

We further examined the reaction using alternative solvent systems such as 1,2-dichloroethane (DCE) and a number of Lewis acids, including $AlCl_3$, $EtAlCl_2$, BBr_3, and BF_3 or $AlCl_3$ supported on silica. Replacing DCM with DCE or using aluminum trichloride prominently reduced the reaction efficiency, yielding **4a** at

32% (5 h, −10 °C) and 22% (8 h, rt), respectively. While the reaction with BBr_3 at −10 °C for 6 h resulted in only 41% conversion of **4a**, warming to room temperature caused complete degradation of the product. Lastly, we tested ethylaluminum dichloride and heterogeneous BF_3 or $AlCl_3$ which were proven entirely ineffective.

To assess the scalability of protocol, we performed the reaction at 2mmol scale of **3a**. The protocol remained effective under these conditions, yielding a regioisomeric mixture of **4a** and **5a** (90:10) with a 69% yield, providing a comparable value to the yield obtained on a smaller scale (**Table 2.3, entry g**).

To identify the configuration of the newly formed double bond, we conducted NOESY experiments on isomer **4a**, which revealed a strong cross-peak signal between the protons at C-2 and C-5, confirming the 3E geometry of the predominant regioisomer **4a** (**Figure 2.12**).

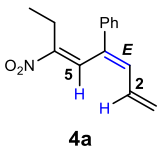

Figure 2.12 NOESY experiment concerning the isomer **4a**.

The formation of the *E* diastereomer can be rationalized by considering the initial generation of carbocation **A**, which can adopt either conformation **B** or **C**, resulting in the *Z* or *E* configuration, respectively.

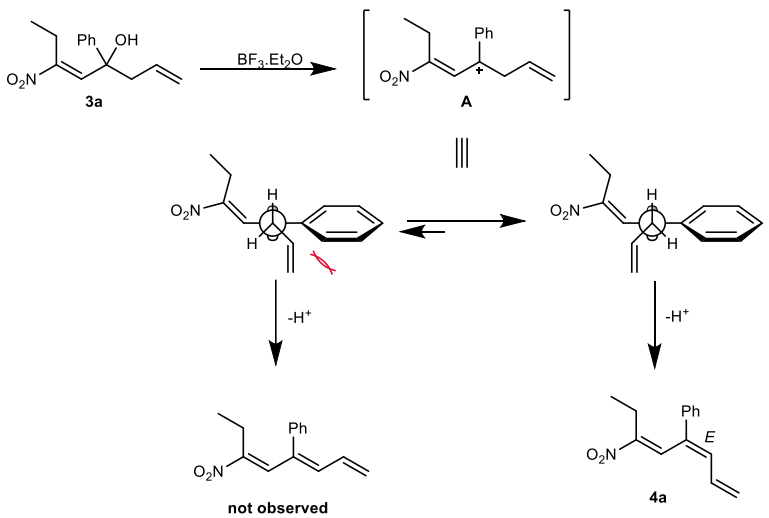

Scheme 2.15 Possible Explanation for the Formation of the ***E*** Diastereomer **4a**.

Specifically, the greater stability of conformation **C**, where steric hindrance and electronic repulsion between the alkyl and phenyl groups are minimized, over conformation **B** leads exclusively to the *E* double-bond geometry (**Scheme 2.15**).

Lastly, we applied the optimized reaction conditions to a range of homoallylic alcohols **3** to observe its substrate scope. We were able to obtain the desired products **4** in satisfactory yields. While approximately 10% of the isomeric product was consistently detected in all the trials except for compound **4i**, which was produced as a single regioisomer (**Figure 2.13**). Additionally, we also attempted the dehydration of the alkyl derivative **3m**, which contains a 4-tert-butyl group. In this case compound **3m** remained unreactive under the reaction conditions, could be due to the reduced stability of the carbocation intermediate.

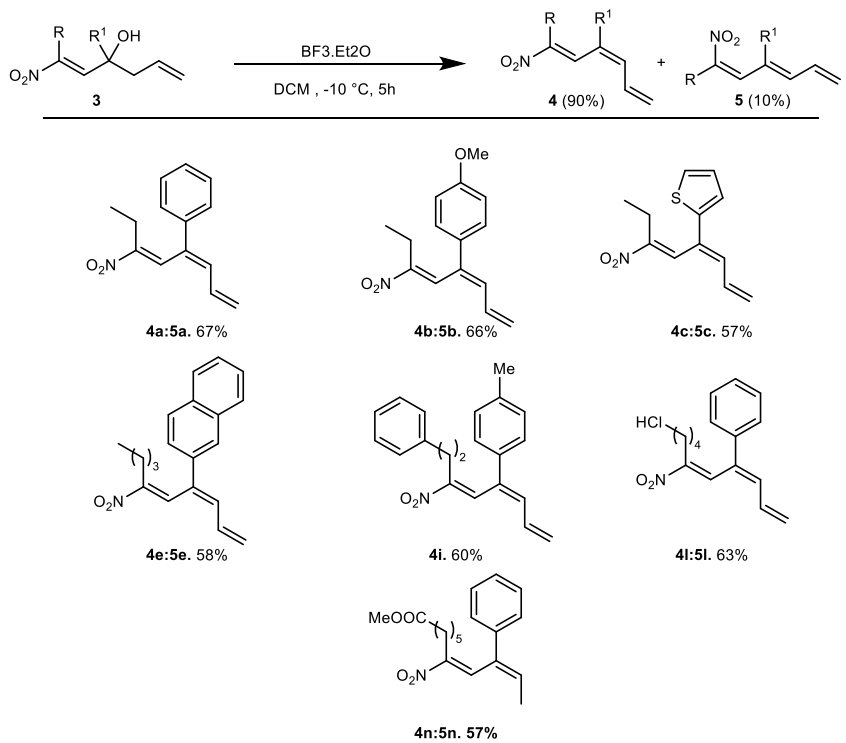

Figure 2.13 Synthesis of conjugated nitrotriene systems **4**.

2.3.3 Conclusions

In summary, the usefulness of *β*-nitroenones as essential starting materials in organic synthesis was once again demonstrated, as we revealed a new significant reactivity of *β*-nitroenones in combination with allylating agents that allows one to prepare a series of polyfunctionalized homoallylic alcohols in excellent yields.

The stereoselective conversion of allylated compounds into functionalized nitrotrienes under mild circumstances has shown their further reactivity and utility.

2.3.4 Experimental section

Analyses were performed using; ^{1}H NMR at 400 MHz on a Varian Mercury Plus 400. ^{13}C NMR at 100 MHz. IR spectra with a PerkinElmer FTIR spectrometer Spectrum Two UATR. Microanalyses were performed with a CHNS-O analyzer model EA 1108 from Fisons Instruments. GS-MS analyses were obtained on a Hewlett-Packard GC/MS 6890N that works with the EI technique (70 eV).

Compounds **1a–o** were synthesized by following documented methods, beginning with nitro compounds and alkyl- and aryl-glyoxals [68, 112], **1a** was a known compound, while compounds **1b–o** were new compounds. Sigma-Aldrich provided the allyltributyltin **2a** (code 271411), Allyl Bromide **2b** (code A29585), allylboronic acid pinacol ester **2c** (code 324647), allylmagnesium chloride **2d** (code 225908), and boron trifluoride diethyl etherate (code 216607), were utilized exactly as they were delivered. Tetrahydrofuran purchased from Sigma-Aldrich (code 87368) was distilled over sodium before usage. Dichloromethane (stabilized with amylene) was purchased from Carlo Erba (code 463314) and used as received. While, Indium(I) iodide was prepared according to the priorly reported method [113]. Compounds **3a–o** were synthesized by heating with a magnetic stirrer equipped with an aluminum heating block. The configuration of compound **4a** was assigned on the basis of additional data obtained from a NOESY experiment.

2.3.4.1. General Procedure for the Preparation of Compounds 3.

A round-bottom flask with a magnetic stir bar were dried over oven and maintained under inert atmosphere, were later charged with the appropriate β-nitroenones **1** (0.5 mmol), the solvent; dry THF (2.5 mL), with the catalyst InI (0.025 mmol, 6 mg), and the allylating reagent **2d** (allylboronic acid pinacol ester (0.75 mmol, 141 μL)).

Subsequently, the resulting reaction mixture was stirred at 40 °C for each of the β-nitroenones **1** till an appropriate time (~5 h). Further, diluted the reaction mixture with dichloromethane (20 mL), and treated with a saturated aqueous solution of $NaHCO_3$ (10 mL). After phase separation, the aqueous phase was extracted with dichloromethane (2 × 20 mL), and the combined organic layers were dried with dry Na_2SO_4. Finally, the solution was filtered and concentrated in vacuo to give the crude products **3**, which were purified by flash column chromatography (hexane/ethyl acetate).

2.3.4.2. Characterization data of Compounds 3.

(*E*)-6-Nitro-4-phenylocta-1,5-dien-4-ol (3a) (94% , 116 mg).

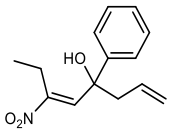

Pale yellow oil. IR (cm^{-1}, neat): 703, 924, 1334, 1520, 1634, 3392. ^{1}H NMR (400 MHz, $CDCl_3$) δ: 7.47–7.42 (m, 2H), 7.40–7.34 (m, 3H), 7.31–7.25 (m, 1H), 5.73–5.60 (m, 1H), 5.32–5.24 (m, 2H), 2.78 (d, 2H, J = 7.7 Hz), 2.76 (q, 2H, J = 7.4 Hz), 2.50 (br s, 1H), 0.92 (t, 3H, J = 7.3 Hz). ^{13}C[114] NMR (100 MHz, $CDCl_3$) δ: 155.8, 144.3, 138.3, 131.7, 128.9, 127.9, 125.3, 122.3, 74.5, 49.1, 20.8, 12.5. GC-MS (70 eV): m/z 206 (59), 159 (100), 131 (12), 105 (37), 77 (32). Anal. Calcd for $C_{14}H_{17}NO_3$ (247.29): C, 68.00; H, 6.93; N, 5.66. Found: C, 68.05; H, 6.96; N, 5.69.

(*E*)-4-(4-Methoxyphenyl)-6-nitroocta-1,5-dien-4-ol (3b) (91% , 126 mg).

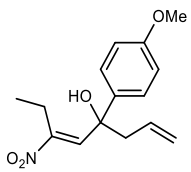

Pale yellow oil. IR (cm^{-1}, neat): 832, 926, 1034, 1176, 1248, 1334, 1513, 1608, 3464. ^{1}H NMR (400 MHz, $CDCl_3$) δ: 7.38–7.32 (m, 3H), 6.89 (d, 2H, J = 8.9 Hz), 5.74–5.60 (m, 1H), 5.29 (s, 1H), 5.27–5.23 (m, 1H), 3.81 (s, 3H), 2.81–2.71 (m, 4H), 2.38 (br s, 1H), 0.95 (t, 3H, J = 7.3 Hz). ^{13}C[114] NMR (100 MHz, $CDCl_3$) δ: 159.2, 155.4, 138.3, 136.2, 131.9, 126.6, 122.1, 114.2, 74.3, 55.6, 48.9, 20.7, 12.6. GC-MS (70 eV): m/z 236 (73), 189 (100), 135 (42), 81 (15), 77 (13). Anal. Calcd for $C_{15}H_{19}NO_4$ (277.32): C, 64.97; H, 6.91; N, 5.05. Found: C, 65.02; H, 6.94; N, 5.02.

(*E*)-6-Nitro-4-(thiophen-2-yl)octa-1,5-dien-4-ol (3c) (95% , 120 mg).

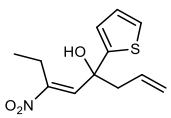

Pale yellow oil. IR (cm^{-1}, neat): 709, 931, 1331, 1434, 1525, 1609, 3528. ^{1}H NMR (400 MHz, $CDCl_3$) δ: 7.27 (dd, 1H, J = 4.4, 1.9 Hz), 7.24 (s, 1H), 7.00–6.96 (m, 2H), 5.82–5.68 (m, 1H), 5.33–5.31 (m, 1H), 5.30–5.26 (m, 1H), 2.92–2.76 (m, 4H), 2.65 (br s, 1H), 1.04 (t, 3H, J = 7.3 Hz). ^{13}C[114] NMR (100 MHz, $CDCl_3$) δ:

155.3, 148.7, 136.8, 131.4, 127.4, 125.6, 124.0, 122.5, 73.9, 49.2, 20.7, 12.9. GC-MS (70 eV): *m*/*z* 212 (61), 165 (100), 111 (47), 81 (19), 39 (17). Anal. Calcd for $C_{12}H_{15}NO_3S$ (253.32): C, 56.90; H, 5.97; N, 5.53; S, 12.66. Found: C, 56.93; H, 6.00; N, 5.56; S, 12.70.

(*E*)-4-(4-Methoxyphenyl)-6-nitrodeca-1,5-dien-4-ol (3d) (90% , 137 mg).

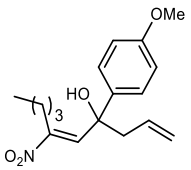

Pale yellow oil. IR (cm^{-1}, neat): 739, 833, 920, 1035, 1177, 1252, 1334, 1508, 1607, 3539. ^1H NMR (400 MHz, $CDCl_3$) δ: 7.35 (d, 2H, *J* = 8.9 Hz), 7.33 (s, 1H), 6.89 (d, 2H, *J* = 8.9 Hz), 5.73–5.61 (m, 1H), 5.29 (s, 1H), 5.27–5.23 (m, 1H), 3.81 (s, 3H), 2.78–2.70 (m, 4H), 2.37 (br s, 1H), 1.39–1.15 (m, 4H), 0.83 (t, 3H, *J* = 7.1 Hz). $^{13}C\{^1H\}$ NMR (100 MHz, $CDCl_3$) δ: 159.2, 154.5, 138.4, 136.3, 131.9, 126.6, 122.1, 114.1, 74.3, 55.5, 48.9, 26.9, 30.2, 22.9, 13.9. GC-MS (70 eV): *m*/*z* 264 (67), 243 (12), 217 (100), 175 (13), 135 (91), 77 (21). Anal. Calcd for $C_{17}H_{23}NO_4$ (305.37): C, 66.86; H, 7.59; N, 4.56. Found: C, 66.91; H, 7.63; N, 4.59.

(*E*)-4-(Naphthalen-2-yl)-6-nitrodeca-1,5-dien-4-ol (3e) (97% , 158 mg).

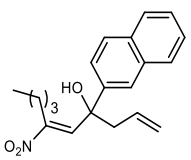

Pale yellow oil. IR (cm^{-1}, neat): 748, 823, 1331, 1426, 1517, 1607, 1635, 3062, 3545. ^1H NMR (400 MHz, $CDCl_3$) δ: 7.94 (d, 1H, *J* = 1.8 Hz), 7.88–7.81 (m, 3H), 7.54–7.48 (m, 3H), 7.47 (s, 1H), 5.74–5.62 (m, 1H), 5.35–5.27 (m, 2H), 2.88 (d, 2H, *J* = 7.3 Hz), 2.74 (dd, 2H, *J* = 8.3, 7.0 Hz), 2.54 (br s, 1H), 1.08–1.37 (m, 4H), 0.74 (t, 3H, *J* = 7.2 Hz). $^{13}C\{^1H\}$ NMR (100 MHz, $CDCl_3$) δ: 155.2, 141.5, 137.9, 133.3, 132.8, 131.7, 128.8, 128.4, 127.8, 126.8, 126.6, 124.1, 123.5, 122.4, 74.6, 49.0, 30.0, 27.0, 22.8, 13.8. GC-MS (70 eV): *m*/*z* 278 (15), 263 (64), 237 (17), 207 (17), 155 (100), 127 (76), 77 (12). Anal. Calcd for $C_{20}H_{23}NO_3$ (325.41): C, 73.82; H, 7.12; N, 4.30. Found: C, 73.78; H, 7.09; N, 4.27.

(*E*)-6-Nitro-4-phenylhepta-1,5-dien-4-ol (3f) (92% , 107 mg).

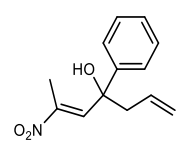

Pale yellow oil. IR (cm^{-1}, neat): 698, 724, 987, 1326, 1519, 1608, 1640, 3062, 3537. ^1H NMR (400 MHz, $CDCl_3$) δ: 7.47–7.45 (m, 2H), 7.44 (s, 1H), 7.40–7.35 (m, 2H), 7.32–7.27 (m, 1H), 5.74–5.61 (m, 1H), 5.33–5.24 (m, 2H), 2.79 (d, 2H, J = 7.4 Hz), 2.46 (br s, 1H), 2.24 (s, 3H). $^{13}C\{^1H\}$ NMR (100 MHz, $CDCl_3$) δ: 150.3, 143.8, 138.3, 131.5, 128.7, 127.7, 125.1, 122.0, 74.2, 48.7, 13.6. GC-MS (70 eV): m/z 192 (60), 145 (100), 105 (29), 77 (31), 67 (32). Anal. Calcd for $C_{13}H_{15}NO_3$ (233.27): C, 66.94; H, 6.48; N, 6.00. Found: C, 66.99; H, 6.52; N, 5.97.

(*E*)-8-Hydroxy-8-(3-methoxyphenyl)-6-nitroundeca-6,10 dienenitrile (3g) (88% , 145 mg).

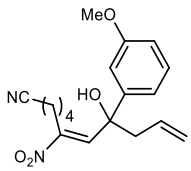

Pale yellow oil. IR (cm^{-1}, neat): 698, 1042, 1247, 1328, 1432, 1520, 1583, 1600, 1640, 2249, 3460. ^1H NMR (400 MHz, $CDCl_3$) δ: 7.40 (s, 1H), 7.30 (t, 1H, J = 7.9 Hz), 7.03–6.96 (m, 2H), 6.87–6.81 (m, 1H), 5.70–5.57 (m, 1H), 5.32 (d, 1H, J = 1.0 Hz), 5.30–5.26 (m, 1H), 3.82 (s, 3H), 2.86–2.69 (m, 4H), 2.52 (br s, 1H), 2.27 (t, 2H, J = 7.2 Hz),1.65–1.34 (m, 4H). $^{13}C\{^1H\}$ NMR (100 MHz, $CDCl_3$) δ: 159.9, 152.9, 145.5, 138.9, 131.2, 129.9, 122.4, 119.5, 117.4, 112.5, 111.4, 74.2, 55.3, 48.7, 26.9, 26.0, 25.0, 16.7. GC-MS (70 eV): m/z 284 (25), 268 (93), 229 (30), 187 (16), 135 (100), 107 (27), 77 (34). Anal. Calcd for $C_{18}H_{22}N_2O_4$ (330.38): C, 65.44; H, 6.71; N, 8.48. Found: C, 65.49; H, 6.74; N, 8.51.

(*E*)-6-Nitro-4-phenyldodeca-1,5,11-trien-4-ol (3h) (89% , 134 mg).

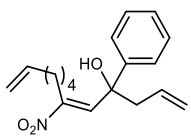

Pale yellow oil. IR (cm^{-1}, neat): 699, 912, 994, 1331, 1521, 1640, 3540. ^1H NMR (400 MHz, $CDCl_3$) δ: 7.47–7.42 (m, 2H), 7.40–7.34 (m, 3H), 7.32–7.26 (m, 1H), 5.80–5.59 (m, 2H), 5.30 (d, 1H, J = 0.8 Hz), 5.28–5.24 (m, 1H), 5.00–4.88 (m, 2H), 2.78 (d, 2H, J = 7.3 Hz), 2.76–2.70 (m, 2H), 2.41 (br s, 1H), 1.96 (q, 2H, J = 6.9 Hz), 1.14–1.12 (m, 4H). $^{13}C\{^1H\}$ NMR (100 MHz, $CDCl_3$) δ: 154.4, 144.0, 138.5, 138.1, 131.5, 128.6, 127.7, 125.1, 122.1, 114.5, 74.2, 48.8, 33.3, 28.6, 27.2, 26.8. GC-MS (70 eV): m/z 260 (7), 213 (11), 186 (18), 105 (100), 91 (10), 77 (26), 41 (14). Anal. Calcd for $C_{18}H_{23}NO_3$ (301.39): C, 71.73; H, 7.69; N, 4.65. Found: C, 71.77; H, 7.73; N, 4.62.

(*E*)-6-Nitro-8-phenyl-4-(*p*-tolyl)octa-1,5-dien-4-ol (3i) (90%, 152 mg).

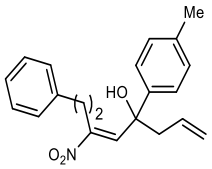

Pale yellow oil. IR (cm^{-1}, neat): 699, 733, 1326, 1453, 1521, 1603, 1640, 3540. ^1H NMR (400 MHz, $CDCl_3$) δ: 7.46 (s, 1H), 7.34–7.29 (m, 4H), 7.26–7.18 (m, 3H), 7.17–7.12 (m, 2H), 5.65–5.54 (m, 1H), 5.27–5.20 (m, 2H), 3.20–3.06 (m, 2H), 2.79–2.60 (m, 4H), 2.38 (s, 3H), 2.05 (br s, 1H). $^{13}C\{^1H\}$ NMR (100 MHz, $CDCl_3$) δ: 152.5, 140.8, 140.7, 139.5, 137.5, 131.5, 129.4, 128.7, 128.5, 126.3, 125.0, 121.6, 74.4, 48.5, 33.9, 29.1, 21.0. GC-MS (70 eV): *m*/*z* 290 (19), 275 (48), 248 (9), 199 (12), 119 (100), 91 (82), 65 (24). Anal. Calcd for $C_{21}H_{23}NO_3$ (337.42): C, 74.75; H, 6.87; N, 4.15. Found: C, 74.79; H, 6.90; N, 4.12.

(*E*)-4-(Naphthalen-2-yl)-6-nitro-8-phenylocta-1,5-dien-4-ol (3j) (92% , 172 mg).

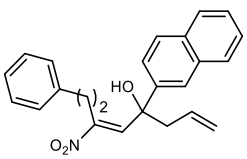

Pale yellow oil. IR (cm^{-1}, neat): 476, 734, 748, 1326, 1521, 1600, 1639, 3027, 3537. ^1H NMR (400 MHz, $CDCl_3$) δ: 7.94–7.85 (m, 4H), 7.59 (s, 1H), 7.58–7.52 (m, 2H), 7.50 (dd, 1H, J = 8.7, 1.9 Hz), 7.29–7.17 (m, 3H), 7.06 (d, 2H, J = 7.0 Hz), 5.67–5.56 (m, 1H), 5.33–5.22 (m, 2H), 3.21–3.07 (m, 2H), 2.87–2.69 (m, 3H), 2.65–2.55 (m, 1H), 2.20 (br s, 1H). $^{13}C\{^1H\}$ NMR (100 MHz, $CDCl_3$) δ: 152.9, 141.0, 140.6, 139.2, 133.1, 132.6, 131.3, 128.7, 128.6, 128.5, 128.2, 127.6, 126.6, 126.4, 126.3, 123.9, 123.2, 122.0, 74.5, 48.5, 33.8, 29.1. GC-MS (70 eV): *m*/*z* 326 (34), 311 (34), 284 (59), 207 (29), 155 (100), 127 (90), 91 (34), 77 (17). Anal. Calcd for $C_{24}H_{23}NO_3$ (373.45): C, 77.19; H, 6.21; N, 3.75. Found: C, 77.24; H, 6.18; N, 3.78.

(*E*)-2-(5-Hydroxy-3-nitro-5-phenylocta-3,7-dien-1-yl)isoindoline-1,3-dione (3k) (91% , 179 mg).

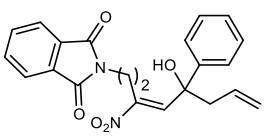

Pale yellow solid. mp: 134–176 °C. IR (cm^{-1}, neat): 701, 716, 935, 1331, 1398, 1517, 1703, 1770, 3073, 3513. ^1H NMR (400 MHz, $CDCl_3$) δ: 7.80–7.77 (m, 2H), 7.72–7.68 (m, 2H), 7.50 (s, 1H), 7.28–7.11 (m, 5H), 5.49–5.37 (m, 1H), 5.08 (dd, 1H, *J* = 10.2, 1.8 Hz), 4.94 (dd, 1H, *J* = 17.1, 1.6 Hz), 3.99–3.84 (m, 2H), 3.28–3.22 (m, 2H), 2.74 (dd, 1H, *J* = 13.7, 6.5 Hz), 2.67 (br s, 1H), 2.51 (dd, 1H, *J* = 13.8, 8.2 Hz). $^{13}C\{^1H\}$ NMR (100 MHz, $CDCl_3$) δ: 168.5, 149.4, 143.4, 141.2, 134.1, 132.4, 131.3, 128.9, 127.9, 125.0, 123.5, 122.2, 74.8, 48.5, 36.0, 26.5. GC-MS (70 eV): *m*/*z* 345 (35), 330 (38), 183 (99), 171 (47), 160 (65), 105 (100), 77 (80). Anal. Calcd for $C_{22}H_{20}N_2O_5$ (392.41): C, 67.34; H, 5.14; N, 7.14. Found: C, 67.38; H, 5.17; N, 7.11.

(*E*)-10-Chloro-6-nitro-4-phenyldeca-1,5-dien-4-ol (3l) (91% , 141 mg).

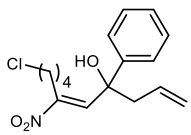

Yellow oil. IR (cm^{-1}, neat): 699, 1331, 1520, 3537. ^1H NMR (400 MHz, $CDCl_3$) δ: 7.47–7.35 (m, 5H), 7.32–7.27 (m, 1H), 5.72–5.59 (m, 1H), 5.33–5.25 (m, 2H), 3.44 (dt, 2H, *J* = 6.8, 0.8 Hz), 2.81–2.74 (m, 4H), 2.47 (br s, 1H), 1.73–1.63 (m, 2H), 1.60–1.46 (m, 1H), 1.44–1.31 (m, 1H). $^{13}C\{^1H\}$ NMR (100 MHz, $CDCl_3$) δ: 153.5, 143.9, 138.7, 131.3, 128.7, 127.8, 125.0, 122.3, 74.3, 48.7, 44.4, 32.2, 26.1, 25.2. GC-MS (70 eV): *m*/*z* 268 (43), 221 (81), 105 (100), 77 (54), 41 (17). Anal. Calcd for $C_{16}H_{20}ClNO_3$ (309.79): C, 62.03; H, 6.51; N, 4.52. Found: C, 62.08; H, 6.48; N, 4.55.

(*E*)-4-(*tert*-Butyl)-6-nitrotrideca-1,5-dien-4-ol (3m) (88% , 131 mg).

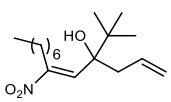

Yellow oil. IR (cm^{-1}, neat): 1329, 1522, 3558. ^1H NMR (400 MHz, $CDCl_3$) δ: 7.10 (s, 1H), 5.80–5.69 (m, 1H), 5.27 (d, 1H, *J* = 10.1 Hz), 5.23 (d, 1H, *J* = 17.0 Hz), 3.06–2.98 (m, 1H), 2.84–2.76 (m, 1H), 2.61 (dd, 1H, *J* = 13.5, 5.5 Hz), 2.34 (dd, 1H, *J* = 13.6, 9.4 Hz), 1.80 (br s, 1H), 1.56–1.47 (m, 1H), 1.43–1.21 (m, 9H), 1.04 (s, 9H), 0.90 (t, 3H, *J* = 7.0 Hz). $^{13}C\{^1H\}$ NMR (100 MHz, $CDCl_3$) δ: 154.6, 136.7, 133.2, 121.0, 78.8, 41.3, 39.2, 31.7, 29.6, 28.9, 28.6, 26.4, 25.4, 22.6, 14.0. GC-MS (70 eV): *m*/*z* 256 (24), 209 (30), 139 (15), 109 (14), 95 (18), 81 (25), 69 (100), 57 (90), 41 (74). Anal. Calcd for $C_{17}H_{31}NO_3$ (297.44): C, 68.65; H, 10.51; N, 4.71. Found: C, 68.60; H, 10.54; N, 4.74.

Methyl (*E*)-9-Hydroxy-7-nitro-9-phenyldodeca-7,11-dienoate (3n) (92% , 160 mg).

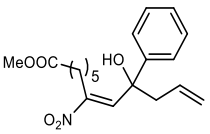

Pale yellow oil. IR (cm^{-1}, neat): 699, 1331, 1520, 1732, 3484. ^1H NMR (400 MHz, $CDCl_3$) δ: 7.46–7.24 (m, 6H), 5.72–5.58 (m, 1H), 5.31–5.23 (m, 2H), 3.65 (s, 3H), 2.78 (d, 2H, *J* = 7.3 Hz), 2.73 (dd, 2H, *J* = 8.5, 6.0 Hz), 2.57 (br s, 1H), 2.23 (t, 2H, *J* = 7.5 Hz), 1.59–1.47 (m, 2H), 1.43–1.11 (m, 4H). $^{13}C\{^1H\}$ NMR (100 MHz, $CDCl_3$) δ: 174.2, 154.2, 144.0, 138.3, 131.5, 128.6, 127.7, 125.1, 122.0, 74.3, 51.5, 48.8, 33.8, 28.7, 27.2, 26.6, 24.3. GC-MS (70 eV): *m*/*z* 300 (6), 285 (13), 199 (22), 197 (18), 105 (100), 77 (41). Anal. Calcd for $C_{19}H_{25}NO_5$ (347.41): C, 65.69; H, 7.25; N, 4.03. Found: C, 65.73; H, 7.28; N, 4.07.

(*E*)-4-Methyl-6-nitrooct-1,5-dien-4-ol (3o) (88% , 81 mg).

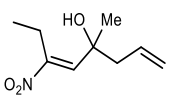

Pale yellow oil. IR (cm^{-1}, neat): 735, 921, 1334, 1457, 1519, 1641, 3533. ^1H NMR (400 MHz, $CDCl_3$) δ: 7.03 (s, 1H), 5.89–5.76 (m, 1H), 5.33–5.19 (m, 2H), 2.95 (dq, 2H, *J* = 7.3, 1.7 Hz), 2.52–2.46 (m, 1H), 2.42–2.35 (m, 1H), 1.94 (br s, 1H), 1.45 (s, 3H), 1.13 (t, 3H, *J* = 7.3 Hz). $^{13}C\{^1H\}$ NMR (100 MHz, $CDCl_3$) δ: 154.6, 138.4, 132.0, 121.1, 71.7, 47.8, 28.4, 20.1, 13.2. GC-MS (70 eV): *m*/*z* 144 (45), 97 (100), 43 (58). Anal. Calcd for $C_9H_{15}NO_3$ (185.22): C, 58.36; H, 8.16; N, 7.56. Found: C, 58.40; H, 8.19; N, 7.58.

2.3.4.3. General Procedure for the Preparation of Compounds 4.

To a stirred solution of the homoallylic alcohol **3** (0.5 mmol) in dichloromethane (5 mL) $BF_3.Et_2O$ (0.75 mmol, 93 μL) was added dropwise at −10 °C. The mixture was stirred at the same temperature (−5 °C for compound 3e) for the appropriate duration, then diluted the reaction mixture with dichloromethane (10 mL) and treated with a saturated aqueous solution of $NaHCO_3$ (10 mL). Followed the phase separation, the aqueous layer was extracted with dichloromethane (2 × 20 mL). The combined organic layers were dried over anhydrous Na_2SO_4, filtered, and concentrated under reduced pressure to afford the crude regioisomeric products **4** and **5**, which were subsequently purified by flash column chromatography using hexane/ethyl acetate eluent system.

2.3.4.4. Characterization data of Compounds 4.

((3*E*,5*E*)-6-Nitroocta-1,3,5-trien-4-yl)benzene (4a) (67% , 77 mg).

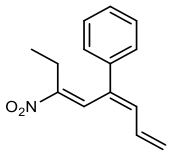

Major regioisomer **4a** 90%. Pale yellow oil. IR (cm^{-1}, neat): 695, 760, 1333, 1520, 1632. ^1H NMR (400 MHz, $CDCl_3$) δ: 7.81 (s, 1H), 7.44–7.29 (m, 5H), 6.73–6.48 (m, 2H), 5.51 (d, 1H, *J* = 16.4 Hz), 5.39 (d, 1H, *J* = 9.9 Hz), 2.42 (q, 2H, *J* = 7.4 Hz), 0.96 (t, 3H, *J* = 7.4 Hz). $^{13}C\{^1H\}$ NMR (100 MHz, $CDCl_3$) δ: 155.7, 138.8, 133.8, 133.1, 132.7, 130.1, 128.5, 128.4, 126.7, 122.0, 21.1, 11.5. GC-MS (70 eV): *m*/*z* 229 ([M^+], 63), 168 (100), 152 (59), 128 (32), 115 (36), 91 (29), 77 (24). Anal. Calcd for $C_{14}H_{15}NO_2$ (229.28): C, 73.34; H, 6.59; N, 6.11. Found: C, 73.38; H, 6.63; N, 6.14.

1-Methoxy-4-((3*E*,5*E*)-6-nitroocta-1,3,5-trien-4-yl)benzene (4b) (66% , 86 mg).

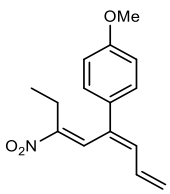

Major regioisomer **4b** 90%. Pale Yellow oil. IR (cm^{-1}, neat): 832, 1030, 1175, 1244, 1333, 1511, 1604. ^1H NMR (400 MHz, $CDCl_3$) δ: 7.76 (s, 1H), 7.28 (d, 2H, *J* = 8.9 Hz), 6.89 (d, 2H, *J* = 8.9 Hz), 6.63–6.44 (m, 2H), 5.45 (dd, 1H, *J* = 16.0, 1.4 Hz), 5.33 (dd, 1H, *J* = 9.5, 1.3 Hz), 3.82 (s, 3H), 2.43 (q, 2H, *J* = 7.4 Hz), 0.97 (t, 3H, *J* = 7.4 Hz). $^{13}C\{^1H\}$ NMR (100 MHz, $CDCl_3$) δ: 160.0, 155.8, 133.5, 131.3, 131.1, 130.7, 128.7, 128.1, 121.3, 114.4, 55.6, 21.4, 11.8. GC-MS (70 eV): *m*/*z* 259 ([M^+], 84), 215 (51), 198 (100), 183 (47), 65 (27), 153 (31), 128 (24), 115 (26). Anal. Calcd for $C_{15}H_{17}NO_3$ (259.31): C, 69.48; H, 6.61; N, 5.40. Found: C, 69.52; H, 6.57; N, 5.42.

2-((3*E*,5*E*)-6-Nitroocta-1,3,5-trien-4-yl)thiophene (4c) (57% , 67 mg).

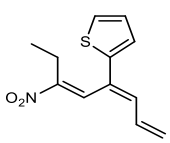

Major regioisomer **4c** 90%. Pale Yellow oil. IR (cm^{-1}, neat): 694, 828, 909, 1329, 1523, 1612, 1656. ^1H NMR (400 MHz, $CDCl_3$) δ: 7.65 (s, 1H), 7.25 (dd, 1H, J = 3.9, 0.8 Hz), 7.01–6.97 (m, 1H), 6.94 (dd, 1H, J = 3.6, 1.0 Hz), 6.68 (d, 1H, J = 11.6 Hz), 6.47–6.33 (m, 1H), 5.48 (dd, 1H, J = 16.7, 0.7 Hz), 5.33 (dd, 1H, J = 10.1, 0.7 Hz), 2.53 (q, 2H, J = 7.4 Hz), 1.05 (t, 3H, J = 7.4 Hz). $^{13}C\{^1H\}$ NMR (100 MHz, $CDCl_3$) δ: 156.4, 142.2, 132.8, 131.2, 129.3, 129.0, 127.8, 125.6, 125.5, 121.4, 21.2, 11.8. GC-MS (70 eV): m/z 235 ([M^+], 76), 174 (100), 147 (26), 128 (35), 115 (33), 97 (24), 77 (19). Anal. Calcd for $C_{12}H_{13}NO_2S$ (235.30): C, 61.25; H, 5.57; N, 5.95; S, 13.63. Found: C, 61.29; H, 5.60; N, 5.89; S, 13.67.

2-((3*E*,5*E*)-6-Nitrodeca-1,3,5-trien-4-yl)naphthalene (4e) (58% , 89 mg).

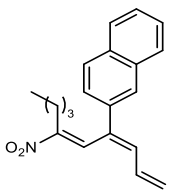

Major regioisomer **4e** 90%. Pale Yellow oil. IR (cm^{-1}, neat): 464, 751, 812, 1325, 1430, 1467, 1519, 3054. ^1H NMR (400 MHz, $CDCl_3$) δ: 7.96 (s, 1H), 7.89–7.83 (m, 3H), 7.76 (d, 1H, J = 1.4 Hz), 7.58–7.49 (m, 3H), 6.84 (d, 1H, J = 11.0 Hz), 6.70–6.58 (m, 1H), 5.58 (d, 1H, J = 16.7 Hz), 5.45 (d, 1H, J = 10.1 Hz), 2.45–2.38 (m, 2H), 1.42–1.33 (m, 2H), 1.15–1.05 (m, 2H), 0.70 (t, 3H, J = 7.3 Hz). $^{13}C\{^1H\}$ NMR (100 MHz, $CDCl_3$) δ: 154.9, 136.0, 133.6, 133.3, 133.2, 133.1, 130.5, 128.8, 128.5, 128.2, 127.6, 126.7, 126.5, 126.1, 124.2, 122.2, 29.1, 27.4, 22.3, 13.4. GC-MS (70 eV): m/z 307 ([M^+], 50), 264 (37), 218 (100), 202 (92), 165 (14), 41 (14). Anal. Calcd for $C_{20}H_{21}NO_2$ (307.39): C, 78.15; H, 6.89; N, 4.56. Found: C, 78.19; H, 6.92; N, 4.59.

1-Methyl-4-((3*E*,5*E*)-6-nitro-8-phenylocta-1,3,5-trien-4-yl)benzene (4i)
(60%, 96 mg).

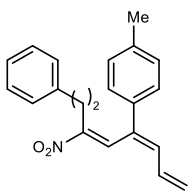

Pale yellow oil. IR (cm^{-1}, neat): 699, 821, 915, 1330, 1520, 3025. ^1H NMR (400 MHz, $CDCl_3$) δ: 7.89 (s, 1H), 7.29–7.07 (m, 7H), 6.93–6.89 (m, 2H), 6.62–6.45 (m, 2H), 5.47 (dd, 1H, J = 16.0, 1.7 Hz), 5.37 (dd, 1H, J = 9.4, 1.6 Hz), 2.66 (s, 4H), 2.37 (s, 3H). $^{13}C\{^1H\}$ NMR (100 MHz, $CDCl_3$) δ: 153.1, 140.1, 138.4, 136.0, 133.6, 133.0, 132.9, 131.8, 129.5, 128.4, 128.3, 126.8, 126.3, 122.0, 33.0, 29.9, 21.2. GC-MS (70 eV): m/z 319 ([M^+], 7), 227 (100), 182 (92), 165 (50), 152 (17), 91 (58).

Anal. Calcd for $C_{21}H_{21}NO_2$ (319.40): C, 78.97; H, 6.63; N, 4.39. Found: C, 79.01; H, 6.60; N, 4.42.

((3*E*,5*E*)-10-Chloro-6-nitrodeca-1,3,5-trien-4-yl)benzene (4l) (63% . 92 mg).

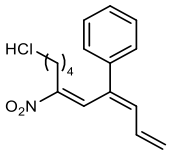

Major regioisomer **4l** 90%. Pale Yellow oil. IR (cm^{-1}, neat): 700, 1326, 1519, 1640. ^1H NMR (400 MHz, $CDCl_3$) δ: 7.93 (s, 1H), 7.43–7.27 (m, 5H), 6.70–6.51 (m, 2H), 5.52 (dd, 1H, *J* = 15.9, 1.5 Hz), 5.42 (dd, 1H, *J* = 9.4, 1.5 Hz), 3.34 (t, 2H, *J* = 6.2 Hz), 2.40–2.34 (m, 2H), 1.62–1.44 (m, 4H). $^{13}C\{^1H\}$ NMR (100 MHz, $CDCl_3$) δ: 153.7, 138.8, 133.7, 133.6, 132.8, 131.0, 128.9, 128.5, 126.8, 122.6, 44.1, 32.0, 26.9, 24.4. GC-MS (70 eV): *m*/*z* 291 (29), 214 (43), 168 (100), 167 (70), 165 (53), 153 (32), 152 (59), 115 (22), 91 (20), 41 (21). Anal. Calcd for $C_{16}H_{18}ClNO_2$ (291.77): C, 65.86; H, 6.22; N, 4.80. Found: C, 65.91; H, 6.19; N, 4.83.

Methyl (7*E*,9*E*)-7-Nitro-9-phenyldodeca-7,9,11-trienoate (4n) (57% , 94 mg).

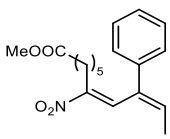

Major regioisomer **4n** 90%. Yellow oil. IR (cm^{-1}, neat): 697, 732, 1331, 1521, 1734. ^1H NMR (400 MHz, $CDCl_3$) δ: 7.87 (s, 1H), 7.40–7.27 (m, 5H), 6.68–6.49 (m, 2H), 5.50 (dd, 1H, *J* = 16.3, 1.5 Hz), 5.39 (dd, 1H, *J* = 9.8, 1.5 Hz), 3.63 (s, 3H), 2.37–2.31 (m, 2H), 2.16 (t, 2H, *J* = 7.5 Hz), 1.49–1.30 (m, 4H), 1.15–1.04 (m, 2H). $^{13}C\{^1H\}$ NMR (100 MHz, $CDCl_3$) δ: 174.0, 154.2, 138.8, 133.7, 133.2, 132.9, 130.7, 128.8, 128.4, 126.8, 122.3, 51.5, 33.7, 28.7, 27.4, 26.6, 24.2. GC-MS (70 eV): *m*/*z* 294 (10), 220 (81), 210 (80), 168 (100), 167 (94), 115 (40), 87 (41), 55 (35). Anal. Calcd for $C_{19}H_{23}NO_4$ (329.40): C, 69.28; H, 7.04; N, 4.25. Found: C, 69.33; H, 7.07; N, 4.21.

2.4 A New One-Pot Synthesis of 3,6-Disubstituted Pyridazines Starting from β-Nitro-β,γ-Unsaturated Ketones

This section is based on the results derived from:

Khan, M. E. I., Yuan, L., Petrini, M., & Palmieri, A. (2023). A New One-Pot Synthesis of 3, 6-Disubstituted Pyridazines Starting from β-Nitro-β, γ-Unsaturated Ketones. *Synthesis*, *55*(19), 3204-3208.

2.4.1 Introduction

Compounds with an aromatic six-member ring having two vicinal nitrogen atoms are known as pyridazines. Their numerous pharmacological properties, including analgesic, antifungal, anti-inflammatory, and anticancer effects, are being thoroughly studied [115-118]. The pyridazine core is also present in various natural products, like Azamerone, which was extracted from a saline culture of a newly discovered marine-derived bacterium belonging to the genus *Streptomyces* [119] and Pyridazomycin, a novel antifungal antibiotic synthesized by *Streptomyces violaceoniger* sp. *Griseofuscus* [120]. Because of its importance, the pyridazine scaffold has now been identified as a privileged structure [121, 122], recently the renowned pharmaceutical company GSK plc has recognized these structures as one of the promising heteroaromatic rings for drug design [123].

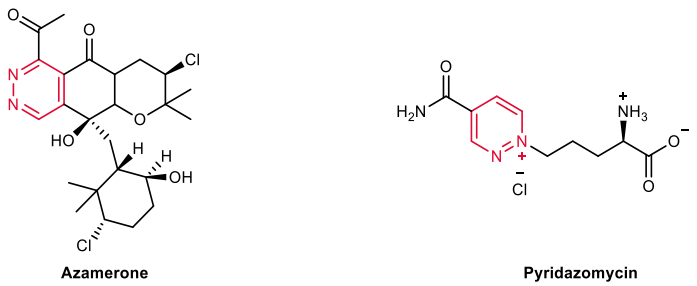

Figure 2.14 Examples of natural products containing the pyridazine core.

In this context, a number of synthetic methodologies for the synthesis of pyridazines have been documented in the literature. These methods primarily rely on multistep approaches, utilizing carbonyl or dicarbonyl compounds in combination with hydrazine or substituted hydrazines for nitrogen atom source [124-127]. Alternatively, tetrazines and diazo compounds have also been employed for the same purpose of nitrogen source [128, 129]. However, these synthetic methods often encounter significant drawbacks, including the use of complex starting materials, strong acids, metal catalysts, and labor-intensive workups, all of these present clear ecological disadvantages.

Building on our ongoing research for the exploration of sustainable protocols that utilizes the reactivity of functionalized nitroolefins [59, 62, 130, 131], we came up with a novel one-pot, promoter-free approach for the synthesis of 3,6-disubstituted pyridazines. This protocol employs *β*-nitro-*β*,*γ*-unsaturated ketones **1** and hydrazine as starting materials.

These compounds **1** are highly reactive species featuring two electrophilic centers positioned in a relative 1,4-configuration. Due to their ability to lose nitrous acid and water undergoing a cyclization reaction, they serve as valuable starting materials for the synthesis of aromatic systems. In this regard, two illustrative

synthetic applications of compounds **1** for the preparation of pyrroles and carbazoles are presented in **Scheme 2.16** [60, 132].

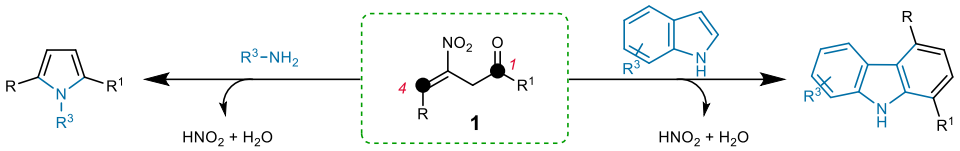

Scheme 2.16 Applications of **1** as precursor of N-containing aromatic systems.

This new reported protocol involves two consecutive steps carried out within the same reactor, each step via domino reactions, as illustrated in **Scheme 2.17**. The initial step involves the reaction of compound **1** with hydrazine to produce cyclic tetrahydropyridazine **2**. In the subsequent step, aromatization of cyclized **2** occurs to afford the pyridazine **3** by the loss of water and nitrous acid, as commonly observed in similar molecules [133].

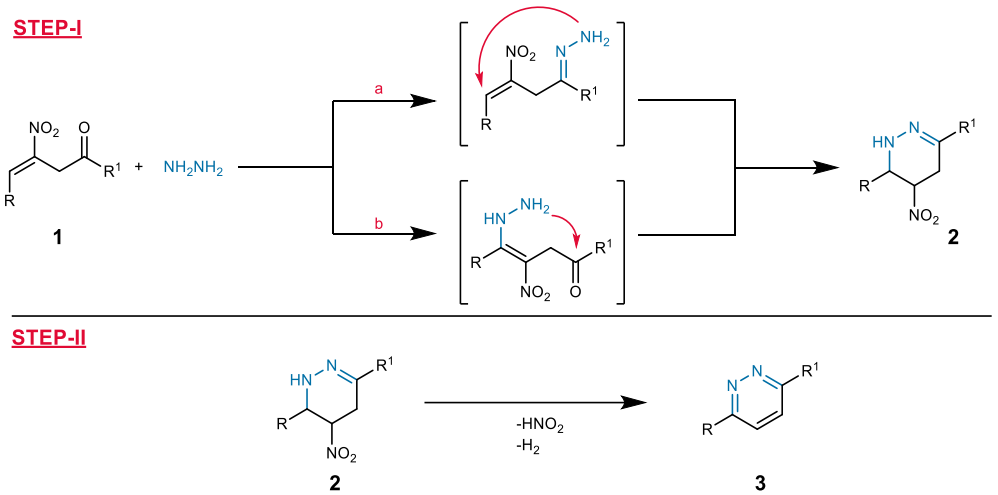

Scheme 2.17 One-pot Synthesis of pyridazines **3**.

In the first step, both the pathway (a), which initiates with the hydrazone formation followed by intramolecular Michael addition reaction, and pathway (b), which involves Michael addition followed by cyclization, are equally feasible.

2.4.2 Results and discussion

To optimize the overall process, we first concentrated on the initial step, specifically the conversion of **1a** into **2a**. To this end, a series of preliminary experiments were conducted to evaluate the reaction's performance with respect to temperature, time, solvent, concentration, and stoichiometry (**Table 2.4**).

Table 2.4 Optimization Studies of the **Step I**.

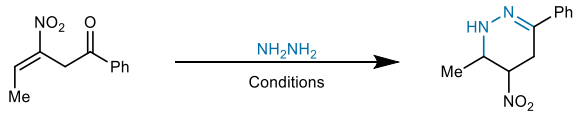

1 **2a**

Entry	NH_2NH_2 (equiv)	Solvent (M)	Time (min)	Temperature (ºC)	2a Yield (%)
a	1	MeCN [0.1]	90	rt	36
b	1	Toluene [0.1]	90	rt	33
c	1	$CHCl_3$ [0.1]	90	rt	31
d	1	EtOAc [0.1]	90	rt	47
e	1.2	EtOAc [0.1]	90	rt	53
f	1.4	EtOAc [0.1]	90	rt	51
g	1.2	EtOAc [0.1]	90	rt	58
h	1.2	EtOAc [0.1]	90	rt	56
i	1.2	EtOAc [0.1]	120	0	64
j	1.2	EtOAc [0.1]	120	-10	53

The highest yield (64%) was obtained by conducting the reaction in ethyl acetate 0.05 M solution at 0 °C for two hours, using 1.2 equivalents of hydrazine monohydrate (**Table 2.4, entry i**). Notably, under these optimal conditions, the conversion of **1a** was complete, though a complex mixture of inseparable by-products was also observed.

Next, we optimized the optimal conditions for the second step, focusing on the conversion of **2a** into **3a**. To achieve this, crude **2a** was subjected to various reaction conditions (Table 2). In the very first trial we studied the reaction progress at 100 ºC using a Biotage® initiator microwave reactor, however the **3a** was isolated in only 8% of yield (**Table 2.4, entry a**). Subsequently, we decided to change the solvent and performed further trials for aromatization of **2a**, using alternative solvents, like cyclopentyl methyl ether (CPME), toluene, γ-valerolactone (GVL), and chloroform (**Table 2.4, entries b–d**). However, only chloroform led the formation of product **2a** in not negligible amount (21% of yield) To our delight, optimizing the reaction temperature and concentration (120 °C, 0.05 M) enabled the isolation of **3a** with a 60% overall yield from **1a**, that corresponds to over 90% yield for the second step (**Table 2.4, entries e–h**).

Table 2.5 Optimization Studies of the **Step II**.

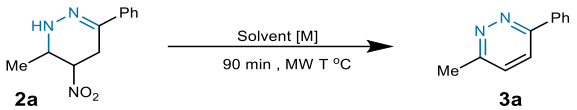

Entry	Solvent (M)	Temperature (°C)	3a Yield (%)
a	EtOAc [0.05]	100	8
b	CPME [0.05]	100	traces
c	GVL [0.05]	100	traces
d	$CHCl_3$ [0.05]	100	21
e	$CHCl_3$ [0.05]	120	60
f	$CHCl_3$ [0.05]	140	36
g	$CHCl_3$ [0.01]	120	52
h	$CHCl_3$ [0.025]	120	58

Finally with the optimal reaction conditions in hand, we applied them to a range of *β*-nitro-*β,γ*-unsaturated ketones **1** to further evaluate the generality of the protocol (**Scheme 2.18**).

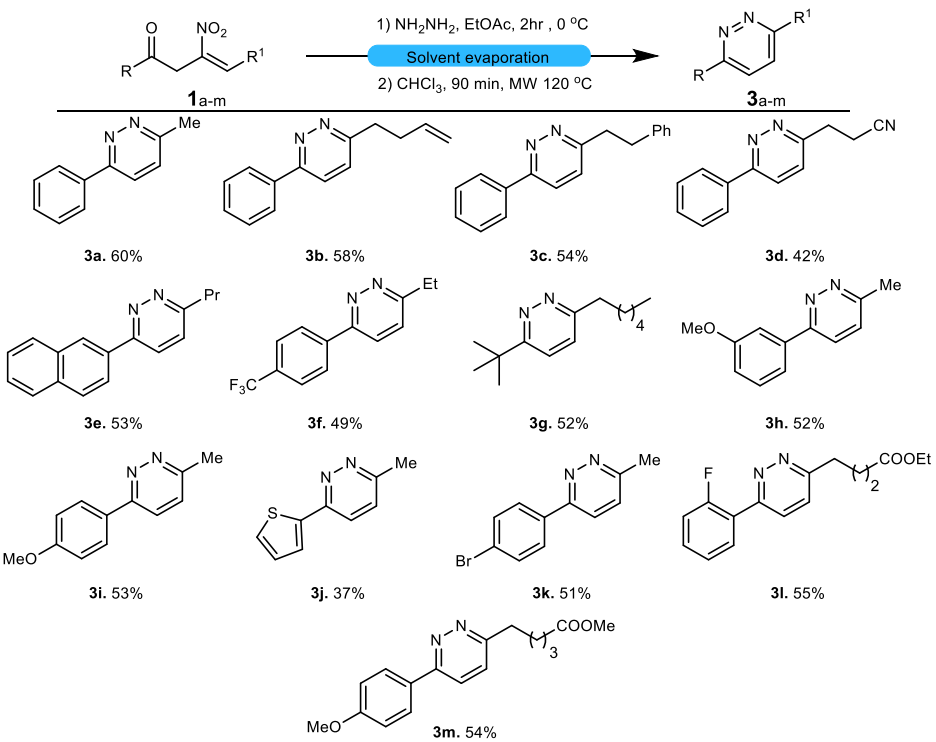

Scheme 2.18 Substrate scope investigation.

Overall, we were able to obtain satisfactory overall yields (49–60%), with the exceptions of products **3d** and **3j**, which were isolated in yields of 42% and 37%, respectively.

2.4.3 Conclusion

In conclusion, we have developed and reported an efficient one-pot protocol for the synthesis of 3,6-disubstituted pyridazines using readily available *β*-nitro-*β*, *γ*-unsaturated ketones. This protocol highlights the versatility of these nitroolefinic compounds as precursors of nitrogen containing heterocycles and allows the incorporation of diverse functional groups including double bonds, esters, ethers, cyano groups, and halides. Notably, the simplified workup (just solvent evaporation) efficiently mitigates the need for conventional and wasteful aqueous treatments. Moreover, this streamlined approach significantly reduces material usage and energy consumption, by offering a clear advantage in terms of sustainability.

2.4.4 Experimental section

^{1}H NMR spectra were recorded at 400 MHz on a Varian Mercury Plus 400 spectrometer, ^{13}C NMR spectra were recorded at 100 MHz. IR spectra were obtained using a PerkinElmer Spectrum Two UATR FT-IR spectrometer. Mass spectra were acquired on a GC/MS system utilizing electron impact (EI) ionization at 70 eV. Elemental microanalyses were carried out with a Fisons Instruments CHNS-O analyzer (Model EA1108). Microwave irradiations were performed using a Biotage® Initiator instrument. While compounds 1a–m were synthesized according to previously reported methods [60].

2.4.4.1. Synthesis of Pyridazines 3a–m; General Procedure

In a 20 mL Biotage® vial, a 0.05 M solution of compound **1** (0.5 mmol) in EtOAc (10 mL) with hydrazine monohydrate (0.6 mmol) was stirred at 0 °C for 120 minutes. Upon reaction completion, the solvent was removed under reduced pressure. Subsequently, the resulting residue was diluted with $CHCl_3$ (10 mL) and subjected to microwave irradiation at 120 °C for 90 minutes using a Biotage® Initiator microwave reactor. Finally, the solvent was evaporated, and the crude product **3** was purified via flash column chromatography using a hexane : EtOAc eluent system.

2.4.4.2. Characterization data

3-Methyl-6-phenylpyridazine (3a) (60% , 51 mg).

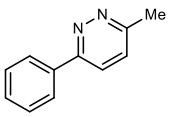

Pale brown solid; mp 97–99 °C. IR (neat): 3061, 1450, 1415, 850, 770, 740, 690, 565 cm^{-1}. ^{1}H NMR ($CDCl_3$, 400 MHz): d = 8.10–8.03 (m, 2 H), 7.79 (d, J = 8.7 Hz, 1H), 7.56–7.46 (m, 3 H), 7.42 (d, J = 8.7 Hz, 1 H), 2.78 (s, 3 H). ^{13}C {^{1}H} NMR ($CDCl_3$, 100 MHz): d = 158.5, 157.3, 136.2, 129.9, 129.0, 127.6, 126.9, 124.3, 21.9. MS (EI): m/z (%) = 170 (54, [M+]), 141 (15), 115 (13), 102 (100), 76(12). Anal. Calcd for $C_{11}H_{10}N_2$ (170.22): C, 77.62; H, 5.92; N, 16.46. Found: C, 77.66; H, 5.95; N, 16.43.

3-(But-3-en-1-yl)-6-phenylpyridazine (3b) (58% , 61 mg).

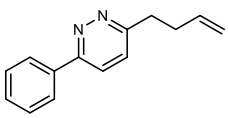

Yellow sticky oil. IR (neat): 3061, 1639, 1594, 1450, 1421, 904, 753, 694 cm^{-1}. ^{1}H NMR ($CDCl_3$, 400 MHz): d = 8.11–8.03 (m, 2 H), 7.80 (d, J = 8.8 Hz, 1H), 7.55–7.47 (m, 3 H), 7.41 (d, J = 8.8 Hz, 1 H), 5.96–5.83 (m, 1 H), 5.11–4.99 (m, 2 H), 3.14 (t, J = 7.6 Hz, 2 H), 2.65–2.55 (m, 2 H). ^{13}C {^{1}H} NMR ($CDCl_3$, 100 MHz): d = 161.3, 157.5, 136.9, 136.1, 129.9, 129.0, 127.2, 126.9, 124.2, 115.9, 35.0, 33.2. MS (EI): m/z (%) = 210 (75, [M+]), 209 (100), 195 (56), 115 (18), 102 (14). Anal. Calcd for $C_{14}H_{14}N_2$ (210.28): C, 79.97; H, 6.71; N, 13.32. Found: C, 80.01; H, 6.73; N, 13.34.

3-Phenethyl-6-phenylpyridazine (3c) (54% , 70 mg).

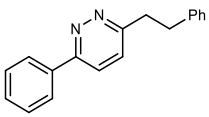

Pale brown solid; mp 80–82 °C. IR (neat): 3059, 3027, 1601, 1451, 1419, 744, 691cm^{-1}. ^{1}H NMR ($CDCl_3$, 400 MHz): d = 8.09 (dd, J = 1.4 Hz, 2 H), 7.77 (d, J = 8.7 Hz, 1 H), 3.58–3.50 (m, 3 H), 7.35–7.20 (m, 6 H), 3.36 (dd, J = 9.0, 6.7 Hz, 2 H), 3.20 (dd, J = 9.0, 6.7 Hz, 2 H). ^{13}C {^{1}H} NMR ($CDCl_3$, 100 MHz): d = 161.2, 157.6, 140.7, 136.2, 129.9, 129.0, 128.6, 128.5, 127.3, 127.0, 126.3, 124.1, 37.5, 35.5. MS (EI): m/z (%) = 260 (70, [M+]), 259 (100), 183 (29), 115 (18), 91

(20). Anal. Calcd for $C_{18}H_{16}N_2$ (260.34): C, 83.04; H, 6.19; N, 10.76. Found: C, 83.00; H, 6.17; N, 10.79.

3-(6-Phenylpyridazin-3-yl)propanenitrile (3d) (42% , 44 mg).

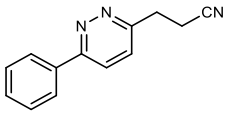

Pale brown solid; mp 69–71 °C. IR (neat): 3060, 2247, 1587, 1546, 1451, 1422, 751, 694 cm^{-1}. ^1H NMR ($CDCl_3$, 400 MHz): d = 8.09–8.03 (m, 2 H), 7.84 (d, J = 8.8 Hz, 1H), 7.55–7.54 (m, 4 H), 3.34 (t, J = 7.3 Hz, 2 H), 3.03 (t, J = 7.3 Hz, 2 H). ^{13}C {^1H} NMR ($CDCl_3$, 100 MHz): d = 158.4, 157.5, 135.8, 130.2, 129.1, 127.3, 127.0, 124.4, 119.1, 31.4, 16.4. MS (EI): m/z (%) = 210 (15, [M + 1+]), 209 (100, [M+]), 208 (55), 156 (12), 141 (13), 115 (24), 102 (71), 76 (15), 51 (7). Anal. Calcd for $C_{13}H_{11}N_3$ (209.25): C, 74.62; H, 5.30; N, 20.08. Found: C, 74.58; H, 5.33; N, 20.11.

3-(Naphthalen-2-yl)-6-propylpyridazine (3e) (53% , 66 mg).

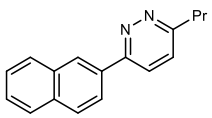

Brown solid; mp 88–90 °C. IR (neat): 3053, 1599, 1460, 1420, 815, 748, 492, 482 cm^{-1}. ^1H NMR ($CDCl_3$, 400 MHz): d = 8.52 (s, 1 H), 8.25 (dd, J = 8.6, 1.8 Hz, 1H), 8.00–7.84 (m, 4 H), 7.55–7.49 (m, 2 H), 7.40 (d, J = 8.8 Hz, 1 H), 3.04–2.98 (m, 2 H), 1.93–1.80 (m, 2 H), 1.04 (t, J = 7.4 Hz, 3 H). ^{13}C {^1H} NMR ($CDCl_3$, 100 MHz): d = 162.1, 157.2, 134.0, 133.6, 133.3, 128.8, 127.7, 127.0, 126.9, 126.6, 126.5, 124.3, 124.1, 37.8, 22.8, 13.8. MS (EI): m/z (%) = 248 (16, [M+]), 234 (18), 220 (100), 152 (23), 110 (9). Anal. Calcd for $C_{17}H_{16}N_2$ (248.33): C, 82.22; H, 6.49; N, 11.28. Found: C, 82.26; H, 6.51; N, 11.32.

3-Ethyl-6-(4-(trifluoromethyl)phenyl)pyridazine (3f) (49% , 62 mg).

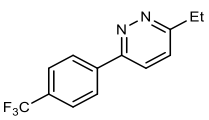

Brown solid; yield: mp 89–91 °C. IR (neat): 3053, 1617, 1586, 1546, 1426, 1321, 1109, 835, 602 cm^{-1}. ^1H NMR ($CDCl_3$, 400 MHz): d = 8.19 (d, J = 8.2 Hz, 2 H), 7.84 (d, J = 8.8 Hz, 1 H), 7.77 (d, J = 8.2 Hz, 2 H), 7.47 (d, J = 8.8 Hz, 1 H), 3.10 (q, J = 7.6 Hz, 2 H), 1.43 (t, J = 7.6 Hz, 3 H). ^{13}C {^1H} NMR ($CDCl_3$, 100 MHz): d = 164.0, 156.1, 139.7, 131.6 (q, J = 32.2 Hz), 127.2, 126.7, 125.9 (q, J = 3.7 Hz),

124.5, 29.1, 13.5. MS (EI): m/z (%) = 252 (99, [M+]), 251 (100), 209 (18), 170 (25). Anal. Calcd for $C_{13}H_{11}F_3N_2$ (252.24): C, 61.90; H, 4.40; N, 11.11. Found: C, 61.94; H, 4.43; N, 11.08.

3-(tert-Butyl)-6-hexylpyridazine (3g) (52% , 57 mg).

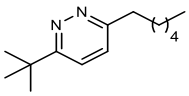

Brown oil. IR (neat): 1664, 1478, 1459, 1428, 1364, 1149, 844, 734 cm^{-1}. ^1H NMR ($CDCl_3$, 400 MHz): d = 7.43 (d, J = 8.8 Hz, 1 H), 7.25 (d, J = 8.8 Hz, 1 H), 2.97–2.91 (m, 2 H), 1.83–1.74 (m, 2 H), 1.47–1.25 (m, 6 H), 1.44 (s, 9 H), 0.89 (t, J = 7.0 Hz, 3 H). ^{13}C {^1H} NMR ($CDCl_3$, 100 MHz): d = 167.9, 161.2, 126.3, 123.3, 36.6, 35.7, 31.6, 30.0, 29.3, 29.0, 22.5, 14.0. MS (EI): m/z (%) = 220 (3, [M+]), 177 (12), 163 (39), 150 (100), 135(36). Anal. Calcd for $C_{14}H_{24}N_2$ (220.36): C, 76.31; H, 10.98; N, 12.71. Found: C, 76.34; H, 11.00; N, 12.74.

3-(3-Methoxyphenyl)-6-methylpyridazine (3h) (52% , 52 mg).

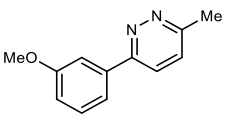

Pale yellow solid; mp 42–44 °C. IR (neat): 3052, 1592, 1458, 1453, 1221, 1041, 863, 841, 798, 700 cm^{-1}. ^1H NMR ($CDCl_3$, 400 MHz): d = 7.75 (d, J = 8.8 Hz, 1 H), 7.73–7.70 (m, 1H), 7.55 (d, J = 7.7 Hz, 1H), 7.44–7.36 (m, 2 H), 7.02 (dd, J = 8.0, 2.3 Hz, 1 H), 3.89 (s, 3 H), 2.76 (s, 3 H). ^{13}C {^1H} NMR (CDCl3, 100 MHz): d = 160.2, 158.7, 157.0, 137.7, 129.9, 127.4, 124.2, 119.1, 116.1, 111.8, 55.4, 22.0. MS (EI): m/z (%) = 200 (76, [M+]), 199 (100), 170 (36), 132 (35), 102 (24), 89 (12). Anal. Calcd for $C_{12}H_{12}N_2O$ (200.24): C, 71.98; H, 6.04; N, 13.99. Found: C, 72.03; H, 6.07; N, 14.02.

3-(4-Methoxyphenyl)-6-methylpyridazine (3i) (53% , 53 mg).

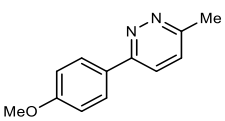

Pale brown solid; mp 131–133 °C. IR (neat): 3047, 1606, 1508, 1427, 1250, 1172, 532, 815, 672, 566 cm^{-1}. ^1H NMR (CDCl3, 400 MHz): d = 8.02 (d, J = 8.9 Hz, 2 H), 7.70 (d, J = 8.8 Hz, 1 H), 7.34 (d, J = 8.8 Hz, 1 H), 7.02 (d, J = 8.9 Hz, 2 H), 3.86 (s, 3 H), 2.73 (s, 3 H). ^{13}C {^1H} NMR ($CDCl_3$, 100 MHz): d = 161.1, 157.8, 156.8, 128.8, 128.2, 127.3, 123.4, 114.3, 55.4, 21.9. MS (EI): m/z (%) = 200 (98,

[M+]), 132 (100), 117 (24), 89 (23). Anal. Calcd for $C_{12}H_{12}N_2O$ (200.24): C, 71.98; H, 6.04; N, 13.99. Found: C, 72.02; H, 6.01; N, 13.96.

3-Methyl-6-(thiophen-2-yl)pyridazine (3j) (37% , 33 mg).

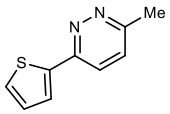

Pale brown solid; mp 135–137 °C. IR (neat): 3028, 1676, 1586, 1543, 1432, 832, 720, 588 cm^{-1}. ^1H NMR ($CDCl_3$, 400 MHz): d = 7.67 (d, J = 8.8 Hz, 1 H), 7.62 (dt, J = 3.7, 1.0 Hz, 1 H), 7.45 (dt, J = 5.0, 1.0 Hz, 1 H), 7.31 (d, J = 8.7 Hz, 1 H), 7.14–7.11 (m, 1 H), 2.69 (s, 3 H). ^{13}C {^1H} NMR ($CDCl_3$, 100 MHz): d = 158.3, 153.1, 140.8, 128.7, 127.9, 127.3, 125.8, 122.5, 22.0. MS (EI): m/z (%) = 176 (48, [M+]), 147 (12), 108 (100), 44 (58), 32 (19). Anal. Calcd for $C_9H_8N_2S$ (176.24): C, 61.34; H, 4.58; N, 15.90; S, 18.19. Found: C, 61.30; H, 4.61; N, 15.93; S, 18.22.

3-(4-Bromophenyl)-6-methylpyridazine (3k) (51% , 33 mg).

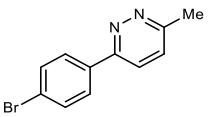

Pale brown solid; mp 125–127 °C. IR (neat): 3044, 1591, 1424, 1397, 1071, 1001, 814, 553 cm^{-1}. ^1H NMR ($CDCl_3$, 400 MHz): d = 7.93 (d, J = 8.7 Hz, 2 H), 7.71 (d, J = 8.7 Hz, 1 H), 7.62 (d, J = 8.7 Hz, 2 H), 7.38 (d, J = 8.7 Hz, 1 H), 2.75 (s, 3 H). ^{13}C {^1H} NMR ($CDCl_3$, 100 MHz): d = 158.8, 156.2, 135.3, 132.1, 128.4, 127.3, 124.4, 123.6, 22.1. MS (EI): m/z (%) = 250 (94, [M + 2+]), 248 (97, [M+]), 182 (99), 180 (100), 139 (16), 115 (14), 101 (33), 75 (20). Anal. Calcd for $C_{13}H_9BrN_2$ (249.11): C, 53.04; H, 3.64; N, 11.25. Found: C, 53.08; H, 3.67; N, 11.22.

Ethyl 4-(6-(2-Fluorophenyl)pyridazin-3-yl)butanoate (3l) (55% , 79 mg).

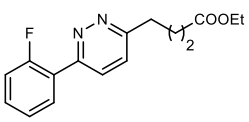

Brown oil. IR (neat): 3064, 1728, 1615, 1579, 1545, 1492, 1452, 1421, 1208, 829, 757 cm^{-1}. ^1H NMR ($CDCl_3$, 400 MHz): d = 8.15 (dt, J = 7.9, 1.8 Hz, 1 H), 7.88 (dd, J = 8.8, 2.2 Hz, 1 H), 7.48–7.37 (m, 2 H), 7.30 (dt, J = 7.6, 1.2 Hz, 1 H), 7.17 (ddd, J = 11.4, 8.3, 1.2 Hz, 1 H), 4.12 (q, J = 7.1 Hz, 2 H), 3.09–3.03 (m, 2 H), 2.43 (t, J = 7.3 Hz, 2 H), 2.24–2.10 (m, 2 H), 1.24 (t, J = 7.1 Hz, 3 H). ^{13}C {^1H} NMR ($CDCl_3$, 100 MHz): d = 173.2, 161.6 (d, J = 53.2 Hz), 159.4, 154.4, 131.5, (d, J = 8.6 Hz), 130.8 (d, J = 2.6 Hz), 127.7 (d, 9.6 Hz), 126.4, 124.8 (d, J = 3.5

Hz), 124.4 (d, J = 11.3 Hz), 116.2 (d, J = 22.6 Hz), 60.4, 35.0, 33.5, 24.4, 14.2. MS (EI): m/z (%) = 288 (10, [M+]), 243 (23), 215 (45), 188 (100), 133 (18), 120 (19). Anal. Calcd for $C_{16}H_{17}FN_2O_2$ (288.32): C, 66.65; H, 5.94; N, 9.72. Found: C, 66.69; H, 5.91; N, 9.69.

Methyl 5-(6-(4-Methoxyphenyl)pyridazin-3-yl)pentanoate (3m) (54% ,81 mg)

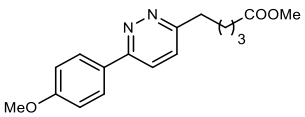

Brown solid; yield:; mp 59–61 °C. IR (neat): 3066, 1727, 1606, 1509, 1248, 1187, 1029, 825, 793, 581 cm^{-1}. ^1H NMR ($CDCl_3$, 400 MHz): d = 8.03 (d, J = 8.9 Hz, 2 H), 7.74 (d, J = 8.8 Hz, 1 H), 7.36 (d, J = 8.8 Hz, 1 H), 7.02 (d, J = 8.9 Hz, 2 H), 3.87 (s, 3 H), 3.66 (s, 3 H), 3.03 (t, J = 7.6 Hz, 2 H), 2.38 (t, J = 7.3 Hz, 2 H), 1.91–1.68 (m, 4 H). ^{13}C {^1H} NMR ($CDCl_3$, 100 MHz): d = 173.9, 161.2, 161.0, 157.0, 128.6, 128.2, 127.0, 123.7, 114.4, 55.4, 51.5, 35.3, 33.7, 28.7, 24.4. MS (EI): m/z (%) = 300 (3, [M+]), 269 (12), 227 (20), 200 (100), 184 (14), 132 (10), 89 (6). Anal. Calcd for $C_{17}H_{20}N_2O_3$ (300.36): C, 67.98; H, 6.71; N, 9.33. Found: C, 68.01; H, 6.68; N, 9.30.

2.5 Synthesis of 3,5-disubstituted isoxazoles by domino reductive Nef reaction/cyclization of β-nitroenones

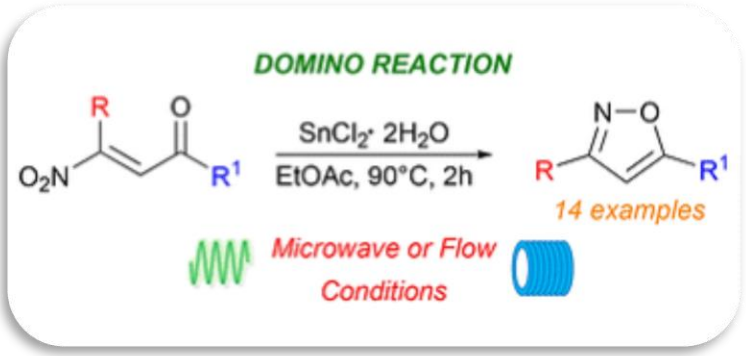

The results presented in this section are extracted from the following paper:

Khan, M. E. I., Cassini, T. L., Petrini, M., & Palmieri, A. (2024). Synthesis of 3, 5-disubstituted isoxazoles by domino reductive Nef reaction/cyclization of β-nitroenones. *Organic & Biomolecular Chemistry*, *22*(16), 3299-3303.

2.5.1 Introduction

The isoxazole ring is regarded as a favored structural motif in isoxazoles, a highly significant class of five-membered heterocyclic compounds that include nitrogen and oxygen [134-136]. In fact, the ability of isoxazole molecules to interact with a wide variety of protein targets, their derivatives show a wide range of biological activity [137]. Specifically, the therapeutic qualities of isoxazole derivatives include antituberculosis, antiviral, antimicrobial, anticancer, and antibacterial activity (**Figure 2.15**) [138-140]. Additionally, the isoxazole moieties also act as a key starting material to access more complex molecular architectures [141].

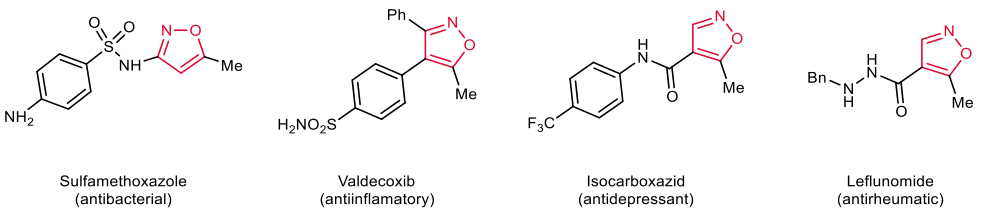

Figure 2.15 Examples of biologically active isoxazole derivatives.

Given their significance, a number of methods for synthesizing poly-functionalized isoxazoles have been reported in the literature (**Scheme 2.19**) [142-146]. The most efficient synthetic methods rely on 1,3-dipolar cycloaddition reactions between electronically rich alkynes and nitrile oxides, which are generated in situ from nitroalkanes **A** or oximes **B**.

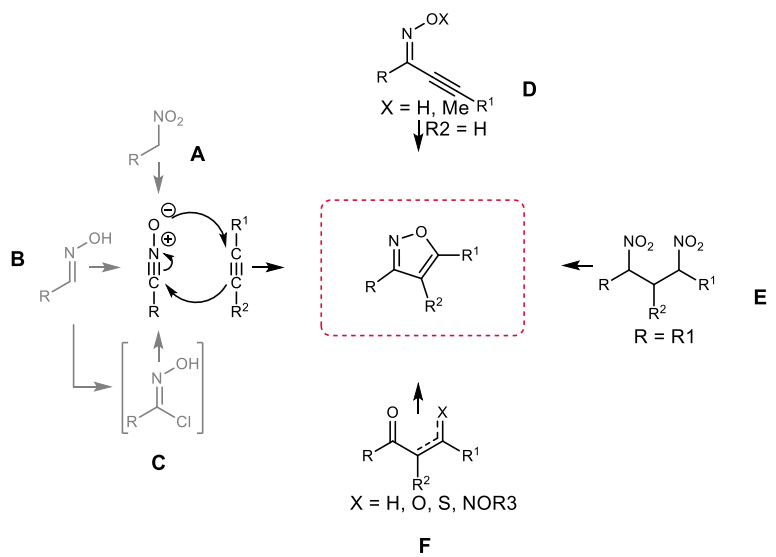

Scheme 2.19 Main synthetic routes to prepare isoxazoles.

As the conversion of **A** to corresponding nitrile oxides is generally effective, it often requires harsh reaction conditions and/or the use of hazardous and toxic reagents like $POCl_3$, phenyl isocyanate, PPA, and DMTMM [147-150]. In contrast, **B** undergoes direct conversion to nitrile oxides using oxidizing agents such as hypervalent iodine reagents, NaOCl, or Oxone®, Alternatively, **B** can be converted into nitrile oxides via imidoyl chlorides **C** by chlorination, followed by a base-promoted elimination step [151-155]. Despite the effectiveness of this synthetic method, employing unsymmetrical alkynes can make it difficult to achieve exact regiochemical control in isoxazole synthesis. Alternative techniques that include the intramolecular cyclization of particular structures have been investigated in order to address the regiochemical control issue. In this regard, α,β-acetylenic oximes **D** are especially well suited for metal catalysis with $AuCl_3$, CuCl, or $Pd(OAc)_2$ to cyclize into isoxazoles [146, 156, 157]. Similarly, under mild basic conditions, dinitro compounds **E** readily transform into the isoxazole core; however, to avoid the production of regioisomeric products, R and R^1 must be similar [158-161]. Lastly, 1,3-dielectrophiles **F** can serve as functionalized isoxazole beginning materials; however, even in this scenario, choosing the right starting scaffold is essential to avoid regioisomeric problems [162].

A particular subclass of nitroolefins known as *β*-nitroenones is distinguished by the simultaneous presence of a ketone and a nitro group at the *α*- and *β*-positions with respect to the double bond, respectively (**Figure 2.16**) [62]. The reactivity and synthetic adaptability of *β*-nitroenones are greatly enhanced by the presence of these two electron-withdrawing groups, making them useful precursors for the synthesis of heterocyclic systems and highly functionalized materials [51, 61, 163-166].

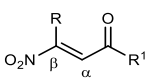

1

Figure 2.16 General structure of *β*-nitroenones.

We have discovered a general and effective conversion of **1** into 3,5-disubstituted isoxazoles **2** as a result of our continuous research on the chemistry of *β*-nitroenones **1**, which was motivated by the groundbreaking studies by Viel in 1979 (limited to *α*-acyl *β*-nitrostilbenes) and Wieland at the turn of the century. The procedure is predicated on the nitroalkene **1**'s first reductive Nef interaction with the corresponding oxime **I** [167], which intramolecularly combines with the carbonyl function to produce the five-membered ring **II**, which ultimately yields the isoxazole system **2** upon dehydration (**Scheme 2.20**).

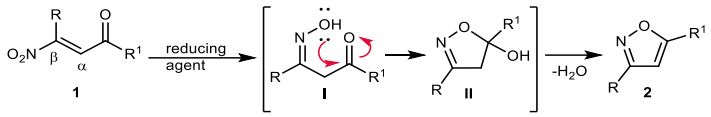

Scheme 2.20 Probable reaction mechanism.

2.5.2 Results and discussion

We profiled the conversion of **1a** into **2a** in terms of solvent, temperature, reaction time, stoichiometry, and reducing species in order to determine the ideal reaction conditions. We tested the reaction using two equivalents of tin(ii) chloride dihydrate in various solvents at room temperature because of its known ability to give oximes [47, 168, 169] (**Table 2.6, entries a–e**). While performing the reaction in dichloromethane (DCM) and toluene, the reaction was totally unsuccessful; however, dioxane, 2-methyltetrahydrofuran (2-MeTHF), and ethyl acetate produced significant yields of **2a**. We examined various reaction temperatures after determining that 2-MeTHF and EtOAc were the most promising solvents for the reaction.

Table 2.6 Optimization studies.

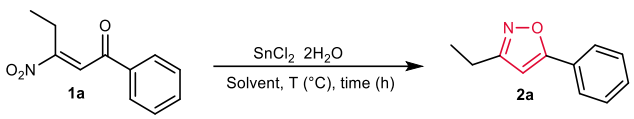

Entry	Solvent	SnCl2.2H2O	Temp. (°C)	Time (h)	Yield (%) of 2a
a	2-MeTHF	2eq	rt	8	34 + 1a
b	Dioxane	″	rt	8	8 + 1a
c	DCM	″	rt	8	1a
d	Toluene	″	rt	8	1a
e	EtOAc	″	rt	8	32 + 1a
f	2-MeTHF	″	50	8	42 + 1a
g	2-MeTHF	″	Reflux	2	69
h	2-MeTHF	″	90°C (MW)	2	74
i	EtOAc	″	50	8	44 + 1a
j	EtOAc	″	Reflux	2	70
k	EtOAc	″	90°C (M.W)	2	79
l	EtOAc	″	90°C (Sand Bath)	2	73
m	EtOAc	1.5 eq	90°C (M.W)	2	50
n	EtOAc	2.5 eq	90°C (M.W)	2	77

Increasing the temperature up to 50 °C, provided similar results to those obtained at room temperature, with **2a** produced in a slightly improved yield (**Table 2.6, entries f and i**). Subsequently, we increased the reaction temperature to reflux conditions, which led to the complete consumption of **1a** within two hours, yielding **2a** in 69% and 70%, respectively (boiling points: 2-MeTHF ≈ 80 °C; EtOAc ≈ 77 °C; (**Table 2.6, entries g and j**). Finally, we employed microwave heating using a Biotage® Initiator microwave synthesizer and raised the temperature further to 90 °C. This resulted in a cleaner reaction mixture and higher yields, with the best yield (79%) achieved in EtOAc (**Table 2.6, entries f–k**). This outcome most likely results from the more effective energy transfer that takes place under microwave irradiation as opposed to the traditional heating method [170]. To further optimize the reaction conditions, we repeated it at 90 °C in a sealed vial using a sand bath, which resulted in a lower yield of **2a** (**Table 2.6, entry l**). Importantly, decreasing the amount of tin(II) chloride dihydrate from 2.0 to 1.5 equivalents significantly suppresses the yield, while increasing it to 2.5 equivalents results in no improvement (**Table 2.6, entries m & n**). In very last, we attempted to conversion of **1a** into **2a** using $FeCl_3$, $FeCl_2.4H_2O$, CuCl, and $CrCl_2$, however, only chromium(II) chloride supported the isolation of **2a**, albeit in a very low yield (8%).

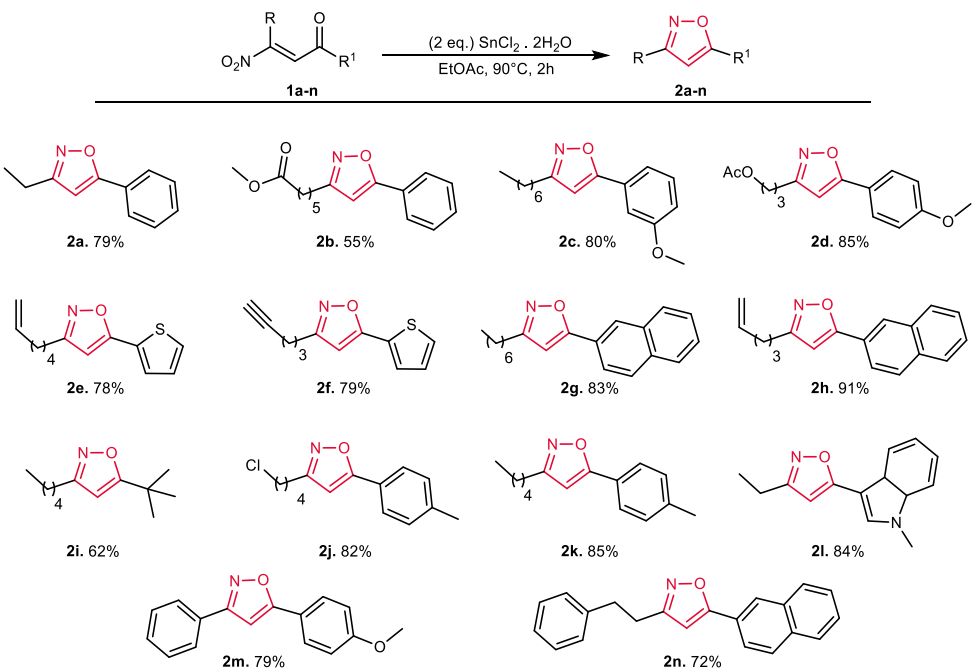

Scheme 2.21 Substrate scope.

To further demonstrate the versatility of our protocol, we tested the optimized reaction conditions to a number of *β*-nitroenones (**1a–n**) (**Scheme 2.21**).

In all cases, the desired isoxazoles derivatives (**2a–n**) were isolated in good to very good yields (55–91%). Additionally, the mild reaction conditions allowed for the inclusion of various functional groups including chlorine, ester, thiophene, ether, and both double and triple bonds, within the substrate.

As expansion, to study the process from automation perspective, we explored the conversion of β-nitroenones **1a–c** under continuous flow chemical conditions using a Uniqsis FlowLab™ system. This setup comprised two HPLC pumps and two reservoirs: among them the reservoir **A** carried the ethyl acetate solution of β-nitroenones **1**, and reservoir **B** contained $SnCl_2.2H_2O$ in ethyl acetate. The system also included a T-connector (T) at the intersection of both the reservoirs, a pre heated reactor equipped with a 10 mL PTFE coil reactor (R), and a back-pressure regulator (BPR) adjusted at 40 psi (**Figure 2.17**).

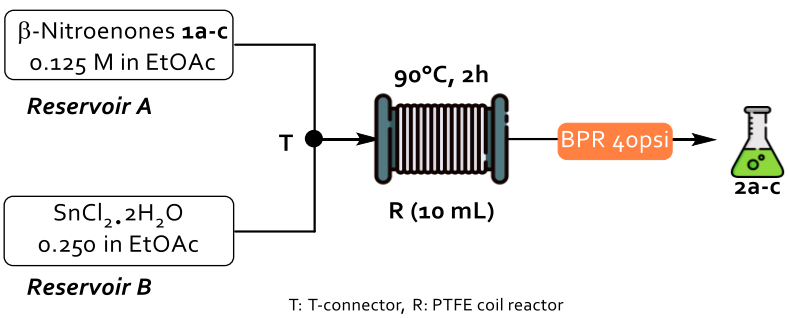

Figure 2.17 Scheme of the flow chemical equipment.

By applying the optimal batch conditions to the flow chemical setup (90 °C with a 2-hour residence time), the targeted isoxazole derivatives **2a–c** were obtained in higher yields in comparison to the batch process, which is most likely attributable to the enhanced efficiency of mass and energy transfer in the flow system than the batch approach [171-177] (**Table 2.7**).

Table 2.7 Trials under flow conditions.

Entry	Yield in M.W	Yield in Flow
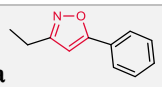 **2a**	79%	84%
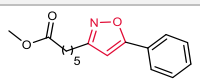 **2b**	55%	68%
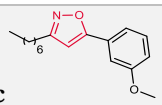 **2c**	80%	86%

2.5.3 Conclusion

To sum up, we have further explored the versatility of *β*-nitroenones as essential building blocks of favored structures in medicinal chemistry. More precisely, we reported a novel, straightforward, and universal method for microwave-induced conversion of *β*-nitroenones into 3,5-disubstituted isoxazoles. Use of mild reaction conditions promoted the compatibility with various functional groups, the methodology enables the production of the subject compounds in very good yields. Moreover, yield improvement and simple process automation were made possible by the expansion of our methodology to flow chemical conditions.

2.5.4 Experimental section

1H NMR spectra were recorded at 400 MHz using a Varian Mercury Plus 400 spectrometer, while 13C NMR spectra were acquired at 100 MHz. IR spectra were obtained with a PerkinElmer Spectrum Two UATR FTIR spectrometer. Elemental analyses were conducted using a Fison Instruments CHNS-O analyzer (Model EA 1108). GC-MS analyses were performed on a Hewlett-Packard 6890 N GC/MS system employing the EI technique at 70 eV. Flow chemical reactions were carried out using a Uniqsis FlowLab™ system, and microwave irradiation experiments were conducted with a Biotage® Initiator. The compounds **1a–n** were synthesized from alkyl- and arylglyoxals and nitro compounds, following established procedures.

2.5.4.1. Batch general procedure

Using a Biotage® Initiator, a solution of the suitable *β*-nitroenone **1a–n** (1 mmol) and tin(II) chloride dihydrate (2 mmol) in 13 mL of ethyl acetate was microwave-irradiated for two hours at 90 °C. The mixture was then moved to a separatory funnel, treated with 30 milliliters of 0.5 N aqueous HCl, and extracted using three milliliters of fresh ethyl acetate. Anhydrous Na_2SO_4 was used to dry the mixed organic layers. The crude product **2a–n** was purified using flash column

chromatography (Hexane: EtOAc = 95:5) after the drying agent was filtered out and the solvent was evaporated under low pressure.

2.5.4.2. Flow general procedure

The appropriate *β*-nitroenone **1a–c** (1 mmol) was dissolved in ethyl acetate (6.5 mL) and charged in reservoir A, while tin(II) chloride dihydrate (2 mmol) was dissolved in ethyl acetate (6.5 mL) and loaded in reservoir B. Both solutions were simultaneously pumped at a flow rate of 0.042 mL min^{-1} per pump into a T-connector, then directed through a 10 mL PTFE coil reactor pre-heated at 90 °C, ensuring a residence time of 2 hours. The reactor outflow was collected in a flask containing 30 mL of stirring 0.5 N aqueous HCl. The layers were separated, the aqueous phase was extracted with fresh ethyl acetate (3 × 30 mL), and the combined organic layers were dried over anhydrous Na_2SO_4. After filtration of sodium sulfate and removing the solvent under reduced pressure, the crude product **2a–c** was purified by flash column chromatography (hexane : EtOAc = 95 : 5).

2.5.4.3. Characterization data

3-Ethyl-5-phenylisoxazole (2a)

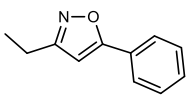

Yellow oil. IR (cm^{-1} , neat): 1615, 1575, 1450, 1420, 947, 762, 689. ^{1}HNMR (400 MHz, $CDCl_3$) δ: 7.79-7.72 (m, 2H), 7.50-7.36 (m, 3H), 6.38 (s, 1H), 2.74 (q, 2H, J = 7.6 Hz), 1.32 (t, 3H, J = 7.6 Hz). ^{13}C-NMR (100 MHz, $CDCl_3$) δ: 169.7, 165.9, 130.1, 129.0, 127.8, 125.9, 99.0, 19.8, 12.8. GC-MS (EI, 70 eV): m/z: 173 ([M+], 98), 131 (12), 105 (100), 77 (56), 68 (18), 51 (17). Anal. Calcd. For $C_{11}H_{11}NO$ (173.21): C, 76.28; H, 6.40; N, 8.09. Found: C, 76.32; H, 6.37; N, 8.12.

Methyl 6-(5-phenylisoxazol-3-yl)hexanoate (2b)

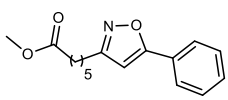

White solid; m.p. = 30-34°C. IR (cm^{-1} , neat): 2940, 1722, 614, 1593, 1575, 1453, 1431, 1203, 1175, 767, 691. ^{1}H-NMR (400 MHz, $CDCl_3$) δ: 7.75 (dd, 2H, J = 8.0, 1.6 Hz), 7.48-7.38 (m, 3H), 6.37 (s, 1H), 3.66 (s, 3H), 2.71 (t, 2H, J = 7.6 Hz), 2.32 (t, 2H, J = 7.5 Hz), 1.79-1.63 (m, 4H), 1.48-1.37 (m, 2H). ^{13}C-NMR (100 MHz, $CDCl_3$) δ: 174.2, 169.7, 164.5, 130.1, 129.0, 127.8, 125.9, 99.2, 51.6, 34.0, 28.8, 28.1, 26.1, 24.7. GC-MS (EI, 70 eV): m/z: 273 ([M+], 7), 272 (9), 242 (17), 200

(18), 172 (42), 159 (100), 131 (14), 105 (34), 77 (23). Anal. Calcd. For $C_{16}H_{19}NO_3$ (273.33): C, 70.31; H, 7.01; N, 5.12. Found: C, 70.28; H, 7.03; N, 5.10.

3-Heptyl-5-(3-methoxyphenyl)isoxazole (2c)

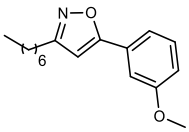

Yellow oil. IR (cm^{-1} , neat): 2926, 1601, 1576, 1466, 1436, 1228, 1041, 779, 685. ^{1}H-NMR (400 MHz, $CDCl_3$) δ: 7.38-7.27 (m, 3H), 6.95 (dt, 1H, J = 6.7, 2.6 Hz), 6.36 (s, 1H), 3.85 (s, 3H), 2.72-2.66 (m, 2H), 1.76-1.63 (m, 2H), 1.45-1.20 (m, 8H), 0.88 (t, 3H, J = 6.9 Hz). ^{13}C-NMR (100 MHz, $CDCl_3$) δ: 169.4, 164.9, 160.0, 129.0, 128.8, 118.3, 116.0, 110.9, 99.5, 55.5, 31.8, 29.3, 29.1, 28.5, 26.2, 22.7, 14.2. GC-MS (EI, 70 eV): m/z: 273 ([M+], 18), 230 (19), 202 (64), 189 (100), 161 (14), 135 (23), 107 (12), 77 (10), 41 (10). Anal. Calcd. For $C_{17}H_{23}NO_2$ (273.38): C, 74.69; H, 8.48; N, 5.12. Found: C, 74.73; H, 8.51; N, 5.10.

3-(5-(4-Methoxyphenyl)isoxazol-3-yl)propyl acetate (2d)

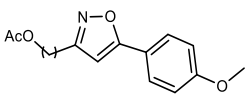

Pale pink solid, m.p. = 85-87°C. IR (cm^{-1} , neat): 1735, 1618, 1514, 1472, 1234, 1175, 1019, 836, 827, 608, 523, 408. ^{1}H-NMR (400 MHz, $CDCl_3$) δ: 7.68 (d, 2H, J = 8.9 Hz), 6.95 (d, 2H, J = 8.9 Hz), 6.25 (s, 1H), 4.15 (t, 1H, J = 6.4 Hz), 3.84 (s, 3H), 2.81-2.73 (m, 2H), 2.11-1.98 (m, 2H), 2.05 (s, 3H). ^{13}C-NMR (100 MHz, $CDCl_3$) δ: 171.1, 169.8, 163.5, 161.0, 127.3, 120.3, 114.3, 97.7, 63.5, 55.4, 27.3, 22.9, 20.9. GC-MS (EI, 70 eV): m/z: 275 ([M+], 21), 232 (12), 189 (100), 161 (11), 135 (47), 77 (10), 43 (16). Anal. Calcd. For $C_{15}H_{17}NO_4$ (275.30): C, 65.44; H, 6.22; N, 5.09. Found: C, 65.48; H, 6.25; N, 5.07.

3-(Hex-5-en-1-yl)-5-(thiophen-2-yl)isoxazole (2e)

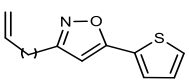

Orange oil. IR (cm^{-1} , neat): 2927, 1638, 1603, 1423, 907, 850, 703. ^{1}H-NMR (400 MHz, $CDCl_3$) δ: 7.47 (dd, 1H, J = 3.7, 1.2 Hz), 7.41 (dd, 1H, J = 5.0, 1.2 Hz), 7.10 (dd, 1H, J = 5.0, 3.7 Hz), 6.23 (s, 1H), 5.86-5.73 (m, 1H), 5.05-4.91 (m, 2H), 2.69 (t, 2H, J = 7.6 Hz), 2.15-2.05 (m, 2H), 1.76-1.64 (m, 2H), 1.54-1.43 (m, 2H). ^{13}C-NMR (100 MHz, $CDCl_3$) δ: 164.7, 164.6, 138.6, 129.7, 128.1, 127.8, 126.8, 114.9, 99.0, 33.5, 28.5, 27.8, 26.0. GC-MS (EI, 70 eV): m/z: 234 ([M+1+], 4), 233 ([M+], 26), 232 (24), 204 (14), 178 (49), 165 (100), 122 (37), 111 (93), 41 (28), 39 (29).

Anal. Calcd. For $C_{13}H_{15}NOS$ (233.33): C, 66.92; H, 6.48; N, 6.00; S, 13.74. Found: C, 66.96; H, 6.51; N, 5.98; S, 13.71.

3-(Pent-4-yn-1-yl)-5-(thiophen-2-yl)isoxazole (2f)

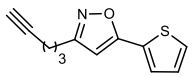

Yellow oil. IR (cm^{-1} , neat): 2115, 1600, 1424, 850, 794, 705. ^{1}H-NMR (400 MHz, $CDCl_3$) δ: 7.48 (dd, 1H, J = 3.7, 1.2 Hz), 7.43 (dd, 1H, J = 5.0, 1.2 Hz), 7.11 (dd, 1H, J = 5.0, 3.7 Hz), 6.27 (s, 1H), 2.85-2.80 (m, 2H), 2.31 (dt, 2H, J = 7.0, 2.7 Hz), 2.01 (t, 1H, J = 2.7 Hz), 1.98-1.89 (m, 2H). ^{13}C-NMR (100 MHz, $CDCl_3$) δ: 164.9, 163.8, 129.6, 128.2, 127.9, 127.0, 99.1, 83.5, 69.4, 27.1, 25.1, 18.1. GC-MS (EI, 70 eV): m/z: 218 ([M+1+], 4), 217 ([M+], 20), 216 (19), 188 (31), 165 (93), 136 (19), 111 (100), 39 (44). Anal. Calcd. For $C_{12}H_{11}NOS$ (217.29): C, 66.33; H, 5.10; N, 6.45; S, 14.75. Found: C, 66.29; H, 5.08; N, 6.48; S, 14.72.

3-Heptyl-5-(naphthalen-2-yl)isoxazole (2g)

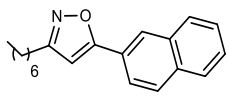

White solid; m.p. = 53-55°C. IR (cm^{-1} , neat): 2919, 1614, 1587, 1567, 1461, 1422, 860, 827, 797, 746, 725, 475. ^{1}H-NMR (400 MHz, $CDCl_3$) δ: 8.28 (s, 1H), 7.95-7.75 (m, 4H), 7.57-7.47 (m, 2H), 6.48 (s, 1H), 2.73 (t, 2H, J = 7.7 Hz), 1.80-1.67 (m, 2H), 1.48-1.22 (m, 8H), 0.90 (t, 3H, J = 6.7 Hz). ^{13}C-NMR (100 MHz, $CDCl_3$) δ: 169.5, 164.9, 133.8, 133.1, 128.8, 128.6, 127.8, 127.2, 126.9, 125.4, 124.9, 123.0, 99.5, 31.7, 29.2, 29.0, 28.4, 26.2, 22.7, 14.1. GC-MS (EI, 70 eV): m/z: 293 ([M+], 24), 250 (15), 222 (55), 209 (100), 181 (18), 155 (27), 127 (35). Anal. Calcd. For $C_{20}H_{23}NO$ (293.41): C, 81.87; H, 7.90; N, 4.77. Found: C, 81.91; H, 7.93; N, 4.80.

5-(Naphthalen-2-yl)-3-(pent-4-en-1-yl)isoxazole (2h)

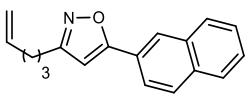

Yellow waxy solid. IR (cm^{-1} , neat): 2929, 1636, 1600, 1425, 855, 825, 799, 745, 723, 479. ^{1}H-NMR (400 MHz, $CDCl_3$) δ: 8.29 (s, 1H), 7.95- 7.77 (m, 4H), 7.57-7.50 (m, 2H), 6.49 (s, 1H), 5.92-5.78 (m, 1H), 5.12-4.99 (m, 2H), 2.76 (t, 2H, J = 7.7 Hz), 2.24-2.13 (m, 2H), 1.92-1.80 (m, 2H). ^{13}C-NMR (100 MHz, $CDCl_3$) δ: 169.6, 164.5, 137.8, 133.8, 133.1, 128.8, 128.6, 127.8, 127.2, 126.9. 125.4, 124.9, 123.0, 115.4, 99.5, 33.2, 27.5, 25.6. GC-MS (EI, 70 eV): m/z: 263 ([M+], 44), 209 (100), 181 (31), 155 (33), 127 (57), 108 (12). Anal. Calcd. For $C_{18}H_{17}NO$ (263.34): C, 82.10; H, 6.51; N, 5.32. Found: C, 82.06; H, 6.48; N, 5.30.

5-(tert-Butyl)-3-pentylisoxazole (2i)

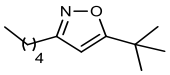

Pale yellow oil. IR (cm^{-1}, neat): 2935, 1614, 1598, 1501, 1464, 1399. ^{1}H-NMR (400 MHz, $CDCl_3$) δ: 5.75 (s, 1H), 2.62-2.56 (m, 2H), 1.70-1.57 (m, 2H), 1.39-1.24 (m, 4H), 1.31 (s, 9H), 0.89 (t, 3H, J = 7.1 Hz). ^{13}C-NMR (100 MHz, $CDCl_3$) δ: 180.8, 163.8, 97.8, 32.6, 31.5, 29.9, 28.0, 26.1, 22.3, 13.9. GC-MS (EI, 70 eV): m/z: 195 ([M+], 5), 166 (11), 152 (55), 139 (100), 82 (16), 57 (15), 40 (20). Anal. Calcd. For $C_{12}H_{21}NO$ (195.31): C, 73.80; H, 10.84; N, 7.17. Found: C, 73.77; H, 10.87; N, 7.15.

3-(4-Chlorobutyl)-5-(p-tolyl)isoxazole (2j)

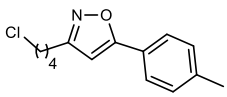

White solid; m.p. = 62-64°C. IR (cm^{-1}, neat): 2946, 1616, 1600, 1514, 1462, 1424, 1328, 829, 789, 771, 506. ^{1}H-NMR (400 MHz, $CDCl_3$) δ: 7.65 (d, 2H, J = 8.1 Hz), 7.25 (d, 2H, J = 8.0 Hz), 6.33 (S, 1H), 3.58 (t, 2H, J = 5.9 Hz), 2.74 (t, 2H, J = 7.0 Hz), 2.39 (s, 3H), 1.92-1.82 (m, 4H). ^{13}C-NMR (100 MHz, $CDCl_3$) δ: 170.0, 163.9, 140.3, 129.6, 125.7, 124.8, 98.4, 44.6, 31.8, 25.4, 25.3, 21.5. GC-MS (EI, 70 eV): m/z: 249 ([M+], 10), 214 (100), 186 (54), 119 (40), 91 (27), 65 (9). Anal. Calcd. For $C_{14}H_{16}ClNO$ (249.74): C, 67.33; H, 6.46; N, 5.61. Found: C, 67.36; H, 6.43; N, 5.59.

3-Pentyl-5-(p-tolyl)isoxazole (2k)

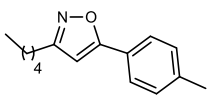

IR (cm^{-1}, neat): 2928, 1621, 1602, 1515, 1465, 1427, 820, 789, 504. ^{1}H-NMR (400 MHz, $CDCl_3$) δ: 7.65 (d, 2H, J = 8.1 Hz), 7.25 (d, 2H, J = 8.0 Hz), 6.32 (s, 1H), 2.69 (t, 2H, J = 7.7 Hz), 2.39 (s, 3H), 1.77-1.58 (m, 2H), 1.45-1.29 (m, 4H), 0.91 (t, 3H, J = 6.7 Hz). ^{13}C-NMR (100 MHz, $CDCl_3$) δ: 169.7, 164.7, 140.2, 129.6, 125.7, 125.0, 98.5, 31.4, 28.1, 26.1, 22.4, 21.4, 13.9. GC-MS (EI, 70 eV): m/z: 229 ([M+], 9), 228 (15), 200 (11), 186 (42), 173 (100), 145 (14), 119 (42), 91 (28). Anal. Calcd. For $C_{15}H_{19}NO$ (229.32): C, 78.56; H, 8.35; N, 6.11. Found: C, 78.60; H, 8.32; N, 6.09.

3-Ethyl-5-(1-methyl-1H-indol-3-yl)isoxazole (2l)

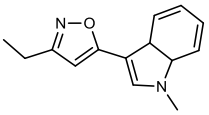

White solid; m.p. = 63-65°C. IR (cm^{-1} , neat): 1624, 1609, 1357, 1344, 1092, 760, 750, 731, 420. ^{1}H-NMR (400 MHz, $CDCl_3$) δ: 7.94 (d, 1H, J = 6.9 Hz), 7.56 (s, 1H), 7.40-7.24 (m, 3H), 6.28 (s, 1H), 3.84 (s, 3H), 2.77 (q, 2H, J = 7.6 Hz), 1.35 (t, 3H, J = 7.6 Hz). ^{13}C-NMR (100 MHz, $CDCl_3$) δ: 166.1, 165.5, 137.1, 128.5, 124.8, 122.7, 121.0, 120.1, 109.9, 104.2, 96.6, 33.2, 19.7, 12.8. GC-MS (EI, 70 eV): m/z: 227 ([M+1+], 16), 226 ([M+], 100), 169 (12), 158 (62), 156 (18). Anal. Calcd. For $C_{14}H_{14}N_2O$ (226.28): C, 74.31; H, 6.24; N, 12.38. Found: C, 74.28; H, 6.22; N, 12.40.

5-(4-Methoxyphenyl)-3-phenylisoxazole (2m)

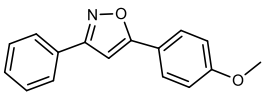

White solid; m.p. = 102-104°C. IR (cm-1 , neat): 1614, 1598, 1501, 1464, 1399, 1260, 1248, 1177, 1033, 840, 800, 768, 690. 1H-NMR (400 MHz, CDCl3) δ: 7.88-7.84 (m, 2H), 7.78 (d, 2H, J = 8.9 Hz), 7.51-7.41 (m, 3H), 7.00 (d, 2H, J = 8.9 Hz), 6.71 (s, 1H), 3.86 (s, 3H). 13C-NMR (100 MHz, CDCl3) δ: 170.4, 162.9, 161.1, 129.9, 129.3, 128.9, 127.4, 126.8, 120.3, 114.4, 96.1, 55.4. GC-MS (EI, 70 eV): m/z: 252 ([M+1+], 14), 251 ([M+], 81), 135 (100), 77 (24). Anal. Calcd. For C16H13NO2 (251.28): C, 76.48; H, 5.21; N, 5.57. Found: C, 76.51; H, 5.19; N, 5.59.

5-(Naphthalen-2-yl)-3-phenethylisoxazole (2n)

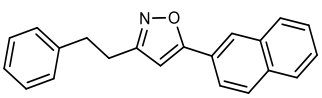

Pale yellow solid; m.p. = 84-89 °C. IR (cm^{-1} , neat): 1602, 1422, 853, 821, 797, 741, 722, 477. ^{1}H-NMR (400 MHz, $CDCl_3$) δ: 8.28 (s, 1H), 7.96-7.83 (m, 3H), 7.79 (dd, 1H, J = 8.6, 1.6 Hz), 7.57-7.51 (m, 2H), 7.37-7.21 (m, 5H), 6.42 (s, 1H), 3.08 (s, 4H). ^{13}C-NMR (100 MHz, $CDCl_3$) δ: 169.6, 164.0, 140.7, 133.8, 133.1, 128.8, 128.7, 128.6, 128.4,127.9, 127.2,126.9, 126.4,125.5, 124.8, 123.0, 99.7, 34.5, 28.1. GC-MS (EI, 70 eV): m/z: 299 ([M+], 100), 270 (16), 195 (25), 155 (71), 144 (47), 127 (62), 91 (41). Anal. Calcd. For $C_{21}H_{17}NO$ (299.37): C, 84.25; H, 5.72; N, 4.68. Found: C, 84.22; H, 5.69; N, 4.70.

2.5.5 References

[1] S. Z. Zard and S. Z. Zard, "Some Aspects of the Chemistry of Nitro Compounds," *Helvetica Chimica Acta,* vol. 95, no. 10, 2012, doi: 10.1002/hlca.201200324.

[2] N. Nishiwaki, "Nitro Compounds and Their Derivatives in Organic Synthesis," 2020, doi: 10.3390/books978-3-03943-149-6.

[3] W. Luo *et al.*, "Nitrogen-containing heterocyclic drug products approved by the FDA in 2023: Synthesis and biological activity," *European Journal of Medicinal Chemistry,* vol. 279, 2024/12/05, doi: 10.1016/j.ejmech.2024.116838.

[4] D. M. Badgujar, M. B. Talawar, S. N. Asthana, and P. P. Mahulikar, "Advances in science and technology of modern energetic materials: An overview," *Journal of Hazardous Materials,* vol. 151, no. 2-3, 2008/03/01, doi: 10.1016/j.jhazmat.2007.10.039.

[5] Guobing Yan, Minghua Yang, Guobing Yan, and Minghua Yang, "Recent advances in the synthesis of aromatic nitro compounds," *Organic & Biomolecular Chemistry,* vol. 11, no. 16, 2013/04/28, doi: 10.1039/C3OB27354G.

[6] S. Noriega *et al.*, "The Diverse Biological Activity of Recently Synthesized Nitro Compounds," *Pharmaceuticals 2022, Vol. 15, Page 717,* vol. 15, no. 6, 2022-06-05, doi: 10.3390/ph15060717.

[7] S. Zlotin, I. Dalinger, N. Makhova, and V. Tartakovsky, "Nitro compounds as the core structures of promising energetic materials and versatile reagents for organic synthesis," *Russian Chemical Reviews,* vol. 89, no. 1, 2020, doi: 10.1070/rcr4908.

[8] A. Kumar *et al.*, "Nitrogen Containing Heterocycles as Anticancer Agents: A Medicinal Chemistry Perspective," *Pharmaceuticals 2023, Vol. 16, Page 299,* vol. 16, no. 2, 2023-02-14, doi: 10.3390/ph16020299.

[9] C. Sahu, A. Chaurasiya, and P. A. Chawla, "Nitrogen-containing heterocycles as topoisomerase II inhibitors for targeting cancer: Recent updates," *Journal of Heterocyclic Chemistry,* vol. 60, no. 6, 2023/06/01, doi: 10.1002/jhet.4588.

[10] S. Bhunia, G. G. Pawar, S. V. Kumar, Y. Jiang, and D. Ma, "Selected Copper-Based Reactions for C−N, C−O, C−S, and C−C Bond Formation," *Angewandte Chemie International Edition,* vol. 56, no. 51, 2017/12/18, doi: 10.1002/anie.201701690.

[11] P. Ruiz-Castillo and S. L. Buchwald, "Applications of Palladium-Catalyzed C–N Cross-Coupling Reactions," *Chemical Reviews,* vol. 116, no. 19, September 30, 2016, doi: 10.1021/acs.chemrev.6b00512.

[12] Marcel Hoogenraad *et al.*, "Accelerated Process Development of Pharmaceuticals: Selective Catalytic Hydrogenations of Nitro Compounds Containing Other Functionalities," *Organic Process Research & Development,* vol. 8, no. 3, March 27, 2004, doi: 10.1021/op0341667.

[13] A. M. Rohit K. Rai, Sushobhan Mukhopadhyay,Sampa Gupta,Pei-Zhou Li,Kim T. Nguyen,Yanli Zhao,Biswarup Pathak,Sanjay K. Singh, "Room-Temperature Chemoselective Reduction of Nitro Groups Using Non-noble Metal Nanocatalysts in Water," *Inorganic Chemistry,* vol. 53, no. 6, 2014, doi: 10.1021/ic402674z.

[14] P. Tomkins, E. Gebauer-Henke, and T. E. Müller, "Molecular Assembly Line: Stepwise Hydrogenation of Multifunctional Substrates over Catalyst Mixtures," *ChemCatChem,* vol. 8, no. 3, 2016/02/01, doi: 10.1002/cctc.201500988.

[15] S.-Z. Song, Y. Dong, G.-P. Ge, Q. Li, and W.-T. Wei, "Recent Advances in Radical Nitration Using tert-Butyl Nitrite," *Synthesis,* vol. 52, no. 06, 2020/03, doi: 10.1055/s-0039-1690789.

[16] R. Ballini, G. Bosica, M. Damiani, and P. Righi, "Nitroalkanes as a new source of 2-alkylidene-1,4-diols, in two steps," *Tetrahedron,* vol. 55, no. 47, 1999/11/19, doi: 10.1016/S0040-4020(99)00829-7.

[17] F. A. Luzzio, "The Henry reaction: recent examples," *Tetrahedron,* vol. 57, no. 6, 2001/02/04, doi: 10.1016/S0040-4020(00)00965-0.

[18] Roberto Ballini, Giovanna Bosica, Dennis Fiorini, a. Alessandro Palmieri, and M. Petrini*, "Conjugate Additions of Nitroalkanes to Electron-Poor Alkenes: Recent Results," February 3, 2005, doi: 10.1021/cr040602.

[19] R. Ballini and M. Petrini, "ChemInform Abstract: Nitroalkanes as Key Building Blocks for the Synthesis of Heterocyclic Derivatives," *ChemInform,* vol. 40, no. 22, 2009/06/02, doi: 10.1002/chin.200922249.

[20] R. Ballini *et al.*, "Acyclic α-nitro ketones : a versatile class of α-functionalized ketones in organic synthesis," *Tetrahedron,* vol. 61, no. 38, 2005, doi: 10.1016/j.tet.2005.06.033.

[21] R. Ballini *et al.*, "Recent developments on the chemistry of aliphatic nitro compounds under aqueous medium," *Green Chemistry,* vol. 9, no. 8, 2007/08/01, doi: 10.1039/B702334K.

[22] B. R, B. L, and G. G, "Nitroalkanes in aqueous medium as an efficient and eco-friendly source for the one-pot synthesis of 1,4-diketones, 1,4-diols, delta-nitroalkanols, and hydroxytetrahydrofurans - PubMed," *The Journal of organic chemistry,* vol. 68, no. 23, 11/14/2003, doi: 10.1021/jo0351163.

[23] R. Ballini, R. Ballini, L. Barboni, L. Barboni, A. Palmieri, and A. Palmieri, "Improved chemoselective, ecofriendly conditions for the conversion of primary alkyl halides into nitroalkanes under PEG400," *Green Chemistry,* vol. 10, no. 9, 2008/09/01, doi: 10.1039/B805985C.

[24] R. Ballini and A. Palmieri, "Synthetic Procedures for the Preparation of Nitroalkanes," *Advanced Synthesis & Catalysis,* vol. 360, no. 12, 2018/06/15, doi: 10.1002/adsc.201800163.

[25] A. Palmieri, S. Gabrielli, R. Ballini, A. Palmieri, S. Gabrielli, and R. Ballini, "Easy and direct conversion of tosylates and mesylates into nitroalkanes," *Beilstein Journal of Organic Chemistry,* vol. 9, no. 1, 2013-03-14, doi: 10.3762/bjoc.9.58.

[26] D. SE and T. A, "Tandem [4+2]/[3+2] Cycloadditions of Nitroalkenes - PubMed," *Chemical reviews,* vol. 96, no. 1, 02/01/1996, doi: 10.1021/cr940277.

[27] Z. Wang *et al.*, "Tandem Michael Addition–Cyclization of Nitroalkenes with 1,3-Dicarbonyl Compounds Accompanied by Removal of Nitro Group," *The Journal of Organic Chemistry,* September 8, 2021, doi: 10.1021/acs.joc.1c01586.

[28] H. Ishitani, Y. Furiya, and S. Kobayashi, "Continuous-flow synthesis using a column reactor packed with heterogeneous catalysts: A convenient production of nitroolefins by using amino-functionalized silicagel," *Bioorganic & Medicinal Chemistry,* vol. 25, no. 23, 2017/12/01, doi: 10.1016/j.bmc.2017.04.017.

[29] M. Hassan *et al.*, "Streamlined One-Pot Synthesis of Nitro Fatty Acids," *European Journal of Organic Chemistry,* vol. 2021, no. 15, 2021/04/22, doi: 10.1002/ejoc.202100247.

[30] M. Hassan, C. N. Nde, and G. Manolikakes, "Synthesis of Nitroolefins via the Direct Nitration of Alkenes," *SynOpen,* vol. 05, no. 03, 2021/07, doi: 10.1055/a-1577-4661.

[31] Stefania Fioravanti, Lucio Pellacani, a. Paolo A. Tardella, and M. C. Vergari, "Facile and Highly Stereoselective One-Pot Synthesis of Either (E)- or (Z)-Nitro Alkenes," February 27, 2008, doi: 10.1021/ol800224.

[32] S. Manna *et al.*, "Synthesis of (E)-nitroolefins via decarboxylative nitration using t-butylnitrite (t-BuONO) and TEMPO," *Chemical Communications,* vol. 49, no. 46, 2013/05/14, doi: 10.1039/C3CC41576G.

[33] Guobing Yan, A. Jyoti Borah, Lianggui Wang, Guobing Yan, A. Jyoti Borah, and Lianggui Wang, "Recent advances in the synthesis of nitroolefin compounds," *Organic & Biomolecular Chemistry,* vol. 12, no. 32, 2014/07/23, doi: 10.1039/C4OB00573B.

[34] J. M. Rodríguez and M. D. Pujol, "Straightforward synthesis of nitroolefins by microwave- or ultrasound-assisted Henry reaction," *Tetrahedron Letters,* vol. 52, no. 21, 2011/05/25, doi: 10.1016/j.tetlet.2011.03.037.

[35] S. M. Soham Maity, Sujoy Rana,Togati Naveen,Arijit Mallick,Debabrata Maiti, "Efficient and Stereoselective Nitration of Mono- and Disubstituted Olefins with AgNO₂ and TEMPO," *Journal of the American Chemical Society,* vol. 135, no. 9, 2013, doi: 10.1021/ja311942e.

[36] S. M. Togati Naveen, Upendra Sharma, Debabrata Maiti, "A Predictably Selective Nitration of Olefin with Fe(NO₃)₃ and TEMPO," *The Journal of Organic Chemistry,* vol. 78, no. 12, 2013, doi: 10.1021/jo400598p.

[37] K. Zhang, B. Jelier, A. Passera, G. Jeschke, and D. Katayev, "Synthetic Diversity from a Versatile and Radical Nitrating Reagent," *Chemistry – A European Journal,* vol. 25, no. 56, 2019/10/08, doi: 10.1002/chem.201902966.

[38] K. Akutu, H. Kabashima, T. Seki, and H. Hattori, "Nitroaldol reaction over solid base catalysts," *Applied Catalysis A: General,* vol. 247, no. 1, 2003/07/10, doi: 10.1016/S0926-860X(03)00124-8.

[39] R. Ballini, G. Bosica, and P. Forconi, "Nitroaldol (Henry) reaction catalyzed by amberlyst A-21 as a far superior heterogeneous catalyst.," *Tetrahedron,* vol. 52, no. 5, 1996/01/29, doi: 10.1016/0040-4020(95)00996-5.

[40] R. Ballini, G. Bosica, D. Livi, A. Palmieri, R. Maggi, and G. Sartori, "Use of heterogeneous catalyst KG-60-NEt2 in Michael and Henry reactions involving nitroalkanes," *Tetrahedron Letters,* vol. 44, no. 11, 2003/03/10, doi: 10.1016/S0040-4039(03)00274-0.

[41] R. Ballini *et al.*, "Isolute®Si-carbonate catalyzes the nitronate addition to both aldehydes and electron-poor alkenes under solvent-free conditions," *Green Chemistry,* vol. 10, no. 5, 2008/05/01, doi: 10.1039/B719477C.

[42] R. C. Roberto Ballini, Marino Petrini, "Chemoselective synthesis of functionalized conjugated nitroalkenes," *The Journal of Organic Chemistry,* vol. 57, no. 7, 1992, doi: 10.1021/jo00033a045.

[43] D. Lucet, S. Sabelle, O. Kostelitz, T. L. Gall, and C. Mioskowski, "Enantioselective Synthesis of α-Amino Acids and Monosubstituted 1,2-Diamines by Conjugate Addition of 4-Phenyl-2-oxazolidinone to Nitroalkenes," *European Journal of Organic Chemistry,* vol. 1999, no. 10, 1999/10/01, doi: 10.1002/(SICI)1099-0690(199910)1999:10<2583::AID-EJOC2583>3.0.CO;2-E.

[44] S. Gabrielli *et al.*, "Eco-friendly synthesis of β-nitro ketones from conjugated enones: an important improvement of the Miyakoshi procedure," *Green Chemistry,* vol. 13, no. 8, 2011/01/08, doi: 10.1039/C1GC15616K.

[45] R. Ballini, S. Gabrielli, and A. Palmieri, "β -Nitroacrylates as an Emerging, Versatile Class of Functionalized Nitroalkenes for the Synthesis of a Variety of Chemicals," *Current Organic Chemistry,* vol. 14, no. 1, 2010, doi: 10.2174/138527210790226429.

[46] R. Ballini, R. Ballini, M. Petrini, and M. Petrini, "Nitroalkanes as key building blocks for the synthesis of heterocyclic derivatives," *ARKIVOC,* vol. 2009, no. 9, 2008-08-14, doi: 10.3998/ark.5550190.0010.912.

[47] G. W. Kabalka, G. M. H. Laila, and R. S. Varma, "Selected reductions of conjugated nitroalkenes," *Tetrahedron,* vol. 46, no. 21, 1990/01/01, doi: 10.1016/S0040-4020(01)89059-1.

[48] G. W. Kabalka and R. S. Varma, "SYNTHESES AND SELECTED REDUCTIONS OF CONJUGATED NITROALKENES. A REVIEW," *Organic Preparations and Procedures International,* vol. 19, no. 4-5, 1987-8-1, doi: 10.1080/00304948709356200.

[49] D. K. Nair, T. Kumar, and I. N. N. Namboothiri, "α-Functionalization of Nitroalkenes and Its Applications in Organic Synthesis," *Synlett,* vol. 27, no. 17, 2016/10, doi: 10.1055/s-0036-1588587.

[50] M. Ahrach, R. Schneider, P. Gérardin, and B. Loubinoux, "Synthesis of 6,6-Disubstituted Tetrahydrothiopheno [3,4-c] Isoxazolines from β-Nitroenones," *Synthetic Communications,* vol. 27, no. 11, 1997-6-1, doi: 10.1080/00397919708006787.

[51] E. Chiurchiù *et al.*, "A New Valuable Synthesis of Polyfunctionalized Furans Starting from β-Nitroenones and Active Methylene Compounds," *Molecules 2019, Vol. 24, Page 4575,* vol. 24, no. 24, 2019-12-13, doi: 10.3390/molecules24244575.

[52] C. He, X. Tang, X. He, Y. Zhou, X. Liu, and X. Feng, "Regio- and enantioselective conjugate addition of β-nitro α,β-unsaturated carbonyls to construct 3-alkenyl disubstituted oxindoles," *Chinese Chemical Letters,* vol. 34, no. 1, 2023/01/01, doi: 10.1016/j.cclet.2022.05.001.

[53] L. R. H. James C. Anderson, Andreas S. Kalogirou,Matthew R. Mills,Gregory J. Stepney,Graham J. Tizzard, "Stereoselective Synthesis of Densely Functionalized Pyrrolidin-2-ones by a Conjugate Addition/Nitro-Mannich/Lactamization Reaction," *The Journal of Organic Chemistry,* vol. 77, no. 14, 2012, doi: 10.1021/jo301000r.

[54] X. Teng, H. Keys, J. Yuan, A. Degterev, and G. D. Cuny, "Structure–activity relationship and liver microsome stability studies of pyrrole necroptosis inhibitors," *Bioorganic & Medicinal Chemistry Letters,* vol. 18, no. 11, 2008/06/01, doi: 10.1016/j.bmcl.2008.04.048.

[55] A. Palmieri *et al.*, "One-pot synthesis of alkyl pyrrole-2-carboxylates starting from β-nitroacrylates and primary amines," *RSC Advances,* vol. 5, no. 6, 2014/12/12, doi: 10.1039/C4RA13094D.

[56] A. Palmieri *et al.*, "Fast, mild, eco-friendly synthesis of polyfunctionalized pyrroles from β-nitroacrylates and β-enaminones," *Green Chemistry,* vol. 13, no. 12, 2011/12/01, doi: 10.1039/C1GC16012E.

[57] R. Ballini, S. Gabrielli, and A. Palmieri, "β-Nitroacrylates as Precursors of Tetrasubstituted Furans in a One-Pot Process and under Acidic Solvent-Free Conditions.," *Synlett,* vol. 2010, no. 16, 2010/10, doi: 10.1055/s-0030-1258031.

[58] R. Ballini, S. Gabrielli, and A. Palmieri, "β-Nitroacrylates as an Emerging, Versatile Class of Functionalized Nitroalkenes for the Synthesis of a Variety of Chemicals," *Current Organic Chemistry,* vol. 14, no. 1, 2010, doi: 10.2174/138527210790226429.

[59] S. Gabrielli, E. Chiurchiù, and A. Palmieri, "β-Nitroacrylates: A Versatile and Growing Class of Functionalized Nitroalkenes," *Advanced Synthesis & Catalysis,* vol. 361, no. 4, 2019/02/19, doi: 10.1002/adsc.201800709.

[60] E. Chiurchiù, S. Xhafa, R. Ballini, G. Maestri, S. Protti, and A. Palmieri, "Diastereoselective Isomerization of (E)-β-Nitroenones into β-Nitro-β,γ-Unsaturated Ketones under Microwave Conditions," *Advanced Synthesis & Catalysis,* vol. 362, no. 21, 2020/11/04, doi: 10.1002/adsc.202000747.

[61] C. Raviola *et al.*, "Visible-Light-Driven Competitive Stereo- and Regioisomerization of (E)-β-Nitroenones," *ChemPhotoChem,* vol. 5, no. 9, 2021/09/01, doi: 10.1002/cptc.202100081.

[62] A. Palmieri, "Synthesis of Heterocyclic Systems Starting from Carbonyl and Carboxyl Functionalized Nitro Compounds by One-Pot Processes," *European Journal of Organic Chemistry,* vol. 2020, no. 28, 2020/08/02, doi: 10.1002/ejoc.202000079.

[63] S. Gabrielli, E. Chiurchiù, and A. Palmieri, "β-Nitroacrylates: A Versatile and Growing Class of Functionalized Nitroalkenes," (in English), *Advanced Synthesis & Catalysis,* vol. 361, no. 4, pp. 630-653, Feb 19 2019, doi: 10.1002/adsc.201800709.

[64] R. Ballini, S. Gabrielli, and A. Palmieri, "β-Nitroacrylates as Precursors of Tetrasubstituted Furans in a One-Pot Process and under Acidic Solvent-Free Conditions," *Synlett,* vol. 2010, no. 16, 2010/10, doi: 10.1055/s-0030-1258031.

[65] a. Paul T. Anastas*, Mary M. Kirchhoff§, "Origins, Current Status, and Future Challenges of Green Chemistry," *Accounts of Chemical Research,* vol. 35, no. 9, 2002, doi: 10.1021/ar010065m.

[66] P. T. A. István T. Horváth, "Innovations and Green Chemistry," *Chemical Reviews,* vol. 107, no. 6, 2007, doi: 10.1021/cr078380v.

[67] J. H. Clark and J. H. Clark, "Green chemistry: challenges and opportunities," *Green Chemistry,* vol. 1, no. 1, 1999/01/01, doi: 10.1039/A807961G.

[68] A. Palmieri, A. Palmieri, S. Gabrielli, S. Gabrielli, R. Ballini, and R. Ballini, "Low impact synthesis of β-nitroacrylates under fully heterogeneous conditions," *Green Chemistry,* vol. 15, no. 9, 2013/08/16, doi: 10.1039/C3GC40936H.

[69] T. K. Behera, S. N. Islam, S. M. Mobin, and V. Singh, "Cycloaddition of cyclohexa-2,4-dienones with β-nitroacrylates: a short and efficient entry into bicyclo[2.2.2]octanes endowed with β-nitro-ester and β-amino ester

functionality," *Tetrahedron Letters,* vol. 55, no. 37, 2014/09/10, doi: 10.1016/j.tetlet.2014.07.097.

[70] J. B. Metternich and R. Gilmour, "Photocatalytic E → Z Isomerization of Alkenes," *Synlett,* vol. 27, no. 18, 2016/11, doi: 10.1055/s-0036-1588621.

[71] N. T, W. M, M. JJ, and G. R, "Advances in the E → Z Isomerization of Alkenes Using Small Molecule Photocatalysts - PubMed," *Chemical reviews,* vol. 122, no. 2, 01/26/2022, doi: 10.1021/acs.chemrev.1c00324.

[72] B. L. Feringa, "The Art of Building Small: From Molecular Switches to Molecular Motors," *The Journal of Organic Chemistry,* vol. 72, no. 18, 2007, doi: 10.1021/jo070394d.

[73] Ben L. Feringa, Richard A. van Delden, a. Nagatoshi Koumura, and E. M. Geertsema, "Chiroptical Molecular Switches," *Chemical Reviews,* vol. 100, no. 5, April 19, 2000, doi: 10.1021/cr9900228.

[74] H.-B. Cheng, S. Zhang, J. Qi, X.-J. Liang, and J. Yoon, "Advances in Application of Azobenzene as a Trigger in Biomedicine: Molecular Design and Spontaneous Assembly," *Advanced Materials,* vol. 33, no. 26, 2021/07/01, doi: 10.1002/adma.202007290.

[75] Z. Wang *et al.*, "Storing energy with molecular photoisomers," *Joule,* vol. 5, no. 12, 2021/12/15, doi: 10.1016/j.joule.2021.11.001.

[76] H. Wang, H. K. Bisoyi, X. Zhang, F. Hassan, and Q. Li, "Visible Light-Driven Molecular Switches and Motors: Recent Developments and Applications," *Chemistry – A European Journal,* vol. 28, no. 18, 2022/03/28, doi: 10.1002/chem.202103906.

[77] K. Zhan, Y. Li, K. Zhan, and Y. Li, "Visible-Light Photocatalytic E to Z Isomerization of Activated Olefins and Its Application for the Syntheses of Coumarins," *Catalysts 2017, Vol. 7, Page 337,* vol. 7, no. 11, 2017-11-09, doi: 10.3390/catal7110337.

[78] L. K, T. M, P. F, D. CG, J. C, and G. R, "Photocatalytic E → Z Isomerization of β-Ionyl Derivatives - PubMed," *Organic letters,* vol. 21, no. 23, 12/06/2019, doi: 10.1021/acs.orglett.9b03842.

[79] H. M, Z. L, P. T, and L. S, "Deracemization through photochemical E/ Z isomerization of enamines - PubMed," *Science (New York, N.Y.),* vol. 375, no. 6583, 02/25/2022, doi: 10.1126/science.abl4922.

[80] P. Martínez-Bescos *et al.*, "Synthesis, structure, and E-Z isomerization of β-(hetero)aryl-α- nitro-α,β-enals," *Journal of Organic Chemistry,* vol. 73, no. 10, 2008, doi: 10.1021/JO702731.

[81] K. Donnelly, M. Baumann, K. Donnelly, and M. Baumann, "Scalability of photochemical reactions in continuous flow mode," *Journal of Flow Chemistry 2021 11:3,* vol. 11, no. 3, 2021-05-17, doi: 10.1007/s41981-021-00168-z.

[82] C. Sambiagio and T. Noël, "Flow photochemistry: shine some light on those tubes!," *Trends in Chemistry,* vol. 2, no. 2, 2020/02/01, doi: 10.1016/j.trechm.2019.09.003.

[83] J. D. Williams and C. O. Kappe, "Recent advances toward sustainable flow photochemistry," *Current Opinion in Green and Sustainable Chemistry,* vol. 25, 2020/10/01, doi: 10.1016/j.cogsc.2020.05.001.

[84] A. A. Takayoshi Arai, Makiko Wasai,Naota Yokoyama,Hyuma Masu, "Catalytic Asymmetric Friedel–Crafts/Protonation of Nitroalkenes and

N-Heteroaromatics," *The Journal of Organic Chemistry,* vol. 76, no. 13, 2011, doi: 10.1021/jo200546a.

[85] N. Arai and K. Narasaka, "Oxidative Generation of 1-Nitroalkyl Radicals and Their Addition Reaction to Olefins," *Bulletin of the Chemical Society of Japan,* vol. 70, no. 10, 1997/10/01, doi: 10.1246/bcsj.70.2525.

[86] M. Lübbesmeyer, E. G. Mackay, M. A. R. Raycroft, J. Elfert, D. A. Pratt, and A. Studer, "Base-Promoted C–C Bond Activation Enables Radical Allylation with Homoallylic Alcohols," *Journal of the American Chemical Society,* January 16, 2020, doi: 10.1021/jacs.9b12343.

[87] F.-L. Q. Xiaowei Lin, "Palladium-Catalyzed Anti-Markovnikov Hydroalkylation of Homoallylic Alcohols Bearing β-Fluorines," *Organic Letters,* vol. 15, no. 17, 2013, doi: 10.1021/ol402032a.

[88] H. Y. Wei Zhang and, "Vanadium-Catalyzed Asymmetric Epoxidation of Homoallylic Alcohols," *Journal of the American Chemical Society,* vol. 129, no. 2, 2007, doi: 10.1021/ja067495y.

[89] J. F. Scott E. Denmark* and, "Catalytic Enantioselective Addition of Allylic Organometallic Reagents to Aldehydes and Ketones," *Chemical Reviews,* vol. 103, no. 8, 2003, doi: 10.1021/cr020050h.

[90] N. A. Yoshinori. Yamamoto, "Selective reactions using allylic metals," *Chemical Reviews,* vol. 93, no. 6, 1993, doi: 10.1021/cr00022a010.

[91] Z. Lu, X. Zhang, Z. Guo, Y. Chen, T. Mu, and A. Li, "Total Synthesis of Aplysiasecosterol A," *Journal of the American Chemical Society,* vol. 140, no. 29, June 25, 2018, doi: 10.1021/jacs.8b05070.

[92] K. C. Nicolaou, D. Rhoades, and S. M. Kumar, "Total Syntheses of Thailanstatins A–C, Spliceostatin D, and Analogues Thereof. Stereodivergent Synthesis of Tetrasubstituted Dihydro- and Tetrahydropyrans and Design, Synthesis, Biological Evaluation, and Discovery of Potent Antitumor Agents," *Journal of the American Chemical Society,* vol. 140, no. 26, June 26, 2018, doi: 10.1021/jacs.8b04634.

[93] J. C. G.-G. Miguel Yus, Francisco Foubelo, "Diastereoselective Allylation of Carbonyl Compounds and Imines: Application to the Synthesis of Natural Products," *Chemical Reviews,* vol. 113, no. 7, 2013, doi: 10.1021/cr400008h.

[94] M. Tissot and A. Alexakis, "Enantio- and Regioselective Conjugate Addition of Organometallic Reagents to Linear Polyconjugated Nitroolefins," *Chemistry – A European Journal,* vol. 19, no. 34, 2013/08/19, doi: 10.1002/chem.201300538.

[95] B. Tan, P. J. Chua, Y. Li, and G. Zhong, "Organocatalytic Asymmetric Tandem Michael−Henry Reactions: A Highly Stereoselective Synthesis of Multifunctionalized Cyclohexanes with Two Quaternary Stereocenters," *Organic Letters,* vol. 10, no. 12, May 20, 2008, doi: 10.1021/ol8007183.

[96] S. Belot, A. Quintard, N. Krause, and A. Alexakis, "Organocatalyzed Conjugate Addition of Carbonyl Compounds to Nitrodienes/Nitroenynes and Synthetic Applications," *Advanced Synthesis & Catalysis,* vol. 352, no. 4, 2010/03/08, doi: 10.1002/adsc.200900814.

[97] R. Ballini, N. Araújo, M. V. Gil, E. Román, and J. A. Serrano, "Conjugated Nitrodienes. Synthesis and Reactivity," *Chemical Reviews,* vol. 113, no. 5, January 11, 2013, doi: 10.1021/cr2002195.

[98] S. R. Salvatore, P. Rowart, and F. J. Schopfer, "Mass spectrometry-based study defines the human urine nitrolipidome," *Free Radical Biology and Medicine,* vol. 162, 2021/01/01, doi: 10.1016/j.freeradbiomed.2020.10.305.

[99] T. Severin and I. Ipach, "Verlängerung CH-acider Verbindungen um eine gerade Anzahl von Methingruppen durch Umsetzung mit Nitroenaminen," *Chemische Berichte,* vol. 111, no. 2, 1978/02/01, doi: 10.1002/cber.19781110226.

[100] C. Jutz and R. M. Wagner, "Die synchrone Sechs-Elektronen-Cyclisierung von Hexatrien-Systemen als neues Syntheseprinzip zur Darstellung von Aromaten und Heteroaromaten," *Angewandte Chemie,* vol. 84, no. 7, 1972/04/01, doi: 10.1002/ange.19720840714.

[101] T. Severin and B. Brück, "Umsetzungen mit 1-Nitro-2-dimethylamino-äthylen," *Chemische Berichte,* vol. 98, no. 12, 1965/12/01, doi: 10.1002/cber.19650981211.

[102] L. A. Yanovskaya, R. N. Stepanova, V. F. Kucherov, L. A. Yanovskaya, R. N. Stepanova, and V. F. Kucherov, "General method of synthesizing esters of ω-nitropolyenic acids," *Bulletin of the Academy of Sciences of the USSR, Division of chemical science 1965 13:11,* vol. 13, no. 11, 1964/11, doi: 10.1007/BF00844504.

[103] P. K. Kalita and P. Phukan, "Facile chemoselective carbonyl allylation of chalcones with allyltributylstannane catalyzed by CuI," *Tetrahedron Letters,* vol. 54, no. 33, 2013/08/14, doi: 10.1016/j.tetlet.2013.06.037.

[104] J. Augé, N. Lubin-Germain, S. Marque, and L. Seghrouchni, "Indium-catalyzed Barbier allylation reaction," *Journal of Organometallic Chemistry,* vol. 679, no. 1, 2003/08/01, doi: 10.1016/S0022-328X(03)00515-1.

[105] H. Dhanjee and T. G. Minehan, "Indium-mediated allylation of aldehydes, ketones and sulfonimines with 2-(alkoxy)allyl bromides," *Tetrahedron Letters,* vol. 51, no. 42, 2010/10/20, doi: 10.1016/j.tetlet.2010.08.064.

[106] Y. Gao *et al.*, "Zinc or indium-mediated Barbier-type allylation of aldehydes with 3-bromomethyl-5H-furan-2-one in aqueous media: an efficient synthesis method for α-methylene-γ-butyrolactone," *Organic & Biomolecular Chemistry,* vol. 10, no. 20, 2012/05/28, doi: 10.1039/C2OB25397F.

[107] U. Schneider and S. Kobayashi, "Catalytic Activation of Pinacolyl Allylboronate with Indium(I): Development of a General Catalytic Allylboration of Ketones," *Angewandte Chemie International Edition,* vol. 46, no. 31, 2007/08/03, doi: 10.1002/anie.200700899.

[108] K. Hema *et al.*, "Topochemical polymerizations for the solid-state synthesis of organic polymers," *Chemical Society Reviews,* vol. 50, no. 6, 2021/03/29, doi: 10.1039/D0CS00840K.

[109] Y. Fang, Z. Yang, and H. Park, "Straightforward and Facile Synthesis of a Bioactive Component from Zingiber cassumunar Roxb.," *Synthetic Communications,* vol. 44, no. 9, 2014-5-3, doi: 10.1080/00397911.2013.846380.

[110] S.-S. Kim, Y. Fang, and H. Park, "Synthesis and Anti-inflammatory Activity of Phenylbutenoid Dimer Analogs," *Bulletin of the Korean Chemical Society,* vol. 36, no. 6, 2015/06/01, doi: 10.1002/bkcs.10321.

[111] G. H. Posner *et al.*, "$BF_3{\cdot}OEt_2$ promotes fast, mild, clean and regioselective dehydration of tertiary alcohols," *Tetrahedron Letters,* vol. 32, no. 45, 1991/11/04, doi: 10.1016/0040-4039(91)80200-P.

[112] R. Ballini, D. Fiorini, and A. Palmieri, "Nitroalkanes and ethyl glyoxalate as common precursors for the preparation of both β-keto esters and α,β-

unsaturated esters," *Tetrahedron Letters,* vol. 45, no. 38, 2004/09/13, doi: 10.1016/j.tetlet.2004.07.141.

[113] B. A. Johns, C. M. Grant, and J. A. Marshall, "Synthesis and Utilization of Indium (I) Iodide for in Situ Formation of Enantioenriched Allenylindium Reagents and their Addition to Aldehydes: (2R,3S,4S)-1-(tert-Butyldiphenylsilyloxy)-2,4-Dimethyl-5-Hexyn-3-ol," *Organic Syntheses,* 2003, doi: 10.1002/0471264180.os079.08.

[114] C.-C. Chien *et al.*, "Photo-Fries rearrangement in flow under aqueous micellar conditions," *Chemical Communications,* vol. 56, no. 98, 2020/12/17, doi: 10.1039/D0CC07331H.

[115] A. A. Alsaiari, M. M. Almehmadi, and M. Asif, "Diverse Pharmacological Potential of Pyridazine Analogs against Various Diseases," *Medicinal Chemistry,* vol. 20, no. 3, 2024, doi: 10.2174/1573406419666230913102835.

[116] Z.-X. He, Y.-P. Gong, X. Zhang, L.-Y. Ma, and W. Zhao, "Pyridazine as a privileged structure: An updated review on anticancer activity of pyridazine containing bioactive molecules," *European Journal of Medicinal Chemistry,* vol. 209, 2021/01/01, doi: 10.1016/j.ejmech.2020.112946.

[117] Y. M. Ali, M. F. Ismail, F. S. M. A. El-Azm, and M. I. Marzouk, "Design, Synthesis, and Pharmacological Assay of Novel Compounds Based on Pyridazine Moiety as Potential Antitumor Agents," *Journal of Heterocyclic Chemistry,* vol. 56, no. 9, 2019/09/01, doi: 10.1002/jhet.3662.

[118] Y. Liu *et al.*, "Pyridazinone derivatives displaying highly potent and selective inhibitory activities against c-Met tyrosine kinase," *European Journal of Medicinal Chemistry,* vol. 108, 2016/01/27, doi: 10.1016/j.ejmech.2015.11.042.

[119] Ji Young Cho, Hak Cheol Kwon,†,Philip G. Williams,,Paul R. Jensen, and,William Fenical*, "Azamerone, a Terpenoid Phthalazinone from a Marine-Derived Bacterium Related to the Genus Streptomyces (Actinomycetales)," *Organic Letters,* vol. 8, no. 12, 2006, doi: 10.1021/ol060630r.

[120] I. TAKAHASHI *et al.*, "DUOCARMYCIN A, A NEW ANTITUMOR ANTIBIOTIC FROM STREPTOMYCES," *The Journal of Antibiotics,* vol. 41, no. 12, 1988/12/25, doi: 10.7164/antibiotics.41.1915.

[121] C. G. Wermuth and C. G. Wermuth, "Are pyridazines privileged structures?," *MedChemComm,* vol. 2, no. 10, 2011/10/05, doi: 10.1039/C1MD00074H.

[122] M. E. Welsch, S. A. Snyder, and B. R. Stockwell, "Privileged scaffolds for library design and drug discovery," *Current Opinion in Chemical Biology,* vol. 14, no. 3, 2010/06/01, doi: 10.1016/j.cbpa.2010.02.018.

[123] T. J. Ritchie *et al.*, "The developability of heteroaromatic and heteroaliphatic rings – do some have a better pedigree as potential drug molecules than others?," *MedChemComm,* vol. 3, no. 9, 2012/08/22, doi: 10.1039/C2MD20111A.

[124] Y. Z. Qinghe Gao, Mi Lian,Meicai Liu,Jingjing Yuan,Guodong Yin,Anxin Wu, "Unexpected C–C Bond Cleavage: A Route to 3,6-Diarylpyridazines and 6-Arylpyridazin-3-ones from 1,3-Dicarbonyl Compounds and Methyl Ketones," *The Journal of Organic Chemistry,* vol. 77, no. 21, 2012, doi: 10.1021/jo301751e.

[125] M.-Y. Chang, Y.-J. Lu, and Y.-C. Cheng, "In(OTf)3-mediated synthesis of substituted pyridazines," *Tetrahedron,* vol. 71, no. 38, 2015/09/23, doi: 10.1016/j.tet.2015.07.025.

[126] Z. Fan, Z. Pan, L. Huang, and J. Cheng, "Copper-Catalyzed Aerobic 6-Endo-Trig Cyclization of β,γ-Unsaturated Hydrazones for the Divergent Synthesis of Dihydropyridazines and Pyridazines," *The Journal of Organic Chemistry,* vol. 84, no. 7, March 18, 2019, doi: 10.1021/acs.joc.9b00228.

[127] P. G. Sergeev, V. N. Khrustalev, and V. G. Nenajdenko, "Construction of 6-Aminopyridazine Derivatives by the Reaction of Malononitrile with Dichloro-Substituted Diazadienes," *European Journal of Organic Chemistry,* vol. 2020, no. 31, 2020/08/23, doi: 10.1002/ejoc.202000807.

[128] O. M. Hassen Bel Abed, Omprakash Bande,Guy Van Lommen,Piet Herdewijn, "Strategy for the Synthesis of Pyridazine Heterocycles and Their Derivatives," *The Journal of Organic Chemistry,* vol. 78, no. 16, 2013, doi: 10.1021/jo400989q.

[129] S. D. Schnell, J. A. González, J. Sklyaruk, A. Linden, and K. Gademann, "Boron Trifluoride-Mediated Cycloaddition of 3-Bromotetrazine and Silyl Enol Ethers: Synthesis of 3-Bromo-pyridazines," *The Journal of Organic Chemistry,* vol. 86, no. 17, August 3, 2021, doi: 10.1021/acs.joc.1c01384.

[130] E. Chiurchiù, Y. Patehebieke, S. Gabrielli, R. Ballini, and A. Palmieri, "β-Nitroacrylates as Starting Materials of Thiophene-2-Carboxylates Under Continuous Flow Conditions," *Advanced Synthesis & Catalysis,* vol. 361, no. 9, 2019/04/23, doi: 10.1002/adsc.201801660.

[131] M. E. I. Khan, L. D. Terlizzi, S. Protti, and A. Palmieri, "Visible-Light-Driven Photocatalyst-Free Preparation of (Z) β-Nitroacrylate Isomers," *European Journal of Organic Chemistry,* vol. 2022, no. 26, 2022/07/14, doi: 10.1002/ejoc.202200635.

[132] G. Lupidi, B. Bassetti, R. Ballini, M. Petrini, and A. Palmieri, "A New and Effective One-Pot Synthesis of Polysubstituted Carbazoles Starting from β-Nitro-β,γ-Unsaturated-Ketones and Indoles," *Asian Journal of Organic Chemistry,* vol. 10, no. 9, 2021/09/01, doi: 10.1002/ajoc.202100342.

[133] R. Ballini, R. Ballini, A. Palmieri, A. Palmieri, L. Barboni, and L. Barboni, "Nitroalkanes as new, ideal precursors for the synthesis of benzene derivatives," *Chemical Communications,* no. 26, 2008/06/27, doi: 10.1039/B800941D.

[134] F. M. Cordero, D. Giomi, and L. Lascialfari, "29.5.7 - Five-membered ring systems with O & N atoms," *PROGRESS IN HETEROCYCLIC CHEMISTRY,* 2019-11-06T20:42:29Z, doi: 10.1016/B978-0-08-102310-5.00011-4.

[135] G. N. Pairas, F. Perperopoulou, P. G. Tsoungas, and G. Varvounis, "The Isoxazole Ring and Its N-Oxide: A Privileged Core Structure in Neuropsychiatric Therapeutics," *ChemMedChem,* vol. 12, no. 6, 2017/03/17, doi: 10.1002/cmdc.201700023.

[136] F. D. Sarlo, F. D. Sarlo, F. Machetti, and F. Machetti, "Primary nitro compounds: progress in the synthesis of isoxazoles by condensation with aldehydes or activated ketones," *Organic & Biomolecular Chemistry,* vol. 21, no. 36, 2023/09/20, doi: 10.1039/D3OB00960B.

[137] J. Zhu, J. Mo, H.-z. Lin, Y. Chen, and H.-p. Sun, "The recent progress of isoxazole in medicinal chemistry," *Bioorganic & Medicinal Chemistry,* vol. 26, no. 12, 2018/07/23, doi: 10.1016/j.bmc.2018.05.013.

[138] C. P. Pandhurnekar, H. C. Pandhurnekar, A. J. Mungole, S. S. Butoliya, and B. G. Yadao, "A review of recent synthetic strategies and biological activities of

isoxazole," *Journal of Heterocyclic Chemistry,* vol. 60, no. 4, 2023/04/01, doi: 10.1002/jhet.4586.

[139] G. C. Arya, K. Kaur, and V. Jaitak, "Isoxazole derivatives as anticancer agent: A review on synthetic strategies, mechanism of action and SAR studies," *European Journal of Medicinal Chemistry,* vol. 221, 2021/10/05, doi: 10.1016/j.ejmech.2021.113511.

[140] N. Agrawal, P. Mishra, N. Agrawal, and P. Mishra, "The synthetic and therapeutic expedition of isoxazole and its analogs," *Medicinal Chemistry Research 2018 27:5,* vol. 27, no. 5, 2018-02-27, doi: 10.1007/s00044-018-2152-6.

[141] M. J. S. D. Ignatius J. Turchi, "Chemistry of oxazoles," *Chemical Reviews,* vol. 75, no. 4, 1975, doi: 10.1021/cr60296a002.

[142] S. Das, S. Das, K. Chanda, and K. Chanda, "An overview of metal-free synthetic routes to isoxazoles: the privileged scaffold," *RSC Advances,* vol. 11, no. 52, 2021/10/04, doi: 10.1039/D1RA04624A.

[143] K. S. Kadam, T. Gandhi, A. Gupte, A. K. Gangopadhyay, and R. Sharma, "Alkyl Nitrites: Novel Reagents for One-Pot Synthesis of 3,5-Disubstituted Isoxazoles from Aldoximes and Alkynes," *Synthesis,* vol. 48, no. 22, 2016/11, doi: 10.1055/s-0035-1561464.

[144] J. Z. Bo Wang, Xinyan Wang,Nan Liu,Wenwen Chen,Yuefei Hu, "Tandem Reaction of 1-Copper(I) Alkynes for the Synthesis of 1,4,5-Trisubstituted 5-Chloro-1,2,3-triazoles," *The Journal of Organic Chemistry,* vol. 78, no. 20, 2013, doi: 10.1021/jo401629x.

[145] Fahmi Himo *et al.*, "Copper(I)-Catalyzed Synthesis of Azoles. DFT Study Predicts Unprecedented Reactivity and Intermediates," *Journal of the American Chemical Society,* vol. 127, no. 1, December 8, 2004, doi: 10.1021/ja0471525.

[146] C. Praveen, A. Kalyanasundaram, and P. T. Perumal, "Gold(III)-Catalyzed Synthesis of Isoxazoles by Cycloisomerization of α,β-Acetylenic Oximes," *Synlett,* vol. 2010, no. 05, 2010/03, doi: 10.1055/s-0029-1219342.

[147] G. Bianchi, G. Bianchi, M. D. Amici, and M. D. Amici, "Synthesis of hentriacontane-14,16-dione, a β-diketone found in plant waxes," *Journal of the Chemical Society, Chemical Communications,* vol. 0, no. 21, 1978/01/01, doi: 10.1039/C39780000962.

[148] Andrew D. White *et al.*, "Heterocyclic Amides: Inhibitors of Acyl-CoA:Cholesterol O-Acyl Transferase with Hypocholesterolemic Activity in Several Species and Antiatherosclerotic Activity in the Rabbit," *Journal of Medicinal Chemistry,* vol. 39, no. 20, September 27, 1996, doi: 10.1021/jm9604033.

[149] A. V. Aksenov *et al.*, "Does electrophilic activation of nitroalkanes in polyphosphoric acid involve formation of nitrile oxides?," *RSC Advances,* vol. 11, no. 57, 2021/11/04, doi: 10.1039/D1RA06503C.

[150] G. Giacomelli, L. D. Luca, and A. Porcheddu, "A method for generating nitrile oxides from nitroalkanes: a microwave assisted route for isoxazoles," *Tetrahedron,* vol. 59, no. 29, 2003/07/14, doi: 10.1016/S0040-4020(03)00859-7.

[151] M. A. P, G. L. Balaji, P. Iniyavan, and H. Ila, "Reaction of 1,3-Bis(het)arylmonothio-1,3-diketones with Sodium Azide: Regioselective Synthesis of 3,5-Bis(het)arylisoxazoles via Intramolecular N–O Bond Formation," *The Journal of Organic Chemistry,* vol. 85, no. 23, November 13, 2020, doi: 10.1021/acs.joc.0c02216.

[152] Y. Ning, Y. Otani, and T. Ohwada, "Contrasting C- and O-Atom Reactivities of Neutral Ketone and Enolate Forms of 3-Sulfonyloxyimino-2-methyl-1-phenyl-1-butanones," *The Journal of Organic Chemistry,* vol. 83, no. 1, December 20, 2017, doi: 10.1021/acs.joc.7b02573.

[153] M. V. Andreev, A. S. Medvedeva, L. I. Larina, and M. M. Demina, "Synthesis of 5-aminoisoxazoles from 3-trimethylsilylprop-2-ynamides," *Mendeleev Communications,* vol. 27, no. 2, 2017/03/01, doi: 10.1016/j.mencom.2017.03.023.

[154] J. H. Shibing Tang, Yongquan Sun,Liuer He,Xuegong She, "Efficient and Regioselective One-Pot Synthesis of 3-Substituted and 3,5-Disubstituted Isoxazoles," *Organic Letters,* vol. 11, no. 17, 2009, doi: 10.1021/ol901626n.

[155] B. MP and R. JT, "A convenient synthesis of 4-alkyl-5-aminoisoxazoles.," *Organic Letters,* vol. 8, no. 17, 2006/08/01, doi: 10.1021/ol061260.

[156] C. Li, J. Li, F. Zhou, C. Li, and W. Wu, "Palladium-Catalyzed Cascade Annulation/Allylation of Alkynyl Oxime Ethers with Allyl Halides: Rapid Access to Fully Substituted Isoxazoles," *The Journal of Organic Chemistry,* vol. 84, no. 18, August 29, 2019, doi: 10.1021/acs.joc.9b01593.

[157] M. Duan, G. Hou, Y. Zhao, C. Zhu, and C. Song, "Synthesis of Isoxazoles via One-Pot Oxidation/Cyclization Sequence from Propargylamines," *The Journal of Organic Chemistry,* vol. 87, no. 16, August 1, 2022, doi: 10.1021/acs.joc.2c00896.

[158] K. HARADA, E. KAJI, and S. ZEN, "Synthesis of Five-membered Heterocycles containing a Nitrogen-Oxygen Bond via O-Acylation of Aliphatic Nitro Compounds," *Chemical and Pharmaceutical Bulletin,* vol. 28, no. 11, 1980/11/25, doi: 10.1248/cpb.28.3296.

[159] W. M. Best, W. M. Best, E. L. Ghisalberti, E. L. Ghisalberti, M. Powell, and M. Powell, "Simple Synthesis of Symmetrical 4-Substituted 3,5-Dialkylisoxazoles," *Journal of Chemical Research, Synopses,* no. 7, 1998/01/01, doi: 10.1039/A801428K.

[160] M. Tu and R. J. Davis, "Cycloaddition of CO2 to Epoxides over Solid Base Catalysts," *Journal of Catalysis,* vol. 199, no. 1, 2001/04/01, doi: 10.1006/jcat.2000.3145.

[161] D. Long *et al.*, "Synthesis, Crystal Structure, and DFT Study of 4-(3,5-Dimethylisoxazol-4-yl)Benzene-1,2-Diol," *Journal of Structural Chemistry 2019 60:8,* vol. 60, no. 8, 2019-09-04, doi: 10.1134/S0022476619080146.

[162] Ulrik S. Sørensen, Erik Falch, and,Povl Krogsgaard-Larsen*, "A Novel Route to 5-Substituted 3-Isoxazolols. Cyclization of N,O-DiBoc β-Keto Hydroxamic Acids Synthesized via Acyl Meldrum's Acids," *The Journal of Organic Chemistry,* vol. 65, no. 4, 2000, doi: 10.1021/jo991409d.

[163] L. Yuan, L. Kachalova, M. E. I. Khan, R. Ballini, M. Petrini, and A. Palmieri, "Overcoming the Usual Reactivity of β-Nitroenones: Synthesis of Polyfunctionalized Homoallylic Alcohols and Conjugated Nitrotriene Systems," *The Journal of Organic Chemistry,* vol. 88, no. 7, March 16, 2023, doi: 10.1021/acs.joc.2c02669.

[164] A. Jorea, B. Bassetti, K. Gervasoni, S. Protti, A. Palmieri, and D. Ravelli, "More Chips to Nitroolefins: Decatungstate Photocatalysed Hydroalkylation Under Batch and Flow Conditions," *Advanced Synthesis & Catalysis,* vol. 365, no. 5, 2023/03/07, doi: 10.1002/adsc.202201314.

[165] E. Chiurchi, S. Xhafa, R. Ballini, G. Maestri, S. Protti, and A. Palmieri, "Diastereoselective Isomerization of (E)-β-Nitroenones into β-Nitro-β,γ-Unsaturated Ketones under Microwave Conditions," *ADVANCED*

SYNTHESIS & CATALYSIS, vol. 362, no. 21, 2020-12-01T10:59:37Z, doi: 10.1002/adsc.202000747.

[166] M. Dell'Aera *et al.*, "Boosting Conjugate Addition to Nitroolefins Using Lithium Tetraorganozincates: Synthetic Strategies and Structural Insights," *Chemistry – A European Journal,* vol. 26, no. 40, 2020/07/17, doi: 10.1002/chem.202001294.

[167] R. Ballini and M. Petrini, "The Nitro to Carbonyl Conversion (Nef Reaction): New Perspectives for a Classical Transformation," *Advanced Synthesis & Catalysis,* vol. 357, no. 11, 2015/08/10, doi: 10.1002/adsc.201500008.

[168] J. Bourgeois, I. Dion, P. H. Cebrowski, F. Loiseau, A.-C. Bédard, and A. M. Beauchemin, "The Tandem Cope-Type Hydroamination/[2,3]-Rearrangement Sequence: A Strategy to Favor the Formation of Intermolecular Hydroamination Products and Enable Difficult Cyclizations," *Journal of the American Chemical Society,* vol. 131, no. 3, January 2, 2009, doi: 10.1021/ja8077895.

[169] M. Koóš, "An alternative route to 2-deoxysugar and 2,3-unsaturated sugar derivatives via the corresponding 1-nitro-1-alkenes," *Tetrahedron Letters,* vol. 41, no. 28, 2000/07/08, doi: 10.1016/S0040-4039(00)00863-7.

[170] D. A. S. Prof. Dr. C. Oliver Kappe, Dr. Doris Dallinger, "Microwaves in Organic and Medicinal Chemistry," 2012, doi: 10.1002/9783527647828.

[171] L. Capaldo, L. Capaldo, Z. Wen, Z. Wen, T. Noël, and T. Noël, "A field guide to flow chemistry for synthetic organic chemists," *Chemical Science,* vol. 14, no. 16, 2023/04/26, doi: 10.1039/D3SC00992K.

[172] C. Holtze and R. Boehling, "Batch or flow chemistry? – a current industrial opinion on process selection," *Current Opinion in Chemical Engineering,* vol. 36, 2022/06/01, doi: 10.1016/j.coche.2022.100798.

[173] C. A. Hone and C. O. Kappe, "Towards the Standardization of Flow Chemistry Protocols for Organic Reactions," *Chemistry - Methods,* vol. 1, no. 11, 2021/11/01, doi: 10.1002/cmtd.202100059.

[174] P. Brandão, M. Pineiro, and T. M. V. D. P. e. Melo, "Flow Chemistry: Towards A More Sustainable Heterocyclic Synthesis," *European Journal of Organic Chemistry,* vol. 2019, no. 43, 2019/11/24, doi: 10.1002/ejoc.201901335.

[175] M. Trojanowicz and M. Trojanowicz, "Flow Chemistry in Contemporary Chemical Sciences: A Real Variety of Its Applications," *Molecules 2020, Vol. 25, Page 1434,* vol. 25, no. 6, 2020-03-21, doi: 10.3390/molecules25061434.

[176] P. R. D. Murray, D. L. Browne, J. C. Pastre, C. Butters, D. Guthrie, and S. V. Ley, "Continuous Flow-Processing of Organometallic Reagents Using an Advanced Peristaltic Pumping System and the Telescoped Flow Synthesis of (E/Z)-Tamoxifen," *Organic Process Research & Development,* vol. 17, no. 9, September 6, 2013, doi: 10.1021/op4001548.

[177] M. B. Plutschack, B. Pieber, K. Gilmore, and P. H. Seeberger, "The Hitchhiker's Guide to Flow Chemistry‖," *Chemical Reviews,* vol. 117, no. 18, June 1, 2017, doi: 10.1021/acs.chemrev.7b00183.

Chapter 3

3. Research work performed during visiting stay at East China Normal University.

During my visiting research at the *State key laboratory of Green Chemistry and Chemical process at* ECNU was comprised of two projects

1) Selective C-H Activation of Alkylbenzenes Via WO_3 Catalyst.

This work is explained in detail in **section 3.1**, a further expansion of this study is underway by *Syed Ali Raza Aal e Ali* at the same group.

2) Machine Learning Advancements in Organic Synthesis: A Focused Exploration of Artificial Intelligence Applications in Chemistry.

In parallel to my core project (**1**), I was also Involved in the co-authorship of a review article based on the Integration of AI in organic synthesis. In **section 3.2** I have just provided a short summary of that review article, while the full article can be openly accessed on following address: (https://doi.org/10.1016/j.aichem.2024.100049).

3.1 Selective C–H Activation of Alkylbenzenes Via WO_3 Catalyst

‘

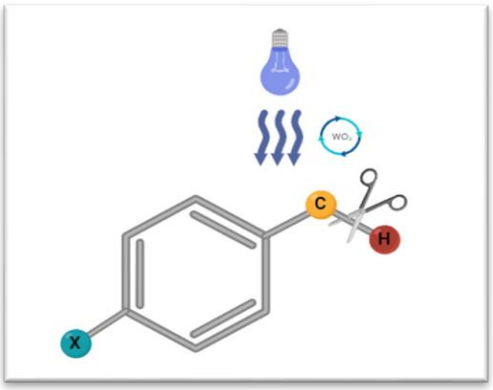

The work presented in this section is unpublished, while performed during the visiting research stray at State Key Laboratory of Green Chemistry and Chemical process, East China Normal University Shanghai.

3.1.1 Introduction

The selective activation of C-H bonds is a fundamental challenge in organic synthesis. The direct functionalization of C-H bonds in alkylbenzenes produces a wide range of valuable compounds, including alcohols, ketones, and carboxylic acids. This is an essential process for increasing the oxidation states of fossil-derived raw materials and is extensively used in the production of pharmaceuticals, agrochemicals, and organic materials [1].

Traditionally, oxygenation of alkyl-benzenes was carried out using highly active oxidants, such as CrO_3, $KMnO_4$, Oxone, ^tBuOOH, *m*-CPBA, H_2O_2, O_3, NHPI, etc. [2, 3]. In accordance with the principles of sustainable chemistry oxygen serves as a major player for benzylic oxygenations with the help of Co, Fe, and Mn catalysis [4-8]. Many literature studies like Fukuzumi, Pandey, Cibulka, Shi, and Wolf, confirmed catalytic systems for benzylic C-H activation under mild photocatalyzed conditions [9-13].

In recent decades scientists developed various elegant aerobic C–H bond photo-oxidation pathways for the synthesis of alcohols, aldehyde, ketones and carboxylic acids [14-20]. WO_3 is a widely used material in various photochemical reactions, as it has a distinctive optical, chemical, and electrochemical properties. In this study, we focused on the utilization of WO_3 as a photocatalyst for the selective C-H activation of alkylbenzenes in the presence of O_2 to synthesize carboxylic acids **Scheme 3.1.**

Previously Professor Jiang's research group explored the C-H activation strategies using uranyl acetate and reported the successive conversions of alkylbenzenes into ketones, alcohols, and carboxylic acids [21], but the use of uranium at larger scale is a clear limitation. On other hand tungsten(VI) oxide (WO_3) is an attractive photocatalyst due to its wide bandgap (ranges between 2.6-3.0 eV), which enables the efficient absorption of visible light. Additionally, WO_3 is a non-toxic, abundant, and cost-effective compound, which makes it a sustainable choice for catalysis.

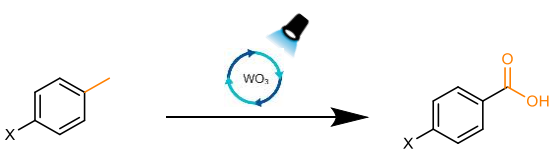

Scheme 3.1 General reaction scheme of light promoted C-H activation of alkyl benzenes using WO_3.

The proposed mechanism for this WO_3 catalyzed oxidation could be as follows; where light source initiates a *via* ligand-to-metal charge transfer (LMCT), producing an oxyl radical, followed by a hydrogen atom transfer (HAT) at benzylic position. In the next step, benzyl radical is captured by oxygen molecule ($^3O_2$) to generate a peroxy radical, which upon hydration gives respective aldehydes. Then this aldehyde goes under a second HAT immediately to form acyl radical. In very last, that acyl radical is further oxidized with dioxygen, to produce carboxylic acids (**Scheme 3.2**).

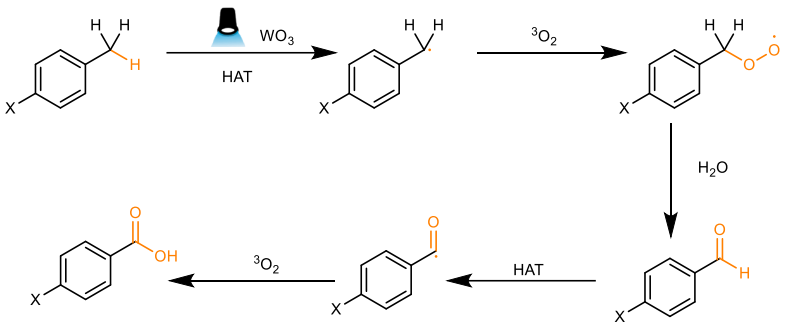

Scheme 3.2 Possible mechanism for photo induced C-H activation using WO_3.

3.1.2 Results and discussion

Studies were commenced with alkylbenzenes, precisely using *p*-phenyl-toluene as a standard molecule. In preliminary trials to optimized suitable reaction conditions, we tested various solvent systems at room temperature, including DCM, DMSO, DMF, Ethanol, MeCN and EtOAc, while best results in terms of yield were obtained in EtOAc as a solvent system. The insolubility of the photocatalyst was observed in all the solvent systems. Different trails were also performed in search of suitable light source, 365 nm UV light was found as the most suitable one, providing best yield of 79% (**Table 3.1, entry b**). With the suitable light source and solvent system in hand we observed the reaction progress by elevating the reaction temperature up to 60 °C but the rection yield dropped to 58% (**Table 3.1, entry e**). In further trials we optimized the concentration of photocatalyst WO_3, which was priorly used as standard 1eq in all experiments. We doubled and halved the amount of photocatalyst in two different trials resulting in no satisfactory yield improvement (**Table 3.1, entries f & g**).

Table 3.1 Optimizations studies for benzylic oxidation.

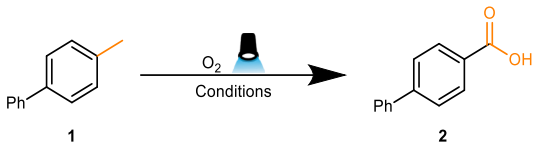

Entry	Solvent	Wavelength	WO_3 (eq)	Temperature	Yield
a	EtOAc	300 nm	1eq	rt	23%
b	EtOAc	365 nm	1eq	rt	79%
c	EtOAc	390 nm	1eq	rt	40%
d	EtOAc	430 nm	1eq	rt	31%
e	EtOAc	365 nm	1eq	60 °C	58%
f	EtOAc	365 nm	2eq	rt	53%
g	EtOAc	365 nm	0.5eq	rt	61%

After optimizing the optimal conditions, we further tested the generality of protocol by applying it on different substrates and we got very good results in terms of yields (**Scheme 3.3**).

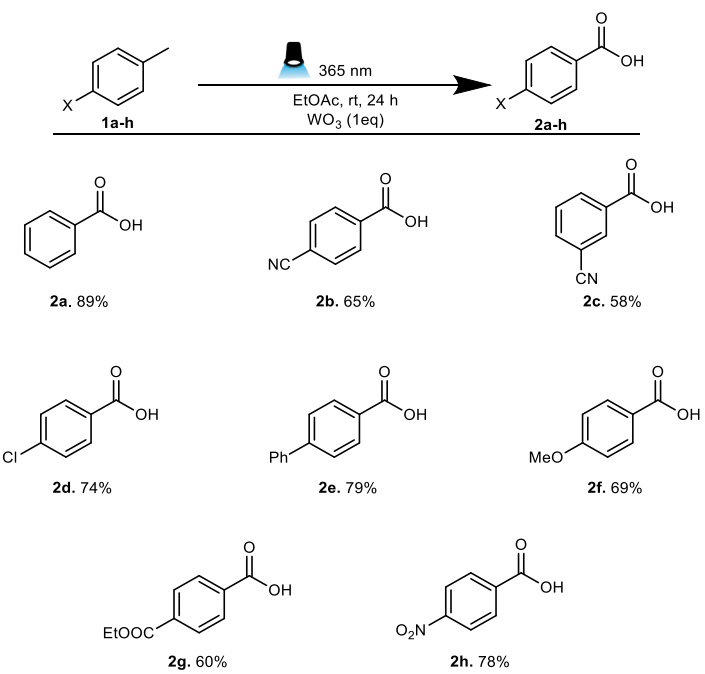

Scheme 3.3 Substrate scope.

3.1.3 Conclusion

In summary, we studied a catalytic strategy for the selective C-H activation of alkylbenzene using WO_3 catalytic system. Ambient conditions like; use of UV and visible light, oxygen, and room temperature supported the sustainability goal of the protocol. While the insolubility of the catalyst provided a handy work up of only filtration, which helped to reduce the use of extra solvents. In expansion to this study, the protocol is being further tested on secondary and tertiary benzylic molecules.

3.1.4 Experimental section

^1H and ^{13}C NMR analysis were performed using 400 MHz or 500 MHz Bruker AVANCE spectrometers. Chemical shifts for proton and Carbon are reported in parts per million (ppm) downfield, for ^1H NMR solvent ($CHCl_3$: δ 7.26, DMSO: δ 2.50, Acetone: δ 2.05). While for ^{13}C NMR solvent ($CHCl_3$: δ 77.0, DMSO: δ 39.52, Acetone: δ 206.26 and δ 29.84) were used. For IR spectra SHIMADZU IR Tracer-100 spectrometer was used.

Green-lab photo chemical apparatus *Photosyn-10* (**Figure 3.1**) was used as apparatus to conduct the reaction.

Figure 3.1 *Photosyn-10* Green-lab photo chemical apparatus.

3.1.4.1. General reaction procedure

In a 50 mL Schlenk tube **1** (0.35 mmol), WO_3 (1 eq) and solvent EtOAc (2ml/mmol) were stirred at room temperature with blue light (365 nm, 5W) under O_2 (1atm) for 24-30 hours. Reaction progress was observed by TLC and upon completion the reaction mixture was filtered to separate the catalyst. Further purification was done by using column chromatography, using 90 : 10 of Hexane ethyl acetate eluent system to afford pure products **2.**

3.1.4.2. Characterization data

Benzoic acid (2a)

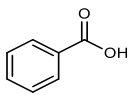

White solid. ^{1}H NMR (400 MHz, DMSO-d6) δ 12.96 (brs, 1H), 7.96-7.94- 7.98 (m, 2H), 7.63-7.59 (m, 1H), 7.51-7.48 (m, 2H). ^{13}C NMR (100 MHz, DMSO-d6) δ 167.4, 132.9, 130.8, 129.3, 128.6. IR (neat) 3007, 1716, 1681, 1421, 1224, 923, 704.

4-Cyanobenzoic acid (2b)

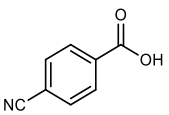

White solid. ^{1}H NMR (400 MHz, DMSO-d6) δ 13.56 (brs, 1H), 8.08 (d, J = 8.0 Hz, 2H), 7.98 (d, J = 8.0 Hz, 2H). ^{13}C NMR (100 MHz, DMSOd6) δ 166.3, 135.0, 132.9, 130.1, 118.4, 115.2. IR (neat) 3410, 2231, 1714, 1566, 1429, 1286, 927.

3-Cyanobenzoic acid (2c)

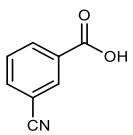

White solid. ^{1}H NMR (400 MHz, DMSO-d6) δ 13.74 (brs, 1H), 8.48-8.45 (m, 1H), 8.36-8.33 (m, 1H), 7.81 (t, J = 8.0 Hz, 1H). ^{13}C NMR (100 MHz, DMSO-d6) δ 165.5, 147.9, 135.4, 132.5, 130.6, 127.4, 123.7. IR (neat) 2924, 2233, 1689, 1616, 1435, 1298, 675.

4-chlorobenzoic acid (2e)

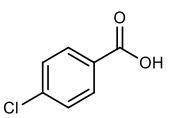

White solid. ^{1}H NMR (400 MHz, DMSO-d6) δ 13.16 (brs, 1H), 7.93 (d, J = 8.0 Hz, 2H), 7.54 (d, J = 8.0 Hz, 2H). ^{13}C NMR (100 MHz, DMSO-d6) δ 166.5, 137.8, 131.2, 129.7, 128.8. IR (neat) 3008, 1716, 1678, 1423, 1365, 1224, 1091.

Biphenyl-4-carboxylic acid (2f)

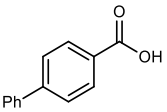

White solid. ^{1}H NMR (400 MHz, DMSO-d6) δ 12.99 (brs, 1H), 8.03 (d, J = 8.0 Hz, 2H), 7.79 (d, J = 8.0 Hz, 2H), 7.72 (d, J = 8.0 Hz, 2H), 7.49 (t, J = 8.0 Hz, 2H), 7.42 (t, J = 8.0 Hz, 1H). ^{13}C NMR (100 MHz, DMSO-d6) δ 167.2, 144.3, 139.0, 129.9, 129.6, 129.1, 128.3, 126.9, 126.8. IR (neat) 2547, 1712, 1674, 1421, 1298, 1286, 746.

4-methoxybenzoic acid (2g)

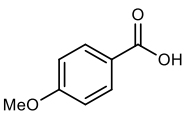

White solid. ^{1}H NMR (400 MHz, DMSO-d6) δ 12.62 (brs, 1H), 7.89 (d, J = 8.0 Hz, 2H), 7.01 (d, J = 8.0 Hz, 2H), 3.82 (s, 3H). ^{13}C NMR (100 MHz, DMSO-d6) δ 167.0, 162.9, 131.4, 123.0, 113.8, 55.4. IR (neat) 2926, 1705, 1678, 1575, 1425, 1230, 1022.

4-(ethoxycarbonyl)benzoic acid (2h)

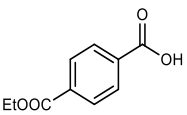

White solid. ^{1}H NMR (400 MHz, DMSOd6) δ 13.33 (brs, 1H), 8.05 (s, 4H), 4.34 (q, J = 6.7 Hz, 2H), 1.33 (t, J = 8.0 Hz, 3H). ^{13}C NMR (100 MHz, DMSO-d6) δ 166.6, 165.1, 134.8, 133.4, 129.6, 129.3, 61.2, 14.1. IR (neat) 3005, 1712, 1573, 1427, 1224, 1014, 729.

4-Nitrobenzoic acid (2i)

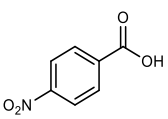

Yellow solid. ^{1}H NMR (400 MHz, DMSO-d6) δ 13.66 (brs, 1H), 8.31 (d, J = 8.0 Hz, 2H), 8.16 (d, J = 8.0 Hz, 2H). ^{13}C NMR (100 MHz, DMSO-d6) δ 165.8, 150.0, 136.4, 130.7, 123.7. IR (neat) 3392, 1685, 1598, 1539, 1425, 1350, 1278.

3.2 Machine Learning Advancements in Organic Synthesis: A Focused Exploration of Artificial Intelligence Applications in Chemistry

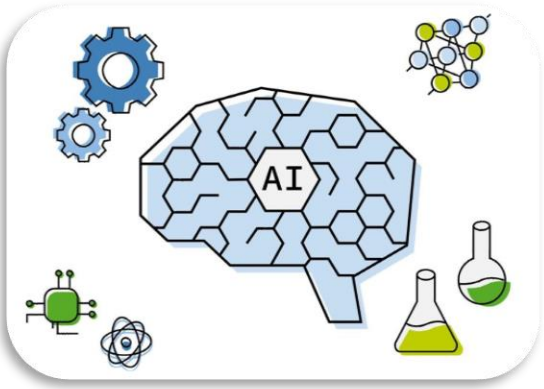

This section is based on short overview of the literature studies performed for following review:

Ali, R. S. A. E., Meng, J., **Khan, M. E. I.**, & Jiang, X. (2024). Machine learning advancements in organic synthesis: A focused exploration of artificial intelligence applications in chemistry. *Artificial Intelligence Chemistry*, *2*(1), 100049.

3.2.1 Summary

Chemistry is undergoing a significant change in the age of digital chemistry, automation, robotics, and artificial intelligence (AI) [22-24]. Nowadays, the field of study is known as "digital chemistry," which includes the use of big data, machine learning algorithms, and sophisticated automation technologies [25, 26]. Its goal is to speed up the discovery and synthesis of new chemicals by fusing traditional experimental chemistry with digital technology [27, 28]. Chemistry is developing more quickly, economically, and sustainably by utilizing digital tools to develop creative workflows [29]. In addition to greatly increasing productivity, this shift also radically changes the way chemists approach their work and creativity. It helps chemists better understand reaction mechanisms and lessens the strain of time-consuming experimental work. One of the most notable uses of AI in this changing environment is found in the field of chemical synthesis [30].

Given the complexity and non-linear nature of organic chemistry, tasks such as retrosynthetic analysis, designing new chemical reactions, and optimizing reaction conditions demands extensive expertise and specialized chemical knowledge [31]. To increase productivity and guarantee the reproducibility of outcomes, there is a rising expectation that these procedures can be streamlined and automated, at least partially or in highly controlled environments. This is especially true when combined with robotic systems [32]. In the field of organic synthesis, AI has had a specifically significant influence. It has instrumental influence in retrosynthetic analysis, where reaction steps are reverse-engineered to develop a pathway for synthesizing a target molecule from readily available compounds [33].

Classically, this process has been labor-intensive and relies on expert knowledge. However, machine learning algorithms and protocols can now generate synthetic pathways by leveraging known reaction data on behalf of databank and established rules [34]. This technique empowers chemists to smoothly design new synthetic routes, accelerating the development and discovery of novel drugs and materials. Additionally, AI has a crucial role in reaction prediction, where algorithms analyze reaction conditions and reactants to predict the resulting products [35]. As organic synthesis involves a wide array of reactions, which have traditionally required massive and extensive experimentation to optimize the optimal reaction conditions. Machine learning algorithms, however, can help to analyze large reaction datasets to uncover patterns, by facilitating the prediction of novel reaction outcomes [36]. This not only helps to save time and resources required, but also facilitates the quicker discovery of new reaction conditions [37]. Additionally, AI can also be used to optimize reaction conditions, enhancing

reaction yields and selectivity [38]. By analyzing extensive experimental data, machine learning algorithms can provide optimal conditions, aiding chemists in planning and designing experiments more efficiently [39].

Digital chemistry has made tremendous strides in organic synthesis, however there are still a number of limitations. The most important of these are from the perspective of data availability and data quality, which are important for machine learning predictions and optimizations to be concise and accurate. High-quality datasets are essential, and by producing vast and varied datasets of reaction results and compound attributes, high-throughput synthesis (HTS), whether automated correction or human, can significantly improve machine learning performance. The volume of data from HTS helps to enhance performance and in directing experiments and refining reaction conditions, as well as prediction accuracy and model generalization. Combining AI and robotics further increase HTS efficiency, which makes it possible to create more reliable and accurate datasets for machine learning. This opens the door for fresh discoveries and starts a cycle of ongoing progress. Thus, gathering, organizing, and disseminating data are quite essential for advancing this field [40].

Many algorithms used AI, especially the deep learning models, are often regarded as black-box systems, which make it difficult to interpret the internal decision-making process of these models. This lack of transparency can lead to promising challenges in chemical research, as chemists must understand the reasoning behind specific predictions or recommendations to ensure trust and safety [41]. As AI algorithms work on data-driven patterns, they could not have deep subject knowledge. Deep comprehension of the complexity and mechanism of chemical reactions is essential for chemical research, and AI systems may not be able to meet this requirement yet [42]. Managing uncertainty remains a significant challenge in complex chemical systems, particularly where reactions and molecular interactions are influenced by factors such as temperature, pressure, and solvents. Additionally, many advanced AI models demand considerable computational resources and specialized hardware, which can possibly limit their accessibility and utilization in practical application.

Particularly In the field of organic synthesis, digital chemistry and artificial intelligence are coming with hitherto unheard-of prospects and difficulties [43]. More discoveries are likely to be made with continued technological progress and the commitment of chemists, while encouraging creativity and improvement in both scientific and practical research applications [44]. Majorly the ongoing broad use of AI in organic synthesis has been discussed in this study, with particular instances used to highlight the inculcation of technology's bright future in chemistry.

Machine learning approaches

The dynamic field of machine learning, which lies at the intersection of statistics and computer science, includes a wide range of learning techniques that enable systems to automatically enhance their efficiency and performance in response to data. These methodologies can be generally divided into three primary paradigms (**Figure 3.2**).

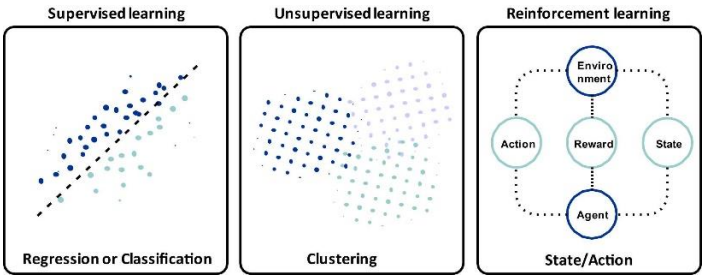

Figure 3.2 Different machine learning approaches.

Machine learning pathway

With an aim to accelerate the discovery and synthesis of new molecules, machine learning is making waves in chemistry. It is a methodical process that combines data analysis, computational techniques, and domain experience. This complex process involves several crucial phases, all of which lead to determine the intended outcomes **Figure 3.3.**

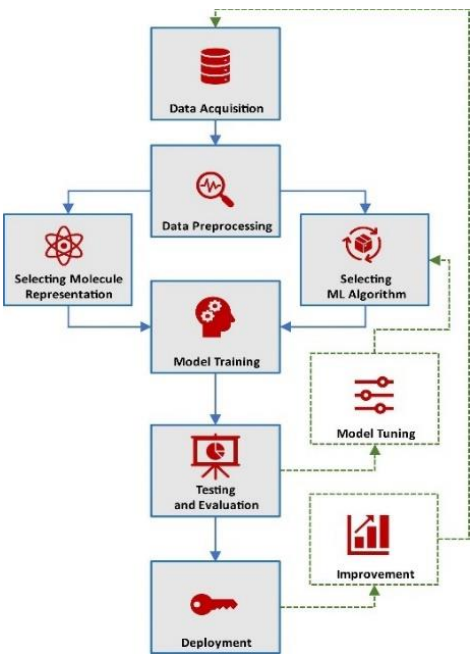

Figure 3.3 Simplified machine learning process.

Reap Benefits

- Yield Prediction
- Selectivity
- Retrosynthesis
- Drug design
- Material design

Challenges

Although applications of AI and ML is being rapidly adapted by the chemistry community but realizing the full potential of AI in chemistry necessitates addressing some key challenges as following.

- Data availability and Quality
- Data Representation
- Reproducibility of AI models
- Interpretability of AI models

3.2.2 Conclusion

Artificial intelligence (AI), specifically machine learning (ML), has brought a huge transformation in organic synthesis, by enabling predictions of retro-synthetic pathways, reaction yields, selectivity, and innovations in drug and material design. While still many challenges persist in these areas, the potential for groundbreaking discoveries is more immense. Addressing these shortcomings paves the way for further innovation, portraying AI as a key driver in accelerating and optimizing chemical processes.

The future of Artificial Intelligence in organic synthesis depends on fostering interdisciplinary collaborations, ensuring transparent reporting of methods and results, and promoting the open sharing of codes and data. While access to computational resources for researchers from diverse backgrounds and with limited resources is equally critical. By combining these efforts, the transformative power of AI can be fully harnessed, ushering in an era of unparalleled efficiency, precision, and creativity in organic synthesis.

3.2.3 References

[1] B. Meunier, *Biomimetic Oxidations Catalyzed by Transition Metal Complexes*.

[2] Stéphane Caron, Robert W. Dugger,,Sally Gut Ruggeri,,John A. Ragan, and,David H. Brown Ripin*, "Large-Scale Oxidations in the Pharmaceutical Industry," *Chemical Reviews,* vol. 106, no. 7, 2006, doi: 10.1021/cr040679f.

[3] M. Costas, "Selective C–H oxidation catalyzed by metalloporphyrins," *Coordination Chemistry Reviews,* vol. 255, no. 23-24, 2011/12/01, doi: 10.1016/j.ccr.2011.06.026.

[4] S. Evans, S. Evans, J. R. L. Smith, and J. R. L. Smith, "The oxidation of ethylbenzene by dioxygen catalysed by supported iron porphyrins derived from iron(III) tetrakis(pentafluorophenyl)porphyrin," *Journal of the Chemical Society, Perkin Transactions 2,* no. 2, 2001/01/01, doi: 10.1039/B007326L.

[5] A. E. Sorochinsky, A. A. Petrenko, V. A. Soloshonok, and G. Resnati, "Regioselective Oxyfunctionalization of Bridgehead Adamantane Derivatives," *Tetrahedron,* vol. 53, no. 17, 1997/04/01, doi: 10.1016/S0040-4020(97)00292-5.

[6] J.-Y. Qi *et al.*, "Synthesis and characterization of cobalt(III) complexes containing 2-pyridinecarboxamide ligands and their application in catalytic oxidation of ethylbenzene with dioxygen," *Chemical Communications,* no. 11, 2003/05/16, doi: 10.1039/B301963B.

[7] S. A. Chavan, S. A. Chavan, D. Srinivas, D. Srinivas, P. Ratnasamy, and P. Ratnasamy, "A novel, zeolite-encapsulated μ3-oxo Co/Mn cluster catalyst for oxidation of para-xylene to terephthalic acid," *Chemical Communications,* no. 12, 2001/01/01, doi: 10.1039/B102016C.

[8] Y. Liang, J. Wei, X. Qiu, and N. Jiao, "Homogeneous Oxygenase Catalysis," *Chemical Reviews,* vol. 118, no. 10, April 9, 2018, doi: 10.1021/acs.chemrev.7b00193.

[9] G. Pandey, S. Pal, and R. Laha, "Direct Benzylic C□ H Activation for C□ O Bond Formation by Photoredox Catalysis," *Angewandte Chemie International Edition,* vol. 52, no. 19, 2013/05/03, doi: 10.1002/anie.201210333.

[10] S. S and G. DP, "Activation of Dioxygen by Iron and Manganese Complexes: A Heme and Nonheme Perspective - PubMed," *Journal of the American Chemical Society,* vol. 138, no. 36, 09/14/2016, doi: 10.1021/jacs.6b05251.

[11] M. B and W. R, "C-H Photooxygenation of Alkyl Benzenes Catalyzed by Riboflavin Tetraacetate and a Non-Heme Iron Catalyst - PubMed," *Angewandte Chemie (International ed. in English),* vol. 55, no. 1, 01/04/2016, doi: 10.1002/anie.201507170.

[12] Z. J *et al.*, "Combining Flavin Photocatalysis and Organocatalysis: Metal-Free Aerobic Oxidation of Unactivated Benzylic Substrates - PubMed," *Organic letters,* vol. 21, no. 1, 01/04/2019, doi: 10.1021/acs.orglett.8b03547.

[13] C.-C. Wang *et al.*, "Photo-induced deep aerobic oxidation of alkyl aromatics," *Science China Chemistry 2021 64:9,* vol. 64, no. 9, 2021-06-23, doi: 10.1007/s11426-021-1032-7.

[14] S. Tripathi, S. Tripathi, S. N. Singh, S. N. Singh, L. D. S. Yadav, and L. D. S. Yadav, "Visible light photocatalysis with CBr4: a highly selective aerobic

photooxidation of methylarenes to aldehydes," *RSC Advances,* vol. 6, no. 18, 2016/02/03, doi: 10.1039/C5RA26623H.

[15] D. M. Schultz *et al.*, "Oxyfunctionalization of the Remote C−H Bonds of Aliphatic Amines by Decatungstate Photocatalysis," *Angewandte Chemie International Edition,* vol. 56, no. 48, 2017/11/27, doi: 10.1002/anie.201707537.

[16] G. Laudadio *et al.*, "Selective C(sp3)−H Aerobic Oxidation Enabled by Decatungstate Photocatalysis in Flow," *Angewandte Chemie International Edition,* vol. 57, no. 15, 2018/04/03, doi: 10.1002/anie.201800818.

[17] L. BJ, D. KS, and Y. TP, "Site-Selective Alkoxylation of Benzylic C-H Bonds by Photoredox Catalysis - PubMed," *Angewandte Chemie (International ed. in English),* vol. 59, no. 1, 01/02/2020, doi: 10.1002/anie.201910602.

[18] K. Ohkubo, K. Ohkubo, K. Hirose, K. Hirose, S. Fukuzumi, and S. Fukuzumi, "Two-phase oxidation of toluene derivatives by dioxygen using the 3-cyano-1-decylquinolinium ion as a photocatalyst," *RSC Advances,* vol. 6, no. 47, 2016/04/22, doi: 10.1039/C6RA05993G.

[19] X. Zhu *et al.*, "Light and oxygen-enabled sodium trifluoromethanesulfinate-mediated selective oxidation of C–H bonds," *Green Chemistry,* vol. 22, no. 13, 2020/07/06, doi: 10.1039/D0GC00383B.

[20] S. Verma, R. B. N. Baig, M. N. Nadagouda, and R. S. Varma, "Hydroxylation of Benzene via C–H Activation Using Bimetallic CuAg@g-C3N4," *ACS Sustainable Chemistry & Engineering,* vol. 5, no. 5, March 23, 2017, doi: 10.1021/acssuschemeng.7b00772.

[21] D. Hu, D. Hu, X. Jiang, and X. Jiang, "Stepwise benzylic oxygenation via uranyl-photocatalysis," *Green Chemistry,* vol. 24, no. 1, 2022/01/04, doi: 10.1039/D1GC04042A.

[22] C. W. Coley *et al.*, "A robotic platform for flow synthesis of organic compounds informed by AI planning," *Science,* vol. 365, no. 6453, 2019-08-09, doi: 10.1126/science.aax1566.

[23] R. L. Greenaway *et al.*, "From alchemist to AI chemist," *Nature Reviews Chemistry 2023 7:8,* vol. 7, no. 8, 2023-07-24, doi: 10.1038/s41570-023-00522-w.

[24] L. M. Roch *et al.*, "ChemOS: Orchestrating autonomous experimentation," *Science Robotics,* vol. 3, no. 19, 2018-06-20, doi: 10.1126/scirobotics.aat5559.

[25] H. Zhu and H. Zhu, "Big Data and Artificial Intelligence Modeling for Drug Discovery," *Annual Review of Pharmacology and Toxicology,* vol. 60, no. Volume 60, 2020, 2020/01/06, doi: 10.1146/annurev-pharmtox-010919-023324.

[26] S. V. Ley, D. E. Fitzpatrick, R. M. Myers, C. Battilocchio, and R. J. Ingham, "Machine-Assisted Organic Synthesis," *Angewandte Chemie International Edition,* vol. 54, no. 35, 2015/08/24, doi: 10.1002/anie.201501618.

[27] X. Yang, Y. Wang, R. Byrne, G. Schneider, and S. Yang, "Concepts of Artificial Intelligence for Computer-Assisted Drug Discovery," *Chemical Reviews,* vol. 119, no. 18, July 11, 2019, doi: 10.1021/acs.chemrev.8b00728.

[28] J. Jiménez-Luna, F. Grisoni, G. Schneider, J. Jiménez-Luna, F. Grisoni, and G. Schneider, "Drug discovery with explainable artificial intelligence," *Nature Machine Intelligence 2020 2:10,* vol. 2, no. 10, 2020-10-13, doi: 10.1038/s42256-020-00236-4.

[29] P. Fantke *et al.*, "Transition to sustainable chemistry through digitalization," *Chem,* vol. 7, no. 11, 2021/11/11, doi: 10.1016/j.chempr.2021.09.012.

[30] S. G. Baird and T. D. Sparks, "What is a minimal working example for a self-driving laboratory?," *Matter,* vol. 5, no. 12, 2022/12/07, doi: 10.1016/j.matt.2022.11.007.

[31] Y. Shen *et al.*, "Automation and computer-assisted planning for chemical synthesis," *Nature Reviews Methods Primers 2021 1:1,* vol. 1, no. 1, 2021-03-18, doi: 10.1038/s43586-021-00022-5.

[32] S. V. Ley, "The Engineering of Chemical Synthesis: Humans and Machines Working in Harmony," *Angewandte Chemie International Edition,* vol. 57, no. 19, 2018/05/04, doi: 10.1002/anie.201802383.

[33] V. Duros *et al.*, "Human versus Robots in the Discovery and Crystallization of Gigantic Polyoxometalates," *Angewandte Chemie International Edition,* vol. 56, no. 36, 2017/08/28, doi: 10.1002/anie.201705721.

[34] M. H. S. Segler, M. Preuss, M. P. Waller, M. H. S. Segler, M. Preuss, and M. P. Waller, "Planning chemical syntheses with deep neural networks and symbolic AI," *Nature 2018 555:7698,* vol. 555, no. 7698, 2018-03-29, doi: 10.1038/nature25978.

[35] J. N. Wei, D. Duvenaud, and A. Aspuru-Guzik, "Neural Networks for the Prediction of Organic Chemistry Reactions," *ACS Central Science,* vol. 2, no. 10, October 14, 2016, doi: 10.1021/acscentsci.6b00219.

[36] J. E. Hein and J. E. Hein, "Machine learning made easy for optimizing chemical reactions," *Nature 2021 590:7844,* vol. 590, no. 7844, 2021-02-03, doi: 10.1038/d41586-021-00209-6.

[37] P. S. Gromski *et al.*, "How to explore chemical space using algorithms and automation," *Nature Reviews Chemistry 2018 3:2,* vol. 3, no. 2, 2019-01-15, doi: 10.1038/s41570-018-0066-y.

[38] H. Gao, T. J. Struble, C. W. Coley, Y. Wang, W. H. Green, and K. F. Jensen, "Using Machine Learning To Predict Suitable Conditions for Organic Reactions," *ACS Central Science,* November 16, 2018, doi: 10.1021/acscentsci.8b00357.

[39] C. J. Taylor *et al.*, "Accelerated Chemical Reaction Optimization Using Multi-Task Learning," *ACS Central Science,* vol. 9, no. 5, April 13, 2023, doi: 10.1021/acscentsci.3c00050.

[40] M. Jutel *et al.*, "The artificial intelligence (AI) revolution: How important for scientific work and its reliable sharing," *Allergy,* vol. 78, no. 8, 2023/08/01, doi: 10.1111/all.15778.

[41] V. A., "Explainable Deep Reinforcement Learning: State of the Art and Challenges," *ACM Computing Surveys,* vol. 55, no. 5, 2022-12-03, doi: 10.1145/3527448.

[42] F. Oviedo, J. L. Ferres, T. Buonassisi, and K. T. Butler, "Interpretable and Explainable Machine Learning for Materials Science and Chemistry," *Accounts of Materials Research,* vol. 3, no. 6, June 3, 2022, doi: 10.1021/accountsmr.1c00244.

[43] A. F. de Almeida, R. Moreira, T. Rodrigues, A. F. de Almeida, R. Moreira, and T. Rodrigues, "Synthetic organic chemistry driven by artificial intelligence," *Nature Reviews Chemistry 2019 3:10,* vol. 3, no. 10, 2019-08-21, doi: 10.1038/s41570-019-0124-0.

[44] H. J. Kulik and M. S. Sigman, "Advancing Discovery in Chemistry with Artificial Intelligence: From Reaction Outcomes to New Materials and Catalysts," *Accounts of Chemical Research,* vol. 54, no. 10, May 18, 2021, doi: 10.1021/acs.accounts.1c00232.

4. Activities & Participations

During this three-year journey, I participated in the following activities in parallel:

a) Invited short oral talk at 48th Edition of the "A. CORBELLA" International Sumer School on Organic Synthesis (ISOS 2024), Italy June **16-20, 2024.**

b) The XXIII International Conference on Organic Synthesis (23-ICOS) Shanghai, China October 15-20, 2023.

c) The Shanghai Laboratory Planning, Construction and Management Conference (Labtech China Congress), National Convention and Exhibition Center Shanghai, China July 11-13, 2023.

d) CPHI & PMEC China, Shanghai New International Expo Center, June 19-21, 2023.

e) Assisting in teaching the laboratories of Organic synthesis of Prof. Alessandro Palmieri, May 4-12, 2023.

f) Poster presentation at 2nd Virtual Symposium for Young Organic Chemists promoted by the Organic Division of Societá Chimica Italiana, Itay. October 24-27, 2022.

g) A webinar organized by Scientific Update on " Synthetic Approaches to the New Drugs Approved in 2022, Jan 26, 2023.

La borsa di dottorato cofinanziata con risorse del Programma Operativo Nazionale Ricerca e Innovazione 2014-2020 (CCI 2014IT16M2OP005), risorse Fondo Sociale Europeo REACT-EU, Azione I.1 "Dottorati Innovativi con caratterizzazione industriale", Azione IV.4 "Dottorati e contratti di ricerca su tematiche dell'innovazione" e Azione IV.5 "Dottorati su tematiche Green"